

August 2012

# Influence of Oceanic Forcing on Fate of Nutrients in a Near-Shore-Aquifer

Nawrin Anwar, *Western University*

Supervisor: Dr. Clare Robinson, *The University of Western Ontario*

A thesis submitted in partial fulfillment of the requirements for the Master of Engineering  
Science degree in Civil and Environmental Engineering

© Nawrin Anwar 2012

Follow this and additional works at: <https://ir.lib.uwo.ca/etd>



Part of the [Environmental Engineering Commons](#)

---

## Recommended Citation

Anwar, Nawrin, "Influence of Oceanic Forcing on Fate of Nutrients in a Near-Shore-Aquifer" (2012).  
*Electronic Thesis and Dissertation Repository*. 762.  
<https://ir.lib.uwo.ca/etd/762>

This Dissertation/Thesis is brought to you for free and open access by Scholarship@Western. It has been accepted for inclusion in Electronic Thesis and Dissertation Repository by an authorized administrator of Scholarship@Western. For more information, please contact [wlsadmin@uwo.ca](mailto:wlsadmin@uwo.ca).

# **INFLUENCE OF OCEANIC FORCING ON FATE OF NUTRIENTS IN A NEAR-SHORE AQUIFER**

(Spine title: Effect of oceanic forcing on nutrients in a coastal aquifer)

(Thesis format: Integrated Article)

by

Nawrin Anwar

Graduate Program in Engineering Science  
Department of Civil and Environmental Engineering

A thesis submitted in partial fulfillment  
of the requirements for the degree of  
Master of Engineering Science

The School of Graduate and Postdoctoral Studies  
Western University  
London, Ontario, Canada

© Nawrin Anwar 2012

WESTERN UNIVERSITY  
SCHOOL OF GRADUATE AND POSTDOCTORAL STUDIES

**CERTIFICATE OF EXAMINATION**

Supervisor

Examiners

\_\_\_\_\_  
Dr. Clare Robinson

\_\_\_\_\_  
Dr. Jason Gerhard

\_\_\_\_\_  
Dr. Slobodan Simonovic

\_\_\_\_\_  
Dr. Madhumita B. Ray

The thesis by

**Nawrin Anwar**

entitled:

**Influence of oceanic forcing on fate of nutrients in a near-shore aquifer**

is accepted in partial fulfillment of the  
requirements for the degree of  
Master of Engineering Science

Date \_\_\_\_\_

\_\_\_\_\_  
Chair of the Thesis Examination Board

## Abstract

---

A reactive groundwater transport model has been developed to investigate the fate of nutrients (ammonium, nitrate, and phosphate) in a near-shore coastal aquifer subject to oceanic forcing (tides and waves) and their subsequent discharge to coastal waters. The model is developed by combining the variable-density groundwater flow model SEAWAT-2005 with the reactive multi-component transport model PHT3D v2.10. The influence of tides and waves are typically neglected in prior studies that have examined the transport and transformation of nutrients in coastal aquifers. Oceanic forcing however can induce a highly dynamic surficial salt-freshwater mixing and reaction zone in a near-shore aquifer and this may modify the transport pathways and concentrations of discharging nutrients. The reactions considered in the model include denitrification, nitrification, aerobic degradation of dissolved organic matter, iron oxidation, and phosphate adsorption. The reaction network implemented, including the kinetic rate expressions, has been verified previously by numerical simulations conducted for a near-shore aquifer not exposed to oceanic forcing. The simulations conducted reveal that oceanic forcing significantly modifies the discharge pathway of the groundwater-derived nutrients and the reactions occurring along this pathway. This alters the net production and consumption of nutrients in the near-shore aquifer and their subsequent loading rates to coastal waters. It is further shown that the fate of the nutrients is strongly controlled by the availability of chemical species including dissolved organic matter in seawater recirculating through the near-shore sediments. Moreover, for the conditions simulated, tides led to more intense salt-freshwater mixing in the near-shore aquifer and thus greater transformations of nutrients in the near-shore aquifer compared to regular wave forcing.

This study significantly enhances conceptual understanding of the processes controlling the fate of nutrients in a near-shore aquifer and hence provides a valuable tool for improving prediction of nutrient loading rates to coastal waters.

**Keywords:** submarine groundwater discharge, tides, waves, salt-freshwater mixing, geochemical reactions, subterranean estuary, numerical modeling.

## Co-Authorship

---

Chapter 3: Influence of oceanic forcing on fate of nutrients in a near-shore aquifer, Nawrin Anwar, and Clare Robinson. Nawrin Anwar is the principal author of this manuscript, with 100% intellectual input, 100% modeling work, and 100% writing process. The manuscript was reviewed by Dr. Clare Robinson who provided additional recommendations for further improvement.

## Dedication

---

*To Them I Dedicate*

*My Parents*

*Manjour Murshed Anwar*

*Shirin Akhter*

## Acknowledgement

---

I would first like to express my sincere appreciation and deep gratitude to my supervisor Dr. Clare Robinson for her profound insight, valuable advice, and continuous support throughout my graduate life at Western University. It was my privilege to work with her. I have learned a lot from her dedicated persona, immaculate work ethics, organizational skills, and creative thinking. Her patient guidance and motivation helped me to move forward and complete this thesis. I will always try to embrace all the good virtues learned from her in my future life.

I am sincerely grateful to the members of my examination committee, Dr. Jason Gerhard, Dr. Slobodan Simonovic and Dr. Madhumita Bhounik Ray.

I would like to thank all my UWO friends and officials for making my graduate life wonderful. Special thanks to Stephanie Laurence for her help with all the important paper works throughout my Masters. I would also like to thank all the members from RESTORE for being welcoming, encouraging, supportive and helpful. My special thanks go to Ambareen Atisha and Ahmed Ishtiaque Amin Chowdhury for their continuous support throughout my journey here in Canada.

Financial support provided by Natural Sciences and Engineering Research Council of Canada (NSERC) and by the Faculty of Engineering at Western University is gratefully acknowledged.

I would like to express my deep gratitude to my family for their support for leading me up to this moment. I would also like to thank my uncle, Ashraf Jahangir, for his support



and encouragement. My special appreciation goes to Mahbuboor Rahman Choudhury for believing in me and always being there for me to accomplish this endeavour. My warm gratitude goes to all my friends here in North America and in Bangladesh, especially to Shathi, Nawshin, Ishita, Pushpita, and Toma for being supportive and encouraging all through my journey here at Western.

## Table of Contents

---

<b>CERTIFICATE OF EXAMINATION .....</b>	<b>ii</b>
<b>Abstract.....</b>	<b>iii</b>
<b>Co-Authorship.....</b>	<b>v</b>
<b>Dedication .....</b>	<b>vi</b>
<b>Table of Contents .....</b>	<b>ix</b>
<b>List of Tables .....</b>	<b>xi</b>
<b>List of Figures .....</b>	<b>xii</b>
<b>Chapter 1 .....</b>	<b>1</b>
<b>Introduction.....</b>	<b>1</b>
1.1 Background.....	1
1.2 Research objective .....	4
1.3 Thesis outline.....	4
References.....	5
<b>Chapter 2 .....</b>	<b>9</b>
<b>Literature Review .....</b>	<b>9</b>
2.1 Introduction.....	9
2.2 Coastal water pollution and stressors .....	10
2.3 Submarine groundwater discharge (SGD) .....	11
2.4 The subterranean estuary and influence of oceanic forcing .....	15
2.5 SGD of nutrients and nutrient dynamics in a near-shore aquifer .....	19
2.6 Numerical modeling of reactive contaminant transport in near-shore aquifers .....	24
2.7 Summary .....	26
References.....	26
<b>Chapter 3 .....</b>	<b>35</b>
<b>Influence of oceanic forcing on fate of nutrients in a near-shore aquifer     .....</b>	<b>35</b>

3.1 Introduction.....	35
3.2 Numerical Model.....	40
<b>3.2.1 Groundwater flow and multi-species transport model.....</b>	<b>40</b>
<b>3.2.2 Nutrient concentrations and geochemical model .....</b>	<b>44</b>
3.3 Results and Discussion .....	50
<b>3.3.1 Effect of tides.....</b>	<b>50</b>
<b>3.3.2 Effect of waves .....</b>	<b>64</b>
3.4 Influence of labile DOM from seawater.....	72
<b>3.4.1 Wave effects on nutrients in the presence of labile DOM .....</b>	<b>74</b>
3.5 Conclusions.....	77
References.....	79
<b>Chapter 4 .....</b>	<b>84</b>
<b>Summary and Recommendations .....</b>	<b>84</b>
4.1 Summary .....	84
4.2 Recommendations .....	87
References.....	88
<b>Appendix A.....</b>	<b>89</b>
<b>Numerical Model Verification.....</b>	<b>89</b>
A.1 Introduction.....	89
A.2 Groundwater flow and multi-species transport geochemical model setup .....	89
A.3 Salt distribution.....	91
A.4 Nutrient distribution.....	92
A.5 Conclusion .....	94
References.....	94
<b>Appendix B .....</b>	<b>96</b>
<b>MATLAB code for post processing data .....</b>	<b>96</b>
B.1 Parameters Calculated.....	96
B.2 Extracting data for ammonium .....	96
<b>Vita .....</b>	<b>106</b>

## List of Tables

---

Table 2.1: Major reactions for nutrient transformation in coastal aquifer.....	22
Table 3.1: Reactions and kinetic formulae included (modified from Spiteri et al. 2008(a)) .....	47
Table 3.2: Reaction parameter values .....	48
Table 3.3: Concentration of species in fresh groundwater (landward boundary) and seawater (cells in zone A and along aquifer ocean interface) <sup>a</sup> .....	49
Table 3.4: Summary of simulations conducted to quantify the effect of oceanic forcing.	50
Table 3.5: Production and consumption of species in the near-shore aquifer for simulated cases 1-8 (without the presence of labile DOM). .....	59
Table 3.6: Production and consumption of species in the near-shore aquifer for simulated cases 9-11 with labile DOM. ....	74

## List of Figures

---

Figure 2.1: Near-shore SGD mechanisms. Figure modified from Robinson et al. (2007c). .....	13
Figure 2.2: Conceptual model of the near-shore coastal aquifer with seawater recirculation and salt-freshwater mixing mechanisms: (1) land-derived fresh groundwater ( $Q_f$ ), (2) density-driven convective recirculation ( $Q_d$ ), (3) tide-induced recirculation ( $Q_t$ ), (4) wave-induced recirculation ( $Q_w$ ). The salt distribution is shown with the coloured shading (red-yellow). The aquifer has 3 distinct zones: saltwater wedge, upper saline plume (USP) and the freshwater discharge zone. The wave set-up profile (wave-averaged water level) is denoted by the thick black dotted line (Figure modified from Robinson et al. 2007b). .....	16
Figure 2.3: Schematic diagram of the biogeochemical processes leading to transformation, removal or release of groundwater-derived nutrients and recirculating nutrients in a subterranean estuary where anoxic groundwater mixes with oxic seawater (Figure reproduced from Slomp and van Cappellen 2004). .....	21
Figure 3.1: Conceptual model of a near-shore coastal aquifer showing main water exchange and salt-freshwater mixing mechanisms: (1) terrestrially-derived fresh groundwater ( $Q_f$ ), (2) density-driven convective recirculation ( $Q_d$ ), (3) tide-induced recirculation ( $Q_t$ ), and (4) wave-induced recirculation ( $Q_w$ ). The salinity distribution is shown by the coloured shading (red-yellow). The aquifer has 3 distinct zones: saltwater wedge, upper saline plume (USP) and the freshwater discharge zone. The wave set-up profile (wave-averaged water level) is denoted by the thick black dotted line (Figure modified from Robinson et al. 2007b). .....	36
Figure 3.2: Model domain and flow boundary conditions. ....	42
Figure 3.3: Simulated salt distributions in the near-shore aquifer for simulations (a) without oceanic forcing (Cases 1 and 2) and (b) with tides (Cases 3 and 4), and oxygen distributions for reactive transport simulations (c) without oceanic forcing (Case 2) and (d) with tides (Case 4) after 300 days. ....	52
Figure 3.4: Concentration profiles of nitrate after 300 days for simulations with (a) conservative transport without oceanic forcing (Case 1), (b) reactive transport without	

oceanic forcing (Case 2), (c) change in concentration due to reaction between Cases 1 and 2 (positive change corresponds to a decrease in concentration) (d) conservative transport with tides (Case 3), and (e) reactive transport with tides (Case 4) (f) change in concentration due to reaction between Cases 3 and 4 (positive change corresponds to a decrease in concentration)..... 53

Figure 3.5: Concentration profiles of ammonium after 300 days for simulations with (a) conservative transport without oceanic forcing (Case 1), (b) reactive transport without oceanic forcing (Case 2), (c) change in concentration due to reaction between Cases 1 and 2 (positive change corresponds to a decrease in concentration) (d) conservative transport with tides (Case 3), and (e) reactive transport with tides (Case 4) (f) change in concentration due to reaction between Cases 3 and 4 (positive change corresponds to a decrease in concentration)..... 54

Figure 3.6: Exit concentration of (a) nitrate and (b) ammonium along the aquifer-ocean interface after 300 days for Cases 1-4..... 56

Figure 3.7: Discharge of chemical fluxes of (a) nitrate and (b) ammonium along the aquifer-ocean interface for Cases 1-4 after 300 days..... 58

Figure 3.8: Concentration profiles of dissolved phosphate after 300 days for simulations with (a) conservative transport without oceanic forcing (Case 1), (b) reactive transport without oceanic forcing (Case 2), (c) conservative transport with tides (Case 3), and (d) reactive transport with tides (Case 4)..... 60

Figure 3.9: Concentration profiles of dissolved ferrous iron after 300 days for simulations with (a) conservative transport without oceanic forcing (Case 1), (b) reactive transport without oceanic forcing (Case 2), (c) conservative transport with tides (Case 3), and (d) reactive transport with tides (Case 4)..... 61

Figure 3.10: Concentrations of (a) dissolved phosphate and (b) ferrous iron along the aquifer-ocean interface for Cases 1-4 after 300 days..... 62

Figure 3.11: Discharge fluxes of (a) dissolved phosphate and (b) ferrous iron along the aquifer-ocean interface for Cases 1-4 after 300 days..... 63

Figure 3.12: Salt distribution in the near-shore aquifer for (a)  $H_{rms} = 1$  m (Cases 5, 6) and (b)  $H_{rms} = 2$  m (Cases 7, 8), and oxygen distribution for reactive transport simulations with (c)  $H_{rms} = 1$  m (Case 6) and (d)  $H_{rms} = 2$  m (Case 8) after 300 days. .... 64

Figure 3.13: Concentration profiles from simulations with $H_{rms} = 1$ m with conservative transport (Case 5) of (a) nitrate, (c) ammonium, (e) phosphate, and (g) ferrous iron; and reactive transport (Case 6) of (b) nitrate, (d) ammonium, (f) phosphate, and (h) ferrous iron after 300 days. ....	66
Figure 3.14: Exit concentrations for (a) nitrate, (b) ammonium, (c) dissolved phosphate, and (d) ferrous iron for cases with $H_{rms} = 1$ m (Cases 5, 6) and no oceanic forcing (Cases 1, 2) after 300 days.....	71
Figure 3.15: Simulated (a) oxygen, (c) nitrate and (e) ammonium distributions for reactive transport case with no oceanic forcing and labile DOM (Case 9) and change in concentrations due to reaction for (b) oxygen, (d) nitrate, and (f) ammonium (positive change corresponds to a decrease in concentration) after 300 days. ....	73
Figure 3.16: Simulated (a) oxygen, (c) nitrate and (e) ammonium distributions for reactive transport case with $H_{rms} = 1$ m and labile DOM (Case 10) and change in concentrations due to reaction for (b) oxygen, (d) nitrate, and (f) ammonium (positive change corresponds to a decrease in concentration) after 300 days. ....	75
Figure A.1: Model domain and flow boundary conditions.....	90
Figure A.2: Simulated steady state salt distribution in the coastal aquifer from (a) model developed, and (b) Spiteri et al. (2008a).....	91
Figure A.3: Vertical salt distribution profiles at (a) 35 m, (b) 40 m, (c) 45 m, (d) 50 m, (e) 55 m, and (f) 60 m from landward boundary in the model at steady state. ....	92
Figure A.4: Simulated concentration profiles for (a, b) nitrate, (c, d) ammonium; and (e, f) phosphate from present study and Spiteri et al. (2008a) respectively. The subplots on the right hand side (b), (d) and (f) are modified from Spiteri et al. (2008a).....	93
Figure A.5: Steady state vertical concentration profiles of (a,e) nitrate, (b,f) ammonium, (c,g) phosphate and (d,h) at interface and seaward boundary from present study and Spiteri et al. (2008a) study respectively after 1000 days. Dashed lines represent simulation results conservative transport simulations and solid lines represent simulation results from reactive transport simulations. ....	93

## Chapter 1

---

### Introduction

#### 1.1 Background

It is widely recognized that submarine groundwater discharge (SGD) can be an important source of nutrients (i.e., ammonium, nitrate, and phosphate) to coastal waters (Capone and Bautista 1985; Garrison et al. 2003; Santos et al. 2008). This is because high concentrations of nutrients are often observed in coastal aquifers due to increasing population and urban and agricultural development along shorelines (Postma et al. 1991; Spalding and Exner 1993; Howarth et al. 1996; Iversen et al. 1998). Natural reactive processes occurring in the aquifer (e.g. denitrification, phosphate adsorption) can decrease nutrient fluxes to coastal waters, however, in many cases, subsurface nutrient attenuation is limited and nutrient loading via SGD can be significant (Valiela et al. 1978; Johannes 1980; Capone and Bautista 1985; Valiela et al. 1992). Understanding the transport and transformation of nutrients in a coastal aquifer is therefore important to accurately predict nutrient loading rates.

Nutrient discharge can have severe effects on the coastal ecosystem (Lapointe and O'Connell 1989; Valiela et al. 1990; Valiela et al. 1992). Increase of the nitrogen:phosphate (N:P) ratio in coastal waters due to groundwater discharge has been shown to lead to eutrophication of coastal waters (Capone and Bautista 1985; Valiela et al. 1992; Paerl 1997). This promotes excessive plant growth including harmful algal blooms and in some cases can lead to changes in the biodiversity of near-shore ecosystems (Paerl 1997). Harmful algal blooms can also have acute human health



impacts, for example, some cyanobacteria can cause health effects such as skin irritations (Pilotto et al. 1997) and more severe respiratory problems (McElhenny et al. 1962).

The discharge of nutrients from a coastal aquifer to the sea depends on the landward groundwater sources as well as on the specific subsurface nutrient discharge pathway and the biogeochemical reactions occurring along this pathway (Slomp and van Cappellen 2004; Spiteri et al. 2005; Charette and Sholkovitz 2006). Two mixing zones of fresh groundwater and seawater often exist in the near-shore region of a coastal aquifer exposed to tides or waves: a) the mixing zone along the interface of the saltwater wedge which forms due to the density-driven seawater recirculation across the aquifer-ocean interface (Cooper 1959; Destouni and Prieto 2003; Smith 2004) and b) the upper saline plume formed due to tide- and wave-induced recirculation through an aquifer (Li 1999; Boufadel 2000; Li et al. 2000; Turner and Acworth 2004; Vandenbohede and Lebbe 2005; Robinson et al. 2006; Robinson et al. 2007b; Robinson et al. 2007c; Xin et al. 2010). The zone where recirculating seawater and fresh groundwater mix in a coastal aquifer is often referred to as a subterranean estuary (Moore 1999). This is because it is typically characterized by strong biogeochemical gradients (e.g., pH or redox gradients) and so is an important zone for the transformation of groundwater-derived reactive species. The salt-freshwater mixing zone along the interface of the saltwater wedge was traditionally considered as the primary area of mixing between fresh groundwater and seawater. However, now it has been widely established that in many cases the upper saline plume may be a more dynamic and active zone of mixing and reaction (Robinson et al. 2007b).

A number of studies have demonstrated that significant nutrient production can occur in a subterranean estuary. This means that multiplication of fresh groundwater nutrient concentrations with submarine groundwater discharge (SGD) rates often underestimates nutrient fluxes to coastal waters (Santos et al. 2009). In a near-shore aquifer, land-derived groundwater flows, seawater recirculation rates, aquifer sediment characteristics and biogeochemical reactions determine the transport and transformation of nutrients discharging to coastal waters (Slomp and van Cappellen 2004). While field and numerical investigations have been undertaken to examine the fate of nutrients in near-shore aquifers (Andersen et al. 2007; Beck et al. 2007; Kroeger and Charette 2008; Spiteri et al. 2008a; Spiteri et al. 2008b), most studies have focused on coastal aquifers that are not influenced by oceanic forcing (tides and waves). Tides and waves lead to significant amounts of seawater containing oxygen and reactants including organic matter to recirculate through the near-shore aquifer (subterranean estuary). It is the availability of these reactants that can significantly affect the fate of nutrients in a subterranean estuary (Santos et al. 2009).

As most shorelines are exposed to tides and/or waves, quantifying the effect of these oceanic forcing on nutrient behaviour in a coastal aquifer is critical for predicting their discharge to coastal waters. Measurement of nutrient behaviour in coastal aquifer system exposed to oceanic forcing is complex due to the extremely high temporal and spatial variability occurring at a wide range of scales (e.g., frequency of tides, waves, seasonal variability). Numerical modeling is able to provide valuable conceptual insight into the physical transport and reaction processes that control the fate of nutrients in a near-shore aquifer subject to tides and waves and their subsequent discharge to coastal waters.

## **1.2 Research objective**

For effective coastal management it is essential to understand the complex and dynamic processes associated with the transport and transformation of nutrients in coastal aquifers. The main objective of this thesis is to evaluate the effects of oceanic fluctuations (e.g., tides and waves) on the transport and transformation of nutrients in a near-shore coastal aquifer and nutrient fluxes to coastal waters. This understanding is required to improve prediction of nutrient loading via submarine groundwater discharge. The variable density groundwater flow model SEAWAT-2005 (Guo and Langevin 2002) is used in combination with the reactive multi-component transport model PHT3D v2.10 (Prommer and Post 2010) to simulate the fate of nutrients discharging to the ocean from a coastal aquifer. The numerical model developed is first described and the model is verified using previously reported simulation results without considering effects of tides and waves (Spiteri et al. 2008a). Simulations were performed with oceanic forcing using the verified numerical model (no oceanic forcing) to evaluate the exit concentration, chemical flux, nutrient accumulation and net discharge of nutrients from a coastal aquifer exposed to tides and waves. The numerical model is finally be used to assess the influence of labile dissolved organic matter associated with the seawater recirculating through the aquifer on the nutrient transformations in the subterranean estuary.

## **1.3 Thesis outline**

This thesis is written in “Integrated Article Format”. A brief description of each chapter is presented below.

Chapter 1: Introduces background information and states the objectives of the study.

Chapter 2: Reviews past research focused on submarine groundwater discharge and the influence of oceanic forcing on groundwater flows and the transport and fate of nutrients in coastal aquifers.

Chapter 3: Details the numerical model development, simulation results and provides discussion of the simulations performed to examine nutrient transport and fate in a near-shore aquifer.

Chapter 4: Summarizes the research results and outlines recommendations for future work.

## References

- Andersen, M. S., L. Baron, et al. (2007). "Discharge of nitrate-containing groundwater into a coastal marine environment." Journal of Hydrology 336 (1-2 ): 98-114.
- Beck, A. J., Y. Tsukamoto, et al. (2007). "Importance of geochemical transformations in determining submarine groundwater discharge-derived trace metal and nutrient fluxes." Applied Geochemistry 22(2): 477-490.
- Boufadel, M. C. (2000). "A mechanistic study of nonlinear solute transport in a groundwater-surface water system under steady state and transient hydraulic conditions." Water Resources Research 36(9): 2549-2565.
- Capone, D. G. and M. F. Bautista (1985). "A Groundwater source of nitrate in nearshore marine-sediments." Nature 313: 214-216.
- Charette, M. A. and E. R. Sholkovitz (2006). "Trace element cycling in a subterranean estuary: Part 2. Geochemistry of the pore water." Geochem et Cosmochim Acta 70: 811-826.
- Cooper, H. H. (1959). "A hypothesis concerning the dynamic balance of fresh water and salt water in a coastal aquifer." Journal of Geophysical Research 64(4): 461-467.
- Destouni, G. and C. Prieto (2003). "On the possibility for generic modelling of submarine groundwater discharge." Biogeochemistry 66: 171-186.

- Garrison, G. H., C. R. Glenn, et al. (2003). "Measurement of submarine groundwater discharge in Kahana Bay, O'ahu, Hawai'i." Limnology and Oceanography 48(2): 920-928.
- Guo, W. and C. D. Langevin (2002). User's Guide to SEAWAT: A computer program for simulation of three-dimensional variable-density ground-water flow. Tallahassee, Florida, US Geological Survey: pp. 77.
- Howarth, R. W., G. Billen, et al. (1996). "Regional nitrogen budgets and riverine N&P fluxes for the drainages to the North Atlantic Ocean: Natural and human influences." Biogeochemistry 35(1): 75-139.
- Iversen, T. M., R. Grant, et al. (1998). "Nitrogen enrichment of European inland and marine waters with special attention to Danish policy measures." Environmental Pollution 102: 771-780.
- Johannes, R. E. (1980). "The ecological significance of the submarine discharge of groundwater." Marine Ecology - Progress Series 3: 365-373.
- Kroeger, K. D. and M. A. Charette (2008). "Nitrogen biogeochemistry of submarine groundwater discharge." Limnology and Oceanography 53(3): 1025-1039.
- Lapointe, B. E. and J. D. O'Connell (1989). "Nutrient-enhanced growth of *Cladophora prolifera* in Harrington Sound, Bermuda: Eutrophication of a confined, phosphorus-limited marine ecosystem." Estuarine, Coastal and Shelf Science 28: 347-360.
- Li, L., D. A. Barry, et al. (2000). "Beach water table fluctuations due to spring-neap tides: moving boundary effects." Advances in Water Resources 23: 817-824.
- Li, L., D. A. Barry, et al. (1999). "Submarine groundwater discharge and associated chemical input to a coastal sea." Water Resources Research 35(11): 3252-3259.
- McElhenny, T. R., H. C. Bold, et al. (1962). "Algae: a cause of inhalant allergy in children." Annals of Allergy 20: 739-743.
- Moore, W. S. (1999). "The subterranean estuary: A reaction zone of ground water and sea water." Marine Chemistry 65: 111-125.
- Paerl, H. W. (1997). "Coastal eutrophication and harmful algal blooms: Importance of atmospheric deposition and groundwater as "new" nitrogen and other nutrient sources." Limnology and Oceanography 42(5): 1154-1165.
- Pilotto, L. S., R. M. Douglas, et al. (1997). "Health effects of exposure to cyanobacteria (blue-green algae) due to recreational water-related activities." Australian and New Zealand Journal of Public Health 21(6): 562-566.

- Postma, D., C. Boesen, et al. (1991). "Nitrate reduction in an unconfined sandy aquifer-water chemistry, reduction processes, and geochemical modeling." Water Resources Research 27(8): 2027-2045.
- Prommer, H. and V. Post (2010). A reactive multicomponent transport model for saturated porous media
- Robinson, C., B. Gibbes, et al. (2006). "Driving mechanisms for flow and salt transport in a subterranean estuary." Geophysical Research Letters 33: L03402.
- Robinson, C., L. Li, et al. (2007b). "Effect of tidal forcing on a subterranean estuary." Advances in Water Resources 30: 851-865.
- Robinson, C., L. Li, et al. (2007c). "Tide-induced recirculation across the aquifer-ocean interface." Water Resources Research 43: W07428.
- Santos, I. R., W. C. Burnett, et al. (2009). "Tidal pumping drives nutrient and dissolved organic matter dynamics in a Gulf of Mexico subterranean estuary." Geochimica et Cosmochimica Acta 73(5): 1325-1339.
- Santos, I. R., M. I. Machado, et al. (2008). "Major ion chemistry in a freshwater coastal lagoon from southern Brazil (Mangueira Lagoon): Influence of groundwater inputs." Aquatic Geochemistry 14(2): 133-146.
- Slomp, C. P. and P. van Cappellen (2004). "Nutrient inputs to the coastal ocean through submarine groundwater discharge: controls and potential impact." Journal of Hydrology 295: 64-86.
- Smith, A. J. (2004). "Mixed convection and density-dependent seawater circulation in coastal aquifers." Water Resources Research 40(8): 16.
- Spalding, R. F. and M. E. Exner (1993). "Occurrence of nitrate in groundwater-a review." Journal of Environmental Quality 22(3): 392-402.
- Spiteri, C., P. Regnier, et al. (2005). "pH-dependent iron oxide precipitation in a subterranean estuary." Journal of Geochemical Exploration 88: 399-403.
- Spiteri, C., C. P. Slomp, et al. (2008b). "Flow and nutrient dynamics in a subterranean estuary (Waquoit Bay, MA, USA): Field data and reactive transport modeling." Geochimica et Cosmochimica Acta 72(14): 3398-3412.
- Spiteri, C., C. P. Slomp, et al. (2008a). "Modeling biogeochemical processes in subterranean estuaries: Effect of flow dynamics and redox conditions on submarine groundwater discharge of nutrients." Water Resources Research 44(4): W04701.

- Turner, I. L. and R. I. Acworth (2004). "Field measurements of beachface salinity structure using cross-borehole resistivity imaging." Journal of Coastal Research 20(3): 753-760.
- Valiela, I., J. Costa, et al. (1990). "Transport of groundwater-borne nutrients from watersheds and their effects on coastal waters." Biogeochemistry 10: 177-197.
- Valiela, I., K. Foreman, et al. (1992). "Coupling of watersheds and coastal waters: Sources and consequences of nutrient enrichment in Waquoit Bay, Massachusetts." Estuaries 15(4): 443-457.
- Valiela, I., J. M. Teal, et al. (1978). "Nutrient and particulate fluxes in a salt-marsh ecosystem: Tidal exchanges and inputs by precipitation and groundwater." Limnology and Oceanography 23(4): 798-812.
- Vandenbohede, A. and L. Lebbe (2005). "Occurrence of salt water above fresh water in dynamic equilibrium in a coastal groundwater flow system near De Panne, Belgium." Hydrogeology Journal 14(4): 462 - 472.
- Xin, P., C. Robinson, et al. (2010). "Effects of wave forcing on a subterranean estuary." Advances in Water Resources 46: W12505.

## Chapter 2

---

### Literature Review

#### 2.1 Introduction

Increasing development and population growth along coastlines worldwide has caused elevated levels of nutrients (e.g., ammonium, nitrate, phosphate) in coastal aquifers. Traditionally river inputs have been considered as the main source of nutrients in coastal waters. However, it is now widely recognized that submarine groundwater discharge (SGD) can also transport considerable amounts of nutrients to coastal waters particularly in areas where severe groundwater contamination has been occurred (Simmons 1992; Church 1996; Moore 1996; Li et al. 1999; Burnett et al. 2003; Slomp and van Cappellen 2004; Burnett et al. 2006). Nutrient loading from coastal aquifers to coastal waters depends not only on the landward sources but also the specific nutrient flow pathway and the biogeochemical reactions occurring along this pathway (Slomp and van Cappellen 2004; Spiteri et al. 2005; Charette and Sholkovitz 2006). In particular the flow, transport and reaction processes in a near-shore aquifer strongly control the exit conditions for nutrients discharging to coastal waters. While several studies have examined the fate of nutrients in near-shore aquifers (Andersen et al. 2007; Beck et al. 2007; Kroeger and Charette 2008; Spiteri et al. 2008a), the effect of oceanic fluctuations including tides and waves is typically neglected. However, oceanic fluctuations can lead to a highly dynamic surficial mixing and reaction zone in the near-shore aquifer and significantly alter the transport pathway for discharging nutrients (Robinson et al. 2007b; Robinson et al. 2007c; Robinson et al. 2009; Xin et al. 2010). In this study the variable density



groundwater flow model SEAWAT-2005 (Guo and Langevin 2002) is used in combination with the reactive multi-component transport model PHT3D v2.10 (Prommer and Post 2010) to examine the influence of tides and waves on the transport and transformation of nutrients (ammonium, nitrate, and phosphate) in a near-shore coastal aquifer. This chapter summarizes previous literature that has investigated the behaviour of nutrients in coastal aquifers and their discharge to coastal waters.

## **2.2 Coastal water pollution and stressors**

As populations expand in coastal areas, coastal ecosystems are placed under greater stress due to increasing pollution. There are a variety of sources that deliver nutrients to coastal waters. Sources can be point sources (e.g., wastewater treatment plants or sewage overflows) or they can be diffuse non-point inputs such as agricultural run-off, storm water run-off and groundwater discharge. Point sources are comparatively simple to identify and quantify compared with non-point sources which are often complex and difficult to quantify and to control.

Worldwide, urban shoreline development, wastewater disposal systems and the use of fertilizers, for example, have led to elevated nutrient levels in coastal aquifers (Postma et al. 1991; Spalding and Exner 1993; Howarth et al. 1996; Iversen et al. 1998). While in some cases nutrients are naturally attenuated in the aquifer, often nutrient removal does not occur in the aquifer and the nutrients discharge with the groundwater to the sea (Valiela et al. 1978; Johannes 1980; Capone and Bautista 1985; Valiela et al. 1992). For phytoplankton growth, the optimal ratio of nitrogen (N) to phosphorous (P) is 16:1 (Redfield ratio). If the N/P ratio is lower than the Redfield ratio, it is the indication of a

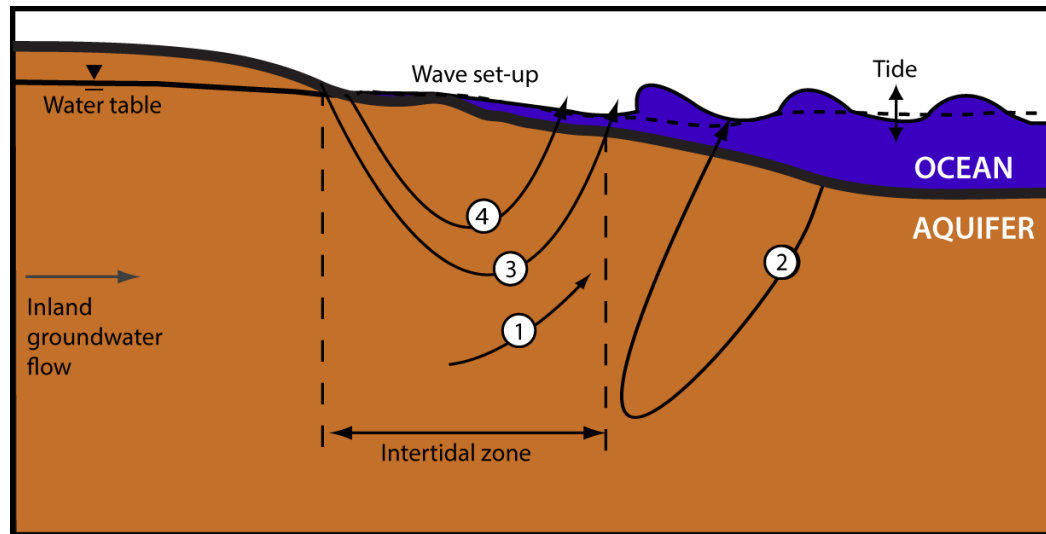
N-limited system. A high N/P ratio indicates a P-limited system. Changes to the Redfield ratio can have a significant effect on the biological state of an ecosystem, including phytoplankton biomass and species composition. Generally, the marine environment is N-limited with a lower N/P ratio (Howarth 1988; Conley 1999). As phosphate is often attenuated in aquifers via adsorption (Krom and Berner 1980; Spiteri et al. 2005), groundwater is often P-limited (Lapointe and O'Connell 1989; Weiskel and Howes 1992). As a result, in some cases where there is significant SGD, N-limited coastal waters become P-limited due to the discharge of excess nitrogen (Valiela et al. 1990; Weiskel and Howes 1992; Paerl 1997). Increase of the N:P ratio in coastal waters due to SGD have been shown to lead to eutrophication (Capone and Bautista 1985; Valiela et al. 1992; Paerl 1997). This promotes excessive plant growth including harmful algal blooms and in some cases can lead to changes in the biodiversity of a near-shore ecosystem (Paerl 1997). Harmful algal blooms can also have human health impacts, for example, some cyanobacteria can cause human health effect such as skin irritations (Pilotto et al. 1997) and more severe respiratory problems (McElhenny et al. 1962).

### **2.3 Submarine groundwater discharge (SGD)**

The importance of groundwater discharge from coastal aquifers as a pollution source was first identified by Johannes (1980) and Bokuniewicz (1980). SGD can be a significant source of fresh water and land-derived chemicals (e.g., nutrients, heavy metals, organic compounds and radionuclides) to coastal waters (Simmons 1992; Moore 1996; Burnett et al. 2001; Taniguchi et al. 2002; Burnett et al. 2003). For example, nutrient inputs via SGD have been shown to be similar in magnitude to surface water inputs in Great South Bay, New York (Capone and Bautista 1985; Capone and Slater 1990), Discovery Bay,

Jamaica (D'Elia et al. 1981), Tomales Bay, California (Oberdorfer 2003) and the eastern part of Florida Bay (Corbett et al. 1999).

SGD is formally defined as all direct discharge of subsurface fluid across the aquifer-ocean interface (Taniguchi et al. 2002). As such SGD is comprised of terrestrially-derived groundwater flow and also seawater recirculating across the aquifer-ocean interface (Li et al. 1999; Taniguchi et al. 2002; Burnett et al. 2003). Direct measurements (Robinson et al. 1998; Kim et al. 2003; Smith and Zawadski 2003; Taniguchi and Iwakawa 2004), geochemical tracer experiments (Moore 1996; Moore and Church 1996; Hussain et al. 1999; Crotwell and Moore 2003; Boehm et al. 2006), and numerical modeling studies (Li et al. 1999; Smith 2004; Kaleris 2006) have shown that the recirculating seawater can be a major portion of total SGD. Recirculation of saltwater across the aquifer-ocean interface is driven by a number of different mechanisms (Riedl et al. 1972; Huettel et al. 1996; Michael et al. 2005; Robinson et al. 2006; Robinson et al. 2007b; Robinson et al. 2007c). In the near-shore region, which is the focus of this study, the main factors driving recirculation are density driven convection, tides, and waves (Figure 2.1).



- |                                 |                               |
|---------------------------------|-------------------------------|
| 1. Fresh groundwater discharge  | 3. Tide-induced recirculation |
| 2. Density-driven recirculation | 4. Wave-induced recirculation |

**Figure 2.1:** Near-shore SGD mechanisms. Figure modified from Robinson et al. (2007c).

These mechanisms that drive seawater recirculation across the aquifer-ocean interface also lead to complex and dynamic flows and transport in the near-shore aquifer (Michael et al. 2005). The relative magnitudes of fresh groundwater discharge and recirculated discharge has been quantified in numerous field studies (Gallagher et al. 1996; Hussain et al. 1999; Kim et al. 2003; Taniguchi and Iwakawa 2004; Boehm et al. 2006; Taniguchi et al. 2006). Nevertheless the significance of the various processes that drive seawater recirculation, for example their importance for nutrient budgets, still requires quantification. The magnitude of seawater recirculation driven by tides and waves in the coastal aquifer was first modeled by Li et al. (1999) who showed analytically that tide- and wave-induced recirculation may account for up to 96% of the total SGD. Their model did not consider density-dependent groundwater flow and hence did not account for density-driven seawater recirculation. Studies were also carried out to examine the effect of the density-dependent flow processes on SGD but without considering oceanic forcing

(Destouni and Prieto 2003; Smith 2004). Prieto and Destouni (2005) later conducted numerical simulations that examined the effects of tides on three different coastal aquifer regions on the Mediterranean Sea. Prieto et al. (2005) found that when the SGD is low, the presence of tides significantly enhances the recirculating component of seawater in the SGD compared to non-tidal conditions. However, when the SGD is large, even if tides are present, they observed higher fresh groundwater components.

Robinson et al. (2007c) presented a detailed parametric study to quantify the factors that influence tide-induced recirculation across the aquifer-ocean interface. They showed that the strength of the tidal forcing relative to the magnitude of groundwater flow strongly controls the tide-induced recirculation rate. The hydraulic conductivity of the beach sediment and aquifer depth has also been shown to influence the magnitude of tide-induced seawater recirculation (Li et al. 2008). More recently, Xin et al. (2010) conducted numerical simulations that demonstrated that wave effects combined with tidal fluctuations further enhance the seawater recirculating rates across the aquifer-ocean interface. For the conditions that Xin et al. (2010) simulated, when both waves and tides were considered, they observed that 61% of the total SGD was comprised of recirculated seawater. When tides and waves were simulated separately, it was found that tide-induced recirculation comprised of 40% of the total SGD whereas wave-induced recirculation comprised of 49% of the total SGD. From previous studies it has been demonstrated that near-shore SGD may have an important role in chemical budgets for coastal waters. However, there is limited understanding of the effect of the different mechanisms driving recirculation across the aquifer-ocean interface. It is important to understand the influence of these recirculation processes in altering the fate of chemicals

in the near-shore aquifer and subsequent chemical fluxes to coastal water. Hence, understanding of SGD is crucial as such discharge can alter the species distribution of the marine environment.

#### **2.4 The subterranean estuary and influence of oceanic forcing**

The recirculating seawater component of SGD is important as it transports not only salt but also other chemicals from the ocean into the aquifer. The recirculating seawater mixes with the fresh groundwater and also interacts with sediments in the near-shore aquifer. As the recirculating seawater and fresh groundwater have distinct chemical compositions the mixing of these waters can set up active biogeochemical reaction zones in the near-shore aquifer (Slomp and van Cappellen 2004; Charette and Allen 2006; Robinson et al. 2007b) (Figure 2.2).

The transport and transformation of groundwater-derived chemicals and subsequent chemical loading to the coastal system is strongly influenced by processes occurring in these salt-freshwater mixing and reaction zone (Charette and Sholkovitz 2002; Ullman et al. 2003; Slomp and van Cappellen 2004; Charette and Sholkovitz 2006). The concept of the subterranean estuary was established by Moore (1999) to highlight the importance of the salt-freshwater mixing zones. In analogy to the surface estuary (Pritchard 1967), Moore defined a subterranean estuary as the mixing zone between the land derived groundwater and recirculating seawater in the coastal aquifer. The composition of groundwater in a subterranean estuary is altered due to the biogeochemical reactions between the mixed waters and aquifer sediments in similar way river particles modify the composition of surface estuarine waters (Moore 1999).

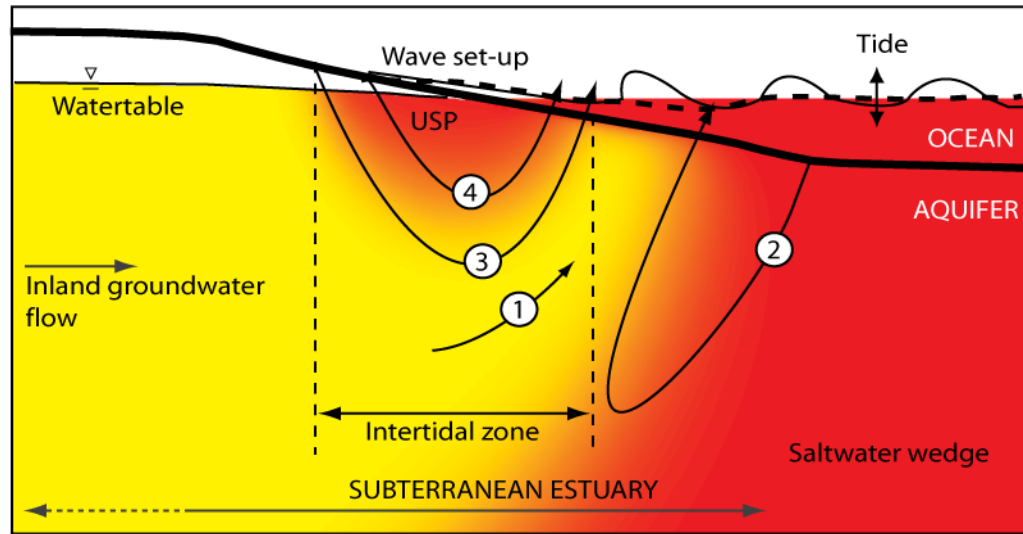


**Figure 2.2:** Conceptual model of the near-shore coastal aquifer with seawater recirculation and salt-freshwater mixing mechanisms: (1) land-derived fresh groundwater ( $Q_f$ ), (2) density-driven convective recirculation ( $Q_d$ ), (3) tide-induced recirculation ( $Q_t$ ), (4) wave-induced recirculation ( $Q_w$ ). The salt distribution is shown with the coloured shading (red-yellow). The aquifer has 3 distinct zones: saltwater wedge, upper saline plume (USP) and the freshwater discharge zone. The wave set-up profile (wave-averaged water level) is denoted by the thick black dotted line (Figure modified from Robinson et al. 2007b).

Land-derived chemical fluxes from a coastal aquifer to the ocean are mostly influenced by (1) landward sources and form of chemicals released; (2) the specific subsurface chemical discharge pathway and flow rate; and (3) the reactions occurring along the discharge pathway that alter the mobility, transformation and removal of chemicals (Slomp and van Cappellen 2004). The distribution of chemicals, including nutrients, in the subterranean estuary and their discharge to coastal waters are strongly controlled by the biogeochemical zonations set up by the mixing zone of fresh groundwater and

recirculating seawater. For example, it has been shown that the mixing of terrestrially-derived anoxic groundwater with oxic seawater can lead to the precipitation of Fe and Mn (hydr)oxides in a coastal aquifer (Charette and Sholkovitz 2002; Charette et al. 2005). The accumulation of these (hydr)oxides in the mixing zone is often referred to as an “iron curtain” as they can act as a geochemical barrier that adsorb other dissolved chemical species such as phosphorous, arsenic, thorium, and barium. The formation of these biogeochemical zonations depends on the flow and mixing of fresh groundwater and recirculating seawater in the near-shore aquifer (Huettel et al. 1998).

The processes that influence the fresh groundwater flow, salt transport and fresh-saltwater mixing in a subterranean estuary are: land-derived fresh groundwater discharge, ( $Q_f$ ), freshwater and seawater density differences ( $Q_d$ ) (Cooper 1959) and oceanic forcing, for example, tides ( $Q_t$ ) and waves ( $Q_w$ ) (Li 1999; Mao et al. 2006; Robinson et al. 2006) (Figure 2.2). The interaction of these processes drives complex and dynamic flow and mixing in the near-shore aquifer. The variation of density between seawater and freshwater and also water level fluctuations by tides create complex flow processes and solute transports in a mildly sloping beach than the vertical beach (Mao et al. 2006).

The density differences between the seawater and fresh groundwater lead to the formation of a saltwater wedge in coastal aquifers (Figure 2.2). Hydrodynamic dispersion at the salt-freshwater interface of the wedge drives convective circulation through the saltwater wedge (Cooper 1959). This density-driven recirculation causes significant water exchange across the aquifer-ocean interface in the near-shore region (Smith 2004; Prieto and Destouni 2005). This salt-freshwater mixing zone of the saltwater wedge was



traditionally viewed as the main area of recirculation and mixing in a subterranean estuary (Moore 1999).

The main oceanic forces acting on coastlines are tides and waves. In the presence of tides, the salinity structure in the near-shore aquifer consists of an upper saline plume in addition to the classical saltwater wedge (Figure 2.2). This has been shown through numerical simulations (Mao et al. 2006; Werner and Lockington 2006; Robinson et al. 2007b; Robinson et al. 2007c) and field observations (Lebbe 1981; Staver and Brinsfield 1996; Robinson et al. 1998; Turner and Acworth 2004; Vandenbohede and Lebbe 2005; Westbrook et al. 2005). The upper saline plume is formed primarily by advective salt transport driven by tide-induced flow circulations through the intertidal zone (Figure 2.2). This flow circulation is caused by seawater infiltration dominating in the upper intertidal zone during high tide and exfiltration occurring near the lower intertidal region during low tide (Mango et al. 2004) (Figure 2.2). Waves also drive a flow circulation through the near-shore region of a coastal aquifer (Longuet-Higgins 1983; Li and Barry 2000). Numerical modeling studies have been conducted to examine wave-induced beach groundwater flow (Li and Barry 2000; Horn 2006; Xin et al. 2010). Xin et al. (2010) presented numerical simulations that showed that wave-induced recirculation also forms an upper saline plume similar to that formed by tides. This upper saline plume extends from the wave run-up zone to the wave set-down zone further offshore. They showed that when both tides and waves act on a sloping beach, the strength of the flow circulation in the aquifer increases further and this subsequently expands the extend of the upper saline plume. A freshwater discharge zone exists as a confined discharge tube in between the upper saline plume and saltwater wedge (Boufadel 2000; Vandenbohede and Lebbe

2005; Mao et al. 2006). The freshwater discharges near the low tide mark with tides present and below the set-down zone with waves present.

The upper saline plume and factors contributing to the formation of this plume are not fully understood but it does represent a potentially important zone of mixing and reaction between fresh groundwater and seawater in a near-shore aquifer in addition to the mixing zone of the saltwater wedge. For example, the upper saline plume has been shown to be associated with faster flow rates and lower transit times for recirculating seawater and so it may be a more dynamic and active zone of mixing than the saltwater wedge (Li et al. 1999; Brovelli et al. 2007; Robinson et al. 2007b; Robinson et al. 2007c). The numerical study of Xin et al. (2010) indicated that, for the conditions simulated, tides led to more intense salt-freshwater mixing around the upper saline plume compared to regular wave forcing. It is important to understand the salt-freshwater mixing processes in a subterranean estuary as it may alter the biogeochemical conditions in the aquifer and thus subsurface species distribution.

## **2.5 SGD of nutrients and nutrient dynamics in a near-shore aquifer**

Several studies have shown that SGD can be a significant source of nutrients to coastal waters particularly in areas where there is a higher concentration of dissolved nutrients in groundwater than in coastal waters (Santos et al. 2008). Previous studies conducted in many different environments, including salt marshes (Charette et al. 2003), coral reefs (Paytan et al. 2006), river-dominated coastal shelves (Burnett et al. 2007) and coastal lagoons (Deborde et al. 2008) have revealed that nutrient inputs from SGD can be comparable and in some cases higher than local surface inputs. In a study conducted in

Great South Bay of New York, it was found that 50% of the land-derived nitrate flux was due to SGD (Capone and Bautista 1985). In Kahana Bay, Hawaii, nitrogen and phosphorous loading via SGD is estimated to be 200-500% higher than the surface water inputs (Garrison et al. 2003).

It has been shown that in some coastal waters N-limited primary production has become P-limited due to the presence of high N:P ratios in discharging groundwater (Slomp and van Cappellen 2004). The typical approach for predicting groundwater derived nutrient loading rates to coastal waters is to multiply the average nutrient concentration in the terrestrial groundwater with the land-derived SGD rate ( $Q_f$ ). This method assumes the conservative transport of nutrients and does not account for important nutrient transformations that may occur in a subterranean estuary. Santos et al. (2009) showed that nutrient production can be significant in a near-shore subterranean estuary and therefore multiplication of fresh groundwater nutrient concentrations with SGD rates is not an accurate method for predicting nutrient fluxes to coastal waters. In the mixing zone of coastal aquifer, groundwater flows, seawater recirculation, aquifer sediment characteristics and biogeochemical reactions determine the transport and transformation of nutrients discharging to coastal waters (Slomp and van Cappellen 2004). Figure 2.3 conceptually illustrates nutrient transformations that may occur in a subterranean estuary where anoxic groundwater and oxic seawater are mixed.

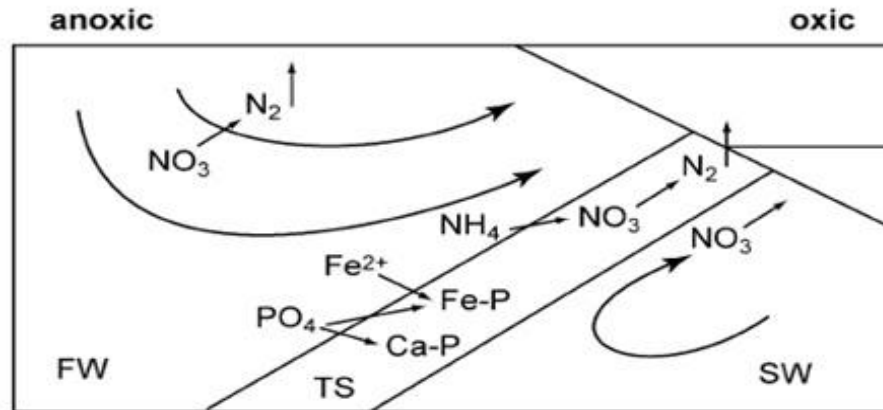


**Figure 2.3:** Schematic diagram of the biogeochemical processes leading to transformation, removal or release of groundwater-derived nutrients and recirculating nutrients in a subterranean estuary where anoxic groundwater mixes with oxic seawater (Figure reproduced from Slomp and van Cappellen 2004).

There are various biogeochemical processes that may transform nutrients in a subterranean estuary (Table 2.1). The major processes are denitrification, nitrification and adsorption of phosphate to iron (hydr)oxides (Charette and Sholkovitz 2002; Charette and Sholkovitz 2006). Denitrification occurs in the absence of oxygen when an electron donor such as organic carbon, ferrous iron or sulphide is present (Postma et al. 1991; Starr and Gillham 1993; Tesoriero et al. 2000). Often the absence of a suitable electron donor or availability of oxygen limits denitrification rates and consequently conservative transport of nitrate occurs through the aquifer (Weiskel and Howes 1992; Wilhelm et al. 1994; DeSimone and Howes 1996). In some coastal aquifers nitrate removal has been observed to occur at freshly precipitated iron (hydr)oxide surfaces by ferrous iron (Kroeger and Charette 2008). Oxidative nitrification or alternatively ammonium oxidation in anoxic groundwater by the reduction of manganese or nitrite (anammox) are the common

ammonium removal processes in aquifers (Kroeger and Charette 2008; Spiteri et al. 2008a) . The general form of reactive phosphorous in groundwater is inorganic dissolved phosphate and this often becomes immobile via sorption to iron hydr(oxides) or co-precipitation with ferrous iron, aluminum or calcium (Weiskel and Howes 1992; Robertson 1995; Zanini et al. 1998). Degradation of dissolved organic matter (DOM) can occur by oxic degradation, denitrification or reduction of iron hydro(oxides) with all these reactions producing ammonium and phosphate (Spiteri et al. 2008a). As tides and waves will likely deliver additional oxygen to near-shore sediments via seawater recirculation it is expected that this enhance nitrification and aerobic respiration of labile DOM from seawater (Ullman et al. 2003).

**Table 2.1:** Major reactions for nutrient transformation in coastal aquifer.

<b>Reaction</b>	<b>Reactants</b>	<b>Products</b>
Denitrification	Nitrate , electron donor (DOM, ferrous iron, sulphide, pyrite)	Nitrite, nitrogen oxide, ammonium, nitrogen gas, phosphate , sulphate, ferrous iron
Nitrification	Ammonium, oxygen	Nitrate
Anammox	Ammonium, nitrite	Nitrogen gas
Oxic degradation	DOM, oxygen	Ammonium, phosphate
Iron (hydr)oxide reduction	Iron (hydr)oxide, DOM	Ammonium, phosphate, ferrous iron
Iron (hydr)oxide precipitation	Ferrous iron, oxygen	Iron-oxides,
Co-precipitation of phosphate	Phosphate, oxygen and ferrous iron, aluminum or calcium	Strengite, varisite, hydroxiapatite
Phosphate adsorption	Phosphate, iron (hydr)oxide	Adsorbed phosphate

Nutrient dynamics in near-shore aquifers have been examined previously but studies have focused primarily on coastal aquifers that are not exposed to oceanic forcing (tides and waves). A field study conducted in West Neck Bay, Long Island, New York demonstrated that DOM acted as conservative species in the near-shore aquifer, whereas nitrate and phosphate were attenuated prior to discharge to coastal waters (Beck et al. 2007). DOM showed conservative behaviour as the change in DOM by decomposition or uptake was not large relative to the delivery of DOM to the aquifer by the recirculating seawater. Phosphate removal occurred by adsorption onto amorphous iron (hydr)oxides. Kroeger and Charette (2008) studied a near-shore subterranean estuary in Waquoit Bay, Massachusetts with low DOM concentrations. They observed significant  $N_2$  production in the near-shore aquifer because of denitrification coupled to oxidation of reduced iron.

In the presence of tides and waves, oxygen and reactants including DOM are delivered to the near-shore aquifer by the recirculating seawater and these chemical species may significantly alter the nutrient dynamics in a near-shore aquifer (Santos et al. 2009). Santos et al. (2009) suggested that oxygen and reactive DOM continuously recirculating into a coastal aquifer on the Gulf of Mexico due to tide-induced recirculation caused significant production of nutrients. Anschutz et al. (2009) also showed that the mineralized products of organic matters delivered to the aquifer via tide-induced recirculation significantly control the nutrient cycling and production in a near-shore aquifer. Therefore, processes occurring in near-shore aquifer subject to tide and/or waves needs to be understood before nutrient fluxes to coastal waters can be accurately predicted.

## **2.6 Numerical modeling of reactive contaminant transport in near-shore aquifers**

Numerical reactive groundwater transport modeling can be used to investigate and quantify the transport and transformation of nutrients in groundwater systems, including coastal aquifers. Numerous studies have used reactive transport models to investigate nutrient transport and fate along the subsurface flow streamlines (Robertson et al. 1991; Harman et al. 1996; Griggs et al. 2003). The various reactions, reaction rates and kinetic parameters are well understood.

Spiteri et al. (2008a) presented a two-dimensional density dependent reactive transport model that conceptually examined the transport and transformation of groundwater-derived nutrients (nitrate, ammonium and phosphate) in a near-shore subterranean estuary discharge to coastal waters. This study did not consider the effects of tides or waves. To evaluate the extent of nutrient removal in the subterranean estuary and subsequent discharge of nitrogen and phosphorous four cases with different redox conditions for the fresh groundwater and seawater were simulated. Their numerical study showed that nutrient discharge via SGD is significantly affected by the biogeochemical reactions occurring in a subterranean estuary and chemical species present in the seawater and fresh groundwater. They identified denitrification and phosphate adsorption as the major processes influencing the fate of nutrients in the subterranean estuary. They more recently applied a modified version of their reactive transport model to simulate observed nutrient concentration in a near-shore subterranean estuary in Waquoit Bay (Spiteri et al. 2008b). At this field site it was found that oxidation of recirculating labile DOM from seawater causes elevated concentrations of ammonium and phosphate in the subterranean estuary. However, they showed that phosphate is strongly adsorbed by iron (hydr)oxides

prior to discharging across the aquifer-ocean interface. This precipitation of iron (hydro)oxides is often significant in subterranean estuaries due to the mixing of oxygen-rich seawater with ferrous iron-rich groundwater (Charette and Sholkovitz 2002).

While Spiteri et al. (2008a, 2008b) quantified the importance of the salt-freshwater mixing in a near-shore aquifer in controlling the fate of nutrients they did not consider the effects of oceanic forcing. As oceanic forcing can significantly enhance the delivery of seawater (and associated chemical constituents) to the near-shore aquifer and also intensify mixing of seawater and fresh groundwater, it is expected that tides and waves may also modify the fate of nutrients transported through a subterranean estuary prior to discharge. While the factors controlling nutrient dynamics in tide- or wave-influenced near-shore aquifers have not been quantified previously, Robinson et al. (2009) did develop a coupled density-dependent flow and multi-species reactive transport model in PHWAT to illustrate the influence of tides on the transport and transformation of BTEX in a near-shore aquifer. This model showed that tide-induced recirculation significantly reduced exit concentrations of the industrial contaminant BTEX (Robinson et al. 2009). Moreover, the BTEX was significantly attenuated in the aquifer by enhanced oxic degradation caused by tide-induced salt-fresh groundwater mixing. For the conditions simulated 79% of the toluene initially released in the aquifer was naturally attenuated prior to discharge to coastal waters with tides present. In comparison, for non-tidal conditions only 1.8% of the toluene was attenuated in the aquifer prior to discharge. In a similar way, it is expected that tide-and wave-induced mixing may also lead to increased transformation of nutrients in a near-shore aquifer. Thus the objective of this study is to



quantify via numerical modeling the effects of oceanic forcing on the fate of nutrients discharging to the coastal water via SGD.

## **2.7 Summary**

This chapter has summarized the relevant background information for this thesis including SGD, the concept of a subterranean estuary, nutrient dynamics in a near-shore aquifer and the importance of oceanic forcing. Previous studies that have examined nutrient dynamics in coastal aquifers and nutrient fluxes to coastal waters via SGD have not accounted the influence of oceanic forcing. Also prior studies that have investigated flow and transport processes in coastal aquifers exposed to oceanic forcing have not quantified the effects on nutrient behaviour. The original contribution of this thesis is that these prior studies are combined to investigate the influence of oceanic forcing on the transport, and fate of nutrients in a near-shore aquifer and subsequent fluxes to the coastal waters. This is achieved through the development of a numerical reactive groundwater transport model.

## **References**

- Andersen, M. S., L. Baron, et al. (2007). "Discharge of nitrate-containing groundwater into a coastal marine environment." Journal of Hydrology 336 (1-2 ): 98-114.
- Anschutz, P., T. Smith, et al. (2009). "Tidal sands as biogeochemical reactors." Estuarine, Coastal Shelf Science 84 84–90.
- Beck, A. J., Y. Tsukamoto, et al. (2007). "Importance of geochemical transformations in determining submarine groundwater discharge-derived trace metal and nutrient fluxes." Applied Geochemistry 22(2): 477-490.
- Boehm, A. B., A. Paytan, et al. (2006). "Composition and flux of groundwater from a California beach aquifer: Implications for nutrient supply to the surf zone." Continental Shelf Research 26(2): 269-282.

- Boufadel, M. C. (2000). "A mechanistic study of nonlinear solute transport in a groundwater-surface water system under steady state and transient hydraulic conditions." Water Resources Research 36(9): 2549-2565.
- Brovelli, A., X. Mao, et al. (2007). "Numerical modeling of tidal influence on density-dependent contaminant transport." Water Resources Research 43(10): 15.
- Burnett, W. C., P. K. Aggarwal, et al. (2006). "Quantifying submarine groundwater discharge in the coastal zone via multiple methods." Science of the Total Environment 367: 498-543.
- Burnett, W. C., H. Bokuniewicz, et al. (2003). "Groundwater inputs to the coastal zone." Biogeochem 66: 3-33.
- Burnett, W. C., M. Taniguchi, et al. (2001). "Measurement and significance of the direct discharge of groundwater into the coastal zone." Journal of Sea Research 46: 109-116.
- Burnett, W. C., G. Wattayakorn, et al. (2007). "Groundwater-derived nutrient inputs to the Upper Gulf of Thailand." Continental Shelf Research 27(2): 176-190.
- Capone, D. G. and M. F. Bautista (1985). "A Groundwater source of nitrate in nearshore marine-sediments." Nature 313: 214-216.
- Capone, D. G. and J. M. Slater (1990). "Interannual patterns of water-table height and groundwater derived nitrate in nearshore sediments." Biogeochemistry 10(3): 277-288.
- Charette, M. A. and M. C. Allen (2006). "Precision ground water sampling in coastal aquifers using a direct-push, shielded-screen well-point system." Ground Water Monitoring and Remediation 26(2): 87-93.
- Charette, M. A. and E. R. Sholkovitz (2002). "Oxidative precipitation of groundwater-derived ferrous iron in the subterranean estuary of a coastal bay." Geophysical Research Letters 29(10): 1444.
- Charette, M. A. and E. R. Sholkovitz (2006). "Trace element cycling in a subterranean estuary: Part 2. Geochemistry of the pore water." Geochem et Cosmochim Acta 70: 811-826.
- Charette, M. A., E. R. Sholkovitz, et al. (2005). "Trace element cycling in a subterranean estuary: Part 1. Geochemistry of the permeable sediments." Geochem et Cosmochim Acta 69(8): 2095-2109.
- Charette, M. A., R. Splivallo, et al. (2003). "Salt marsh submarine groundwater discharge as traced by radium isotopes." Marine Chemistry 84(1-2): 113-121.

- Church, T. (1996). "An underground route for the water cycle." Nature 380: 579-580.
- Conley, D. J. (1999). "Biogeochemical nutrient cycles and nutrient management strategies." Hydrobiologia 410: 87-96.
- Cooper, H. H. (1959). "A hypothesis concerning the dynamic balance of fresh water and salt water in a coastal aquifer." Journal of Geophysical Research 64(4): 461-467.
- Corbett, D. R., J. Chanton, et al. (1999). "Patterns of groundwater discharge into Florida Bay." Limnology and Oceanography 44(4): 1045-1055.
- Crotwell, A. M. and W. S. Moore (2003). "Nutrient and radium fluxes from submarine groundwater discharge to Port Royal Sound, South Carolina." Aquatic Geochemistry 9: 191-208.
- D'Elia, C. F., K. L. Webb, et al. (1981). "Nitrate-rich groundwater inputs to Discovery Bay, Jamaica - a significant source of N to local coral reefs." Bulletin of Marine Science 31(4): 903-910.
- Deborde, J., P. Anschutz, et al. (2008). "Role of tidal pumping on nutrient cycling in a temperate lagoon (Arcachon Bay, France)." Marine Chemistry 109(1-2): 98-114.
- DeSimone, L. A. and B. L. Howes (1996). "Denitrification and Nitrogen Transport in a Coastal Aquifer Receiving Wastewater Discharge." Environmental Science & Technology 30(4): 1152-1162.
- Destouni, G. and C. Prieto (2003). "On the possibility for generic modelling of submarine groundwater discharge." Biogeochemistry 66: 171-186.
- Gallagher, D. L., A. M. Dietrich, et al. (1996). "Ground water discharge of agricultural pesticides and nutrients to estuarine surface water." Ground Water Monitoring and Remediation 16(1): 118-129.
- Garrison, G. H., C. R. Glenn, et al. (2003). "Measurement of submarine groundwater discharge in Kahana Bay, O'ahu, Hawai'i." Limnology and Oceanography 48(2): 920-928.
- Griggs, E. M., L. R. Kump, et al. (2003). "The fate of wastewater-derived nitrate in the subsurface of the Florida Keys: Key Colony Beach, Florida." Estuarine Coastal and Shelf Science 58(3): 517-539.
- Guo, W. and C. D. Langevin (2002). User's Guide to SEAWAT: A computer program for simulation of three-dimensional variable-density ground-water flow. Tallahassee, Florida, US Geological Survey: pp. 77.

- Harman, J., W. D. Robertson, et al. (1996). "Impacts on a sand aquifer from an old septic system: Nitrate and phosphate." Ground Water 34(6): 1105-1114.
- Horn, D. (2006). "Measurements and modelling of beach groundwater flow in the swash-zone: a review." Continental Shelf Research 26: 622-652.
- Howarth, R. W. (1988). "Nutrient limitation of net primary production in marine ecosystems." Annual Review of Ecology and Systematics 19: 89-110.
- Howarth, R. W., G. Billen, et al. (1996). "Regional nitrogen budgets and riverine N&P fluxes for the drainages to the North Atlantic Ocean: Natural and human influences." Biogeochemistry 35(1): 75-139.
- Huettel, M., W. Ziebis, et al. (1996). "Flow-induced uptake of particulate matter in permeable sediments." Limnology and Oceanography 41: 309-322.
- Huettel, M., W. Ziebis, et al. (1998). "Advective transport affecting metal and nutrient distributions and interfacial fluxes in permeable sediments." Geochimica et Cosmochimica Acta 62(4): 613-631.
- Hussain, N., T. M. Church, et al. (1999). "Use of  $^{222}\text{Rn}$  and  $^{226}\text{Ra}$  to trace groundwater discharge into Chesapeake Bay." Marine Chemistry 65: 127-134.
- Iversen, T. M., R. Grant, et al. (1998). "Nitrogen enrichment of European inland and marine waters with special attention to Danish policy measures." Environmental Pollution 102: 771-780.
- Johannes, R. E. (1980). "The ecological significance of the submarine discharge of groundwater." Marine Ecology - Progress Series 3: 365-373.
- Kaleris, V. (2006). "Submarine groundwater discharge: Effects of hydrogeology an of near shore surface water bodies." Journal of Hydrology 325, doi: 10.1016/j.jhydrol.2005.10.008: 96-117.
- Kim, G., K. K. Lee, et al. (2003). "Large submarine groundwater discharge (SGD) from a volcanic island." Geophysical Research Letters 30.
- Kroeger, K. D. and M. A. Charette (2008). "Nitrogen biogeochemistry of submarine groundwater discharge." Limnology and Oceanography 53(3): 1025-1039.
- Krom, M. D. and R. A. Berner (1980). "Adsorption of phosphate in anoxic marine-sediments." Limnology and Oceanography 25(5): 797-806.
- Lapointe, B. E. and J. D. O'Connell (1989). "Nutrient-enhanced growth of *Cladophora* prolifera in Harrington Sound, Bermuda: Eutrophication of a confined,

- phosphorus-limited marine ecosystem." Estuarine, Coastal and Shelf Science 28: 347-360.
- Lebbe, L. C. (1981). The subterranean flow of fresh and salt water underneath the western Belgian beach. In Proceedings of 7th Salt Water Intrusion Meeting, Uppsala, Sweden, Sverigis Geologiska, Rapporten och meddelanden, 27.
- Li, H., M. C. Boufadel, et al. (2008). "Tide-induced seawater-groundwater circulation in shallow beach aquifers." Journal of Hydrology 352(1-2): 211-224.
- Li, L. and D. A. Barry (2000). "Wave-induced beach groundwater flow." Advances in Water Resources 23: 325-337.
- Li, L., D. A. Barry, et al. (1999). "Submarine groundwater discharge and associated chemical input to a coastal sea." Water Resources Research 35(11): 3253-3259.
- Li, L., D. A. Barry, et al. (1999). "Submarine groundwater discharge and associated chemical input to a coastal sea." Water Resources Research 35(11): 3252-3259.
- Longuet-Higgins, M. S. (1983). "Wave set-up, percolation and undertow in the surf zone." Proceedings of the Royal Society of London, Series A 390: 283-291.
- Mango, A. J., M. W. Schmeckle, et al. (2004). "Tidally induced groundwater circulation in an unconfined coastal aquifer modeled with a Hele-Shaw cell." Geology 32(3): 233-236.
- Mao, X., P. Enot, et al. (2006). "Tidal influence on behaviour of a coastal aquifer adjacent to a low-relief estuary." Journal of Hydrology 327: 110-127.
- Mao, X., P. Enot, et al. (2006). "Tidal influence on behaviour of a coastal aquifer adjacent to a low-relief estuary." Journal of Hydrology 327(1-2): 110-127.
- Mao, X., H. Prommer, et al. (2006). "Three-dimensional model for multi-component reactive transport with variable density groundwater flow." Environmental Modelling & Software 21: 615-628.
- McElhenny, T. R., H. C. Bold, et al. (1962). "Algae: a cause of inhalant allergy in children." Annals of Allergy 20: 739-743.
- Michael, H. A., A. E. Mulligan, et al. (2005). "Seasonal oscillations in water exchange between aquifers and the coastal ocean." Nature 436: 1145-1148.
- Moore, W. S. (1996). "Large groundwater inputs to coastal waters revealed by  $^{226}\text{Ra}$  enrichments." Nature 380: 612-614.
- Moore, W. S. (1999). "The subterranean estuary: A reaction zone of ground water and sea water." Marine Chemistry 65: 111-125.

- Moore, W. S. and T. Church (1996). "Submarine groundwater discharge. Reply to Younger." Nature 382: 122.
- Oberdorfer, J. (2003). "Hydrogeologic modeling of submarine groundwater discharge: comparison to other quantitative methods." Biogeochemistry 66: 159-169.
- Paerl, H. W. (1997). "Coastal eutrophication and harmful algal blooms: Importance of atmospheric deposition and groundwater as "new" nitrogen and other nutrient sources." Limnology and Oceanography 42(5): 1154-1165.
- Paytan, A., G. G. Shellenbarger, et al. (2006). "Submarine groundwater discharge: An important source of new inorganic nitrogen to coral reef ecosystems." Limnology and Oceanography 51(1): 343-348.
- Pilotto, L. S., R. M. Douglas, et al. (1997). "Health effects of exposure to cyanobacteria (blue-green algae) due to recreational water-related activities." Australian and New Zealand Journal of Public Health 21(6): 562-566.
- Postma, D., C. Boesen, et al. (1991). "Nitrate reduction in an unconfined sandy aquifer-water chemistry, reduction processes, and geochemical modeling." Water Resources Research 27(8): 2027-2045.
- Prieto, C. and G. Destouni (2005). "Quantifying hydrological and tidal influences on groundwater discharges to coastal waters." Water Resources Research 41: W12427.
- Pritchard, D. W. (1967). What is an estuary: physical viewpoint. Estuaries. G. H. Lauff. Washington DC, American Association of Advanced Science: 37-44.
- Prommer, H. and V. Post (2010). A reactive multicomponent transport model for saturated porous media
- Riedl, R. J., N. Huang, et al. (1972). "The subtidal pump: a mechanism of interstitial water exchange by wave action." Marine Biology 13: 210-221.
- Robertson, W. D. (1995). "Development of steady-state phosphate concentrations in septic system plumes." Journal of Contaminant Hydrology 19(4): 289-305.
- Robertson, W. D., J. A. Cherry, et al. (1991). "Groundwater contamination from 2 small septic systems on sand aquifers." Ground Water 29(1): 82-92.
- Robinson, C., A. Brovelli, et al. (2009). "Tidal influence on BTEX biodegradation in sandy coastal aquifers." Advances in Water Resources 32 16-28.

- Robinson, C., B. Gibbes, et al. (2006). "Driving mechanisms for flow and salt transport in a subterranean estuary." Geophysical Research Letters 33: L03402.
- Robinson, C., L. Li, et al. (2007b). "Effect of tidal forcing on a subterranean estuary." Advances in Water Resources 30: 851-865.
- Robinson, C., L. Li, et al. (2007c). "Tide-induced recirculation across the aquifer-ocean interface." Water Resources Research 43: W07428.
- Robinson, M. A., D. Gallagher, et al. (1998). "Field observations of tidal and seasonal variations in groundwater discharge to tidal estuarine surface water." Ground Water Monitoring and Remediation 18(1): 83-92.
- Santos, I. R., W. C. Burnett, et al. (2009). "Tidal pumping drives nutrient and dissolved organic matter dynamics in a Gulf of Mexico subterranean estuary." Geochimica et Cosmochimica Acta 73(5): 1325-1339.
- Santos, I. R., M. I. Machado, et al. (2008). "Major ion chemistry in a freshwater coastal lagoon from southern Brazil (Mangueira Lagoon): Influence of groundwater inputs." Aquatic Geochemistry 14(2): 133-146.
- Simmons, G. M. (1992). "Importance of submarine groundwater discharge (SGWD) and seawater cycling to material flux across the sediment/water interfaces in marine environments." Marine Ecology Progress Series 84: 173-184.
- Slomp, C. P. and P. van Cappellen (2004). "Nutrient inputs to the coastal ocean through submarine groundwater discharge: controls and potential impact." Journal of Hydrology 295: 64-86.
- Smith, A. J. (2004). "Mixed convection and density-dependent seawater circulation in coastal aquifers." Water Resources Research 40(8): 16.
- Smith, A. J. (2004). "Mixed convection and density-dependent seawater circulation in coastal aquifers." Water Resources Research 40.
- Smith, L. and W. Zawadski (2003). "A hydrogeologic model of submarine groundwater discharge: Florida intercomparison experiment." Biogeochemistry 66: 95-110.
- Spalding, R. F. and M. E. Exner (1993). "Occurrence of nitrate in groundwater-a review." Journal of Environmental Quality 22(3): 392-402.
- Spiteri, C., P. Regnier, et al. (2005). "pH-dependent iron oxide precipitation in a subterranean estuary." Journal of Geochemical Exploration 88: 399-403.

- Spiteri, C., C. P. Slomp, et al. (2008b). "Flow and nutrient dynamics in a subterranean estuary (Waquoit Bay, MA, USA): Field data and reactive transport modeling." Geochimica et Cosmochimica Acta 72(14): 3398-3412.
- Spiteri, C., C. P. Slomp, et al. (2008a). "Modeling biogeochemical processes in subterranean estuaries: Effect of flow dynamics and redox conditions on submarine groundwater discharge of nutrients." Water Resources Research 44(4): W04701.
- Starr, R. C. and R. W. Gillham (1993). "Denitrification and organic-carbon availability in 2 aquifers." Ground Water 31(6): 934-947.
- Staver, K. W. and R. B. Brinsfield (1996). "Seepage of groundwater nitrate from a riparian agroecosystem into the Wye River estuary." Estuaries 19(2B): 359-370.
- Taniguchi, M., W. C. Burnett, et al. (2002). "Investigation of submarine groundwater discharge." Hydrological Processes 16: 2115-2129.
- Taniguchi, M., T. Ishitobi, et al. (2006). "Dynamics of submarine groundwater discharge and fresh-seawater interface." Journal of Geophysical Research 111: C01008.
- Taniguchi, M. and H. Iwakawa (2004). "Submarine groundwater discharge in Osaka Bay." Limnology 5: 25-32.
- Tesoriero, A. J., H. Liebscher, et al. (2000). "Mechanism and rate of denitrification in an agricultural watershed: Electron and mass balance along groundwater flow paths." Water Resources Research 36(6): 1545-1559.
- Turner, I. L. and R. I. Acworth (2004). "Field measurements of beachface salinity structure using cross-borehole resistivity imaging." Journal of Coastal Research 20(3): 753-760.
- Ullman, W. J., B. Chang, et al. (2003). "Groundwater mixing, nutrient diagenesis, and discharges across a sandy beachface, Cape Henlopen, Delaware (USA)." Estuarine, Coastal and Shelf Science 57: 539-552.
- Valiela, I., J. Costa, et al. (1990). "Transport of groundwater-borne nutrients from watersheds and their effects on coastal waters." Biogeochemistry 10: 177-197.
- Valiela, I., K. Foreman, et al. (1992). "Coupling of watersheds and coastal waters: Sources and consequences of nutrient enrichment in Waquoit Bay, Massachusetts." Estuaries 15(4): 443-457.
- Valiela, I., J. M. Teal, et al. (1978). "Nutrient and particulate fluxes in a salt-marsh ecosystem: Tidal exchanges and inputs by precipitation and groundwater." Limnology and Oceanography 23(4): 798-812.



- Vandenbohede, A. and L. Lebbe (2005). "Occurrence of salt water above fresh water in dynamic equilibrium in a coastal groundwater flow system near De Panne, Belgium." Hydrogeology Journal 14(4): 462 - 472.
- Weiskel, P. K. and B. L. Howes (1992). "Differential transport of sewage-derived nitrogen and phosphorus through a coastal watershed." Environ. Sci. Technol. 26: 352-360.
- Werner, A. D. and D. A. Lockington (2006). "Tidal impacts on riparian salinities near estuaries." Journal of Hydrology 328(3-4): 511-522.
- Westbrook, S. J., J. L. Rayner, et al. (2005). "Interaction between shallow groundwater, saline surface water and contaminant discharge at a seasonally and tidally forced estuarine boundary." Journal of Hydrology 302: 255-269.
- Wilhelm, S. R., S. L. Schiff, et al. (1994). "Biogeochemical evolution of domestic wastewater in septic systems. 1. Conceptual-model." Ground Water 32(6): 905-916.
- Xin, P., C. Robinson, et al. (2010). "Effects of wave forcing on a subterranean estuary." Advances in Water Resources 46: W12505.
- Zanini, L., W. D. Robertson, et al. (1998). "Phosphorus characterization in sediments impacted by septic effluent at four sites in central Canada." Journal of Contaminant Hydrology 33: 405-429.

## Chapter 3

---

### **Influence of oceanic forcing on fate of nutrients in a near-shore aquifer**

#### **3.1 Introduction**

Elevated nutrient (nitrate, ammonium, and phosphate) levels in coastal aquifers are increasingly observed due to growing populations and urban and agricultural development along shorelines (Postma et al. 1991; Spalding and Exner 1993; Howarth et al. 1996; Iversen et al. 1998). Nutrients can be attenuated in the aquifer by natural reactive processes, but in many cases nutrient removal does not occur in the aquifer and nutrients discharge with the groundwater to the sea (Valiela et al. 1978; Johannes 1980; Capone and Bautista 1985; Valiela et al. 1992). It is widely established that groundwater discharge can be an important contributor of nutrients to coastal waters (Capone and Bautista 1985; Garrison et al. 2003; Santos et al. 2008).

Understanding the transport and transformation of nutrients in a coastal aquifer is important as nutrient discharge can have severe effects on the coastal ecosystem (Lapointe and O'Connell 1989; Valiela et al. 1990; Valiela et al. 1992). The discharge of groundwater-derived nutrients to coastal waters depends on the landward groundwater sources as well as on the specific subsurface nutrient discharge pathway and the biogeochemical reactions occurring along this pathway (Slomp and van Cappellen 2004; Spiteri et al. 2005; Charette and Sholkovitz 2006). Oceanic forcing (tides and waves) significantly modify the flow and transport of fresh groundwater in a coastal aquifer. These forcings can induce a highly dynamic upper salt-freshwater mixing and reaction zone in a near-shore aquifer (Figure 3.1) and may significantly modify the flow paths for

discharging nutrients (Robinson et al. 2007b; Robinson et al. 2007c; Robinson et al. 2009; Xin et al. 2010).

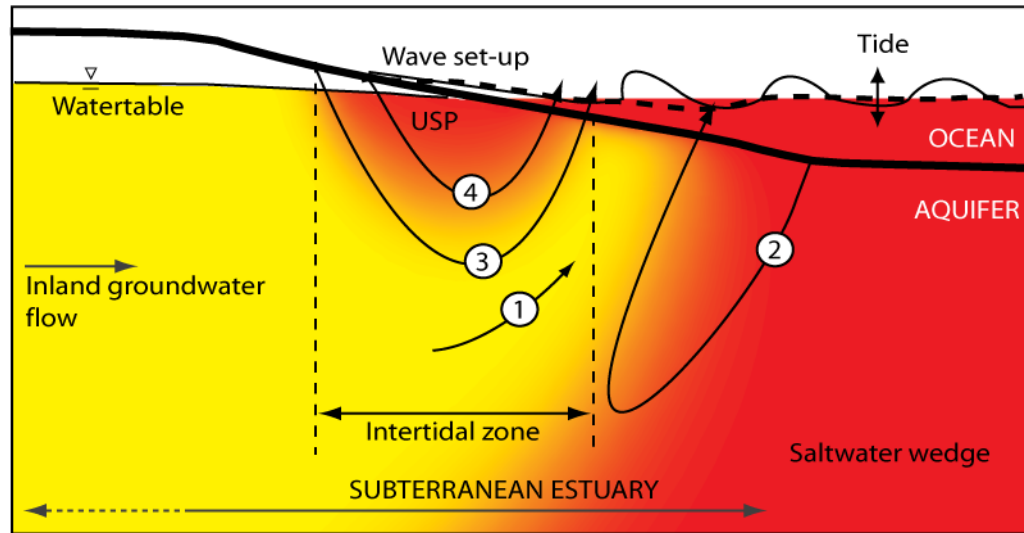


**Figure 3.1:** Conceptual model of a near-shore coastal aquifer showing main water exchange and salt-freshwater mixing mechanisms: (1) terrestrially-derived fresh groundwater ( $Q_f$ ), (2) density-driven convective recirculation ( $Q_d$ ), (3) tide-induced recirculation ( $Q_t$ ), and (4) wave-induced recirculation ( $Q_w$ ). The salinity distribution is shown by the coloured shading (red-yellow). The aquifer has 3 distinct zones: saltwater wedge, upper saline plume (USP) and the freshwater discharge zone. The wave set-up profile (wave-averaged water level) is denoted by the thick black dotted line (Figure modified from Robinson et al. 2007b).

Numerical simulations (Li and Barry 2000; Prieto and Destouni 2005; Mao et al. 2006; Werner and Lockington 2006; Robinson et al. 2007b; Xin et al. 2010) and field observations (Robinson et al. 1998; Horn 2006; Robinson et al. 2006; Robinson et al. 2007a) have been conducted previously to understand the groundwater flow and salt transport processes in a near-shore aquifer exposed to oceanic forcing. It has been

observed in the presence of oceanic forcing two dynamic fresh-saltwater mixing zones exist: i) the saltwater wedge that forms due to the density driven seawater recirculation across the aquifer-ocean interface (Cooper 1959; Destouni and Prieto 2003; Smith 2004) and ii) the upper saline plume that forms due to tide- and wave-induced seawater recirculation (Li 1999; Boufadel 2000; Li et al. 2000; Turner and Acworth 2004; Vandenbohede and Lebbe 2005; Robinson et al. 2006; Robinson et al. 2007b; Robinson et al. 2007c; Xin et al. 2010). The terrestrially-derived fresh groundwater is transported between these two saline plumes and discharges near the low tide mark or wave set-down zone (Figure 3.1) (Boufadel 2000; Robinson et al. 2006). The seawater recirculating across the aquifer-ocean interface mixes with the fresh groundwater, and as these waters have distinct chemical compositions, this mixing sets up an active biogeochemical reaction zone in the near-shore aquifer (Slomp and van Cappellen 2004; Charette and Allen 2006; Robinson et al. 2007b).

The salt-freshwater mixing zone in a coastal aquifer, referred to as a subterranean estuary, (Moore 1999) is important as reactions occurring in this zone may control the fate of groundwater-derived chemical species and also chemical species delivered to the aquifer by the recirculating seawater (Spiteri et al. 2005; Charette and Sholkovitz 2006; Spiteri et al. 2008a; Spiteri et al. 2008b). As a result, processes occurring in a subterranean estuary can significantly alter the chemical loading to coastal waters via SGD (Robinson et al. 2009). The dispersion zone of the saltwater wedge was initially considered the primary area of mixing between fresh groundwater and seawater in a subterranean estuary; however, now it is established that the upper saline plume may be a more active and dynamic zone of mixing as it is associated with lower residence times

and higher flow rates (Robinson et al. 2007b). Tide- or wave-induced seawater recirculations supply ocean-derived chemicals to the mixing zone of the upper saline plume at a high rate. Although the residence time is lower, thus providing less reaction time, this rapid supply will likely create a significant reaction zone in the near-shore aquifer.

Several studies have shown that SGD can be a significant source of nutrients to coastal waters particularly in areas where there is a the higher concentration of dissolved nutrients in groundwater than in surface water (Santos et al. 2008). While the fate of nutrients in near-shore aquifers has been studied previously through field and numerical investigations most studies have focused on systems not exposed to oceanic forcing (i.e., stationary sea water level) (Andersen et al. 2007; Beck et al. 2007; Kroeger and Charette 2008; Spiteri et al. 2008a; Spiteri et al. 2008b). Santos et al. (2009) showed that multiplication of fresh groundwater nutrient concentrations with SGD rates may underestimate the flux of nutrients discharging to the sea as significant nutrient transformations (e.g., nitrate production) can occur in a subterranean estuary.

In a subterranean estuary, groundwater fluxes, seawater recirculation, aquifer sediment characteristics and biogeochemical reactions determine the fate of nutrients discharging to coastal waters (Slomp and van Cappellen 2004). The transport and transformation of groundwater-derived nutrients (nitrate, ammonium, phosphate) in a near-shore aquifer not exposed to oceanic forcing (no tides and no waves) was examined numerically by Spiteri et al. (2008a). They developed a two-dimensional numerical reactive groundwater transport model that conceptually illustrated how nutrient discharge via SGD may be significantly influenced by the biogeochemical reactions occurring in a subterranean

estuary. In simulating an aquifer not subject to oceanic fluctuations, this study revealed the importance of the mixing processes occurring along the interface of the saltwater wedge. Denitrification and phosphate sorption to iron hydr(oxides) were identified as the major processes influencing the fate of nutrients in a subterranean estuary. They later validated and applied a modified version of the reactive transport model to simulate observed nutrient concentration in a subterranean estuary in Waquoit Bay (Spiteri et al. 2008b). At this site it was found that oxidation of recirculating labile dissolved organic matter (DOM) from seawater causes high concentrations of ammonium and phosphate in the near-shore aquifer (Spiteri et al. 2008b). However, they showed numerically that the phosphate produced is rapidly adsorbed by iron hydr(oxides) prior to discharging across the aquifer-ocean interface.

As most coastal shorelines are exposed to tides and/or waves, quantifying the effect of these oceanic forcing on nutrient behaviour in a coastal aquifer is critical to predict their nutrient discharge to coastal waters. For example, tide- and wave-induced seawater circulations through the aquifer deliver chemical species, including oxygen and organic matter, into a near-shore aquifer. These species may react with the groundwater-derived chemical species in the salt-freshwater mixing zones and in doing so significantly alter subsurface biogeochemical conditions and nutrient distributions (Santos et al. 2009).

In this study the variable density groundwater flow model SEAWAT-2005 (Guo and Langevin 2002) is used in combination with the reactive multi-component transport model PHT3D v2.10 (Prommer and Post 2010) to examine the influence of tides and waves on the fate of nutrients (ammonium, nitrate, and phosphate) in a near-shore aquifer. Simulation results are presented for conditions (i) without oceanic forcing, (ii)

with tides, and (iii) with waves to quantitatively compare the nutrient transport and reaction processes in a coastal aquifer and the influence of the oceanic forcing on nutrient discharge rates to coastal waters. The influence of recirculating labile DOM from seawater on nutrient transformations in a near-shore aquifer is also examined.

### 3.2 Numerical Model

A reactive variable-density groundwater transport model was developed to quantify the effect of oceanic forcing on the fate of subsurface nutrients discharging to coastal waters. Simulations were performed by combining SEAWAT-2005 (Guo and Langevin 2002), a variable-density groundwater flow model, with PHT3D v2.10 (Prommer and Post 2010). PHT3D v2.10 incorporates the program MT3DMS v5.3 (Zheng and Wang 1999) for simulation of advective-dispersive multi-species transport with the program PHREEQC v2.17 (Parkhurst and Appelo 1999) which simulates complex geochemical reactions.

#### 3.2.1 Groundwater flow and multi-species transport model

SEAWAT-2005 (Guo and Langevin 2002) was used to simulate two-dimensional variable-density groundwater flow and salt transport in an unconfined shallow coastal aquifer subject to oceanic forcing acting on a sloping beach boundary. The governing equation used by SEAWAT-2005 for density-dependent groundwater flow is:

$$\nabla \cdot \left[ \rho K_f \left( \nabla \cdot h_f + \frac{\rho - \rho_f}{\rho_f} \cdot \nabla z \right) \right] = \rho S_f \frac{\partial h_f}{\partial t} + n_e \frac{\partial \rho}{\partial t} - \rho_s q_s \quad 3.1$$

where  $\rho$  is the fluid density ( $\text{ML}^{-3}$ ),  $K_f$  is the equivalent freshwater hydraulic conductivity ( $\text{LT}^{-1}$ ),  $h_f$  is the equivalent freshwater head (L),  $\rho_f$  is the freshwater density ( $\text{ML}^{-3}$ ),  $z$  is the vertical coordinate in the upward direction (L),  $S_f$  is the equivalent freshwater storage

coefficient ( $L^{-1}$ ),  $t$  is time (T),  $n_e$  is the effective porosity, and  $\rho_s$  ( $ML^{-3}$ ) and  $q_s$  ( $T^{-1}$ ) are the density and flow rate per unit volume of aquifer of a source or sink (Langevin et al. 2003).

The governing equation for multi-species reactive transport used by SEAWAT-2005 for salt transport and in PHT3D v2.10 to transport all other species is:

$$\frac{\partial C^k}{\partial t} = \nabla \cdot (DC^k) - \nabla \cdot (\vec{v}C^k) - \frac{q_s C_s^k}{n_e} + r_k \quad 3.2$$

where,  $C^k$  is the concentration of species  $k$  ( $ML^{-3}$ ),  $D$  is the hydrodynamic dispersion tensor ( $L^2T^{-1}$ ),  $\vec{v}$  is the linear pore water velocity ( $LT^{-1}$ ),  $C_s^k$  is the concentration of species  $k$  from a source or sink ( $ML^{-3}$ ) and  $r_k$  accounts for the reaction of species  $k$  (Prommer and Post 2010). The reactions considered and kinetic expressions adopted are described in Section 3.2.2.

A modified version of the groundwater flow and transport model used by Robinson et al. (2009) to simulate BTEX transport in a tidally-influenced near-shore aquifer was adopted for this study. A brief summary of the model set-up is provided here and a schematic of the model domain is shown in Figure 3.2.



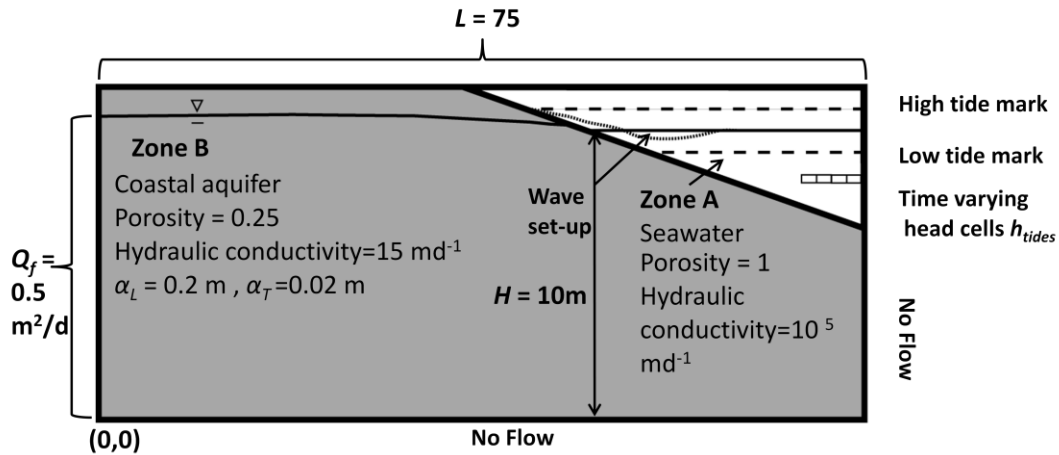


**Figure 3.2:** Model domain and flow boundary conditions.

The model represents a cross-shore transect through a sandy coastal aquifer where oceanic forcing is applied on a mildly sloping beach (slope = 0.1). To simulate the tidal fluctuations the model domain is divided into two zones: a surface water zone (zone A) and an aquifer zone (zone B). A very high hydraulic conductivity of  $10^5 \text{ md}^{-1}$ ,  $n_e = 1$  and a constant salt concentration of  $35 \text{ gL}^{-1}$  is applied in zone A. To simulate a sandy coastal aquifer the hydraulic conductivity is  $15 \text{ md}^{-1}$ , porosity is 0.25, longitudinal dispersivity is 0.2 m ( $\alpha_L$ ) and transverse dispersivity is 0.02 m ( $\alpha_T$ ) in zone B. The model domain is 75 m long and the location of the x-z co-ordinate origin is shown in Figure 3.2. A shallow coastal aquifer system is simulated with an aquifer depth ( $H$ ) of 10 m. The model domain is discretized into 49 layers and 56 columns with greater refinement around the sloping beach interface. The set-up of the groundwater flow model including grid discretization was previously tested by Robinson et al. (2009) to ensure the solution was converged and independent of the grid size.

No flow boundary conditions are applied on the bottom of the aquifer and also at the vertical seaward boundary. To simulate regional groundwater flow, a constant flux of 0.5

$\text{m}^2\text{d}^{-1}$  ( $Q_f$ ) with salt concentration of  $1 \text{ gL}^{-1}$  has been assigned along the vertical landward boundary. The upper boundary is a phreatic surface and recharge to the aquifer is not considered.

To simulate tidal fluctuations a time-varying head ( $h_{tide}$ ) is applied to selected cells in surface water zone (Figure 3.2). This is given as:

$$h_{tide} = A \cos(\omega t) + H \quad 3.3$$

where  $A$  is the tidal amplitude (L) and  $\omega$  is the angular frequency for the tidal fluctuations. For the simulations with tides  $A$  is set to 0.5 m and semi-diurnal tidal period of 0.5 day ( $\omega = 12.567 \text{ rad d}^{-1}$ ) is considered.

To simulate the influence of waves acting on a sloping beach the phase-averaged wave effects described by wave set-up is simulated. The instantaneous pressure fluctuations induced by individual waves are rapidly attenuated in beach sediment due to their high frequency. As a result it is the phase-averaged effect of waves that strongly control the groundwater flow and transport processes in the aquifer (Xin et al. 2010). Therefore simulation of wave set-up acting on the sloping beach interface can be used to adequately and more efficiently simulate the wave effects. For the simulations with wave effects considered, zone A is not included, but rather constant heads are used along the interface to simulate the on-shore pressure gradient of wave set-up. An empirical equation of Nielson (2009) was used to set the head values at each cell along the interface. This empirical equation has been well validated with field data. The mean water level,  $\eta(x)$  (L) is described by:

$$\eta = \frac{H_{rms}}{1 + 10 \frac{D + \eta}{H_{rms}}} \quad 3.4$$

where  $H_{rms}$  (L) is the root mean square wave height, and  $D(x)$  (L) is the still water depth measured from the local beach surface to the still water level ( $z = 10$  m). To examine the effect of waves, simulations were performed with  $H_{rms}$  equal to 1 m and 2 m.

### 3.2.2 Nutrient concentrations and geochemical model

Nine solute species salt, ammonium ( $\text{NH}_4^+$ ), nitrate ( $\text{NO}_3^-$ ), phosphate ( $\text{PO}_4$ ), oxygen ( $\text{O}_2$ ), ferrous iron ( $\text{Fe}^{2+}$ ), dissolved organic matter (DOM), adsorbed phosphate ( $\text{PO}_{4(\text{ads})}$ ), and iron (hydr)oxide ( $\text{Fe}(\text{OH})_3$ ) are considered in the reactive transport model. The reactions and rate expressions included in the model are based on Spiteri et al. (2008a) who examined nutrient dynamics in a sandy near-shore aquifer not exposed to oceanic forcing. The reaction network was validated by a later study by Spiteri et al. (2008b) where they simulated the fate of nutrients in a coastal aquifer in Waquoit Bay and compared the simulation results with field data. The reactions simulated and the kinetic rate expressions and rate constants adopted are shown in Table 3.1 and 3.2 respectively. Spiteri et al. (2008a) took these kinetic parameter values from different literature. These values will likely vary for different field sites. Although the nutrient transformations are sensitive to the pH, the pH is not considered in the kinetic expressions (Table 3.1) and proton exchange was not simulated. The reaction network and model thus focuses on the effect of the redox gradients set-up by the salt-freshwater mixing in the near-shore aquifer rather than the pH effect.

The concentrations of chemical species along the landward boundary and for cells in zone A were set as constant. The concentration values for each species are provided in Table 3.3. These concentrations correspond to the anoxic groundwater and oxic seawater concentrations (Case 3) used by Spiteri et al. (2008a). At the landward boundary nitrate is present in the top 4.5 m of the aquifer and phosphate and ammonium are present in the lower 5.5 m of the aquifer. All other species concentrations (ferrous iron, DOM) are constant over the entire depth at the landward boundary.

The complete reactive transport model was first verified by simulating the model results of Spiteri et al. (2008a). For this verification the model set-up was the same as that for the simulated presented below but with slightly different aquifer properties and flow boundary conditions. The model by Spiteri et al. (2008a) did not consider the effects of tides or waves. A good comparison between the results was observed with the details of the verification provided in Appendix A.

Once verified the model was used to simulate conservative transport and reactive transport for the nutrients in a near-shore aquifer without oceanic forcing, with tides, and with waves. Details of the simulations performed are provided in Table 3.4. The model was first run to steady state for Case 1 (conservative transport without tides and waves). Once steady state was reached, the steady state concentrations were set as the initial concentrations for all the simulation cases. Model simulations were run for 300 days as this time period was required for the nutrient plume to be transported from the landward boundary to the aquifer-ocean interface and for the nutrient distributions in the aquifer to reach a new steady state. Mass balance calculations were performed for each chemical

species for the conservative transport simulations and after 300d the inflow and outflow from the aquifer was equal.

this time period was required for the nutrient plume to be transported from the landward boundary to the aquifer-ocean interface and for the nutrient distributions in the aquifer to reach a new steady state. Once each model simulation was complete, the results were post-processed in MATLAB to extract the concentration distributions and to calculate the exit concentrations, chemical fluxes across the aquifer-ocean interface and total nutrient removal or accumulation in the aquifer. Details of the post-processing are provided in Appendix B.

**Table 3.1:** Reactions and kinetic formulae included (modified from Spiteri et al. 2008(a))

Name	Reaction	Kinetic Formula
Oxic Degradation	$[(\text{CH}_2\text{O})_{106}(\text{NH}_3)_{11}(\text{H}_3\text{PO}_4)] + 106\text{O}_2 \rightarrow$ $97\text{CO}_2 + 9\text{HCO}_3^- + 11\text{NH}_4^+ + \text{HPO}_4^{2-} + 97\text{H}_2\text{O}$	<p>If <math>\text{O}_2 &gt; \text{kmo}_2</math>; <math>\text{Rate} = k_{\text{fox}} [(\text{CH}_2\text{O})_{106}(\text{NH}_3)_{11}(\text{H}_3\text{PO}_4)]</math></p> <p>If <math>\text{O}_2 &lt; \text{kmo}_2</math>; <math>\text{Rate} = k_{\text{fox}} [(\text{CH}_2\text{O})_{106}(\text{NH}_3)_{11}(\text{H}_3\text{PO}_4)] \cdot [\text{O}_2] / [\text{kmo}_2]</math></p>
Denitrification	$[(\text{CH}_2\text{O})_{106}(\text{NH}_3)_{11}(\text{H}_3\text{PO}_4)] + 84.8 \text{NO}_3^- \rightarrow$ $42.4\text{N}_2 + 12.2\text{CO}_2 + 93.8\text{HCO}_3^- + 11\text{NH}_4^+ + \text{HPO}_4^{2-} + 54.6\text{H}_2\text{O}$	<p>If <math>\text{O}_2 &gt; \text{kmo}_2</math>; <math>\text{Rate} = 0</math></p> <p>If <math>\text{O}_2 &lt; \text{kmo}_2</math> and <math>\text{NO}_3^- &gt; \text{kmno}_3</math> ;</p> <p><math>\text{Rate} = k_{\text{fox}} [(\text{CH}_2\text{O})_{106}(\text{NH}_3)_{11}(\text{H}_3\text{PO}_4)] (1 - [\text{O}_2] / [\text{kmo}_2])</math></p> <p>If <math>\text{O}_2 &lt; \text{kmo}_2</math> and <math>\text{NO}_3^- &lt; \text{kmno}_3</math> ;</p> <p><math>\text{Rate} = k_{\text{fox}} [(\text{CH}_2\text{O})_{106}(\text{NH}_3)_{11}(\text{H}_3\text{PO}_4)] (1 - [\text{O}_2] / [\text{kmo}_2]) \cdot [\text{NO}_3^-] / [\text{kmno}_3]</math></p>
Nitrification	$\text{NH}_4^+ + 2\text{O}_2 + 2\text{HCO}_3^- \rightarrow \text{NO}_3^- + 2\text{CO}_2 + 3\text{H}_2\text{O}$	$\text{Rate} = k_{\text{nitr}} [\text{NH}_4^+] [\text{O}_2]$
Fe <sup>2+</sup> oxidation	$\text{Fe}^{2+} + 0.25\text{O}_2 + 2\text{HCO}_3^- + 0.5\text{H}_2\text{O} \rightarrow \text{Fe}(\text{OH})_3 + 2\text{CO}_2$	$\text{Rate} = k_{\text{feox}} [\text{Fe}^{2+}] [\text{O}_2]$
PO <sub>4</sub> adsorption	$K_d * n_e / (1 - n_e) = [\text{PO}_{4(\text{ads})}] / [\text{PO}_4]$	$K_d = K * \text{Fe}(\text{OH})_3$

**Table 3.2:** Reaction parameter values

Parameter	Units	Description	Value
$k_{\text{fox1}}$	$\text{s}^{-1}$	Rate constant for decomposition of DOM	$3.0 \times 10^{-11\text{a}}$
$k_{\text{fox2}}$	$\text{s}^{-1}$	Rate constant for decomposition of DOM	$3.0 \times 10^{-7\text{b}}$
$k_{\text{nitri}}$	$\text{mM}^{-1} \text{s}^{-1}$	Rate constant for nitrification	$4.8 \times 10^{-4\text{c}}$
$k_{\text{foxe}}$	$\text{mM}^{-1} \text{s}^{-1}$	Rate constant for $\text{Fe}^{2+}$ reoxidation	$6.4 \times 10^{-2\text{c}}$
$k_{\text{mo2}}$	$\text{mM}$	Limiting concentration of $\text{O}_2$	$0.008^{\text{c}}$
$k_{\text{mno3}}$	$\text{mM}$	Limiting concentration of $\text{NO}_3^-$	$0.001^{\text{c}}$
$k_{\text{mfe}}$	$\text{mM}$	Limiting concentration of $\text{Fe}(\text{OH})_3$	$18.95^{\text{c}}$
$K$	$\text{dm}^3 \text{mmol}^{-1}$	Adsorption coefficient for $\text{PO}_4$	$1545^{\text{d}}$

<sup>a</sup> (Tromp et al. 1995), <sup>b</sup> (Hunter et al. 1998), <sup>c</sup> (Van Cappellen and Wang 1995), <sup>d</sup> (Krom and Berner 1980)

**Table 3.3:** Concentration of species in fresh groundwater (landward boundary) and seawater (cells in zone A and along aquifer ocean interface)<sup>a</sup>

Species <sup>b</sup>	Concentration in Anoxic Groundwater	Concentration in Oxidic Seawater
NO <sub>3</sub> <sup>-</sup>	0.25 (1) <sup>c</sup>	0.02 (2)
NH <sub>4</sub> <sup>+</sup>	0.2 (3) <sup>c</sup>	— <sup>a</sup>
O <sub>2</sub>	0.0	0.2(2)
DOM	0.75 (3)	— <sup>a</sup>
Fe <sup>2+</sup>	0.1 (4)	— <sup>a</sup>
PO <sub>4</sub>	0.05 (1) <sup>c</sup>	0.001 (2)
Fe(OH) <sub>3</sub> (s)	— <sup>a</sup>	— <sup>a</sup>
PO <sub>4(ads)</sub>	— <sup>a</sup>	— <sup>a</sup>

<sup>a</sup> In the table, Sources within parentheses are as follows: 1. (Slomp and van Cappellen 2004); 2. (Berner and Berner 1996); 3. (Nyvang 2003); 4. (Charette et al. 2005) ‘—’ indicates low concentrations, assumed to be 0.

<sup>b</sup> Units for concentration of species are mM. It is considered that there is no Fe(OH)<sub>3</sub> and PO<sub>4(ads)</sub> in the aquifer initially.

<sup>c</sup> NO<sub>3</sub><sup>-</sup> and PO<sub>4</sub> occur at lower depth ( $z < 4.5$  m) and NH<sub>4</sub><sup>+</sup> occurs at higher depth ( $4.5 \text{ m} < z < 10 \text{ m}$ ).



**Table 3.4:** Summary of simulations conducted to quantify the effect of oceanic forcing

Case	Reactive transport	Tides	Waves	Labile DOM
1	No	No	No	No
2	Yes	No	No	No
3	No	$A=0.5$ m	No	No
4	Yes	$A=0.5$ m	No	No
5	No	No	$H_{rms} = 1$ m	No
6	Yes	No	$H_{rms} = 1$ m	No
7	No	No	$H_{rms} = 2$ m	No
8	Yes	No	$H_{rms} = 2$ m	No
9	Yes	No	No	Yes
10	Yes	No	$H_{rms} = 1$ m	Yes
11	Yes	No	$H_{rms} = 2$ m	Yes

### 3.3 Results and Discussion

#### 3.3.1 Effect of tides

##### 3.3.1.1 Salinity and oxygen distribution

The salt and oxygen distributions in the near-shore aquifer for the reactive transport simulations without oceanic forcing (Case 2) and with tides (Case 4) are shown in Figure 3.3. Salt is conservative in the aquifer and so the salt distribution is the same regardless of whether reactions are considered in the model. The model was first run to steady state for Case 1 and once steady state was reached, the steady state concentrations were set as the initial concentrations for all the simulation cases. As expected, in the absence of tides, a saltwater water wedge is formed due to density driven recirculation (Figure 3.3a). With

tides present, tide-induced seawater recirculation through the intertidal region leads to the formation of an upper saline plume in addition to the saltwater wedge (Figure 3.3b). The recirculating seawater transports both salt and oxygen into the aquifer. As such, for the cases without reactions considered (Cases 1 and 3) the oxygen distribution in the aquifer corresponds to the salt distribution but with different concentration values. With reactions considered, the oxygen delivered to the aquifer via the recirculating seawater is consumed by the reduced species present in the aquifer. For the reactive transport case without oceanic forcing (Case 2), the oxygen is consumed along the salt-freshwater mixing zone of the saltwater wedge as it reacts with the landward-derived DOM, ferrous iron and ammonium (Figure 3.3c). For the reactive transport tidal case (Case 4) oxygen is also consumed in the aquifer as the tide-induced recirculating seawater mixes with the ammonium, and ferrous iron in the fresh groundwater (Figure 3.3d). Despite this consumption of oxygen in the upper saline plume there is a higher availability of oxygen in the aquifer close to the aquifer-ocean interface when the tide is present.

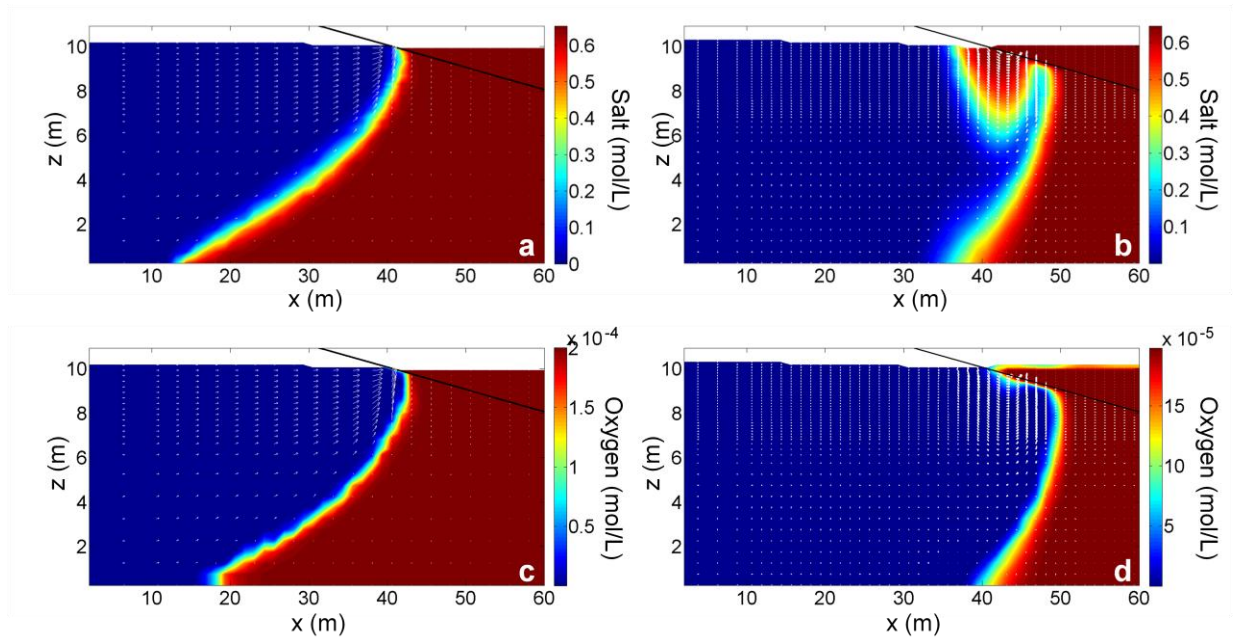


**Figure 3.3:** Simulated salt distributions in the near-shore aquifer for simulations (a) without oceanic forcing (Cases 1 and 2) and (b) with tides (Cases 3 and 4), and oxygen distributions for reactive transport simulations (c) without oceanic forcing (Case 2) and (d) with tides (Case 4) after 300 days.

### 3.3.1.2 Transport and fate of nitrate and ammonium

The nitrate and ammonium distributions in the aquifer after 300 days for the conservative and reactive transport simulations without oceanic forcing and with tides are shown in Figures 3.4 and 3.5. It can be seen that the land-derived nitrate is attenuated (Figure 3.4c) and ammonium is produced (Figure 3.5c) in the upper aquifer when there is no oceanic forcing (Case 2). This is because denitrification is occurring in this region of the aquifer due to the availability of nitrate and DOM and absence of oxygen in the anoxic groundwater. It can also be seen that nitrate increases and ammonium decreases along the mixing zone of the saltwater wedge for Case 2 (Figure 3.4c). This is caused by

nitrification of the land-derived ammonium as it mixes and reacts with the oxygen delivered by recirculating oxic seawater.

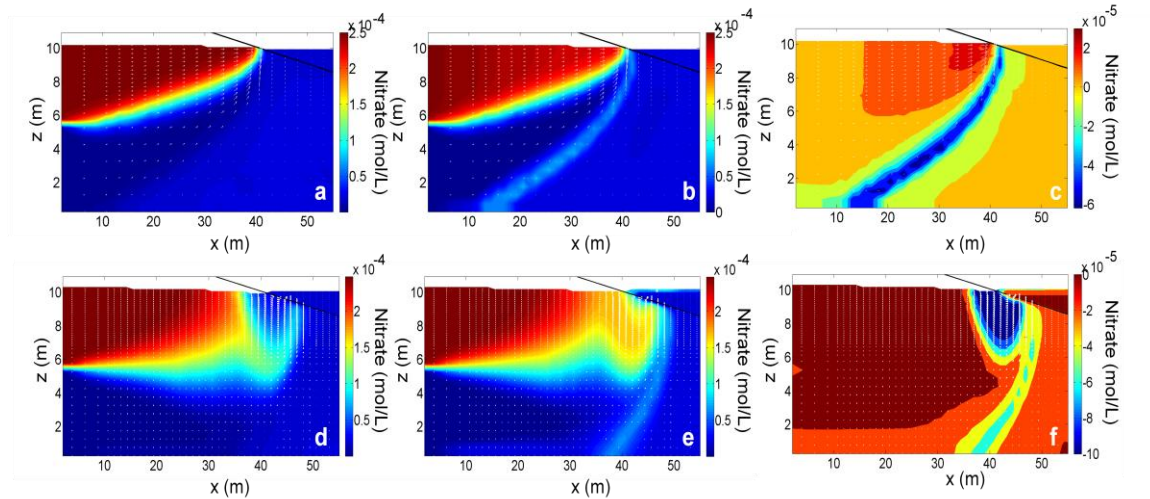


**Figure 3.4:** Concentration profiles of nitrate after 300 days for simulations with (a) conservative transport without oceanic forcing (Case 1), (b) reactive transport without oceanic forcing (Case 2), (c) change in concentration due to reaction between Cases 1 and 2 (positive change corresponds to a decrease in concentration) (d) conservative transport with tides (Case 3), and (e) reactive transport with tides (Case 4) (f) change in concentration due to reaction between Cases 3 and 4 (positive change corresponds to a decrease in concentration).

From the cases with only conservative transport considered (Cases 1 and 3), it is evident that the distribution of species in the near-shore aquifer is significantly altered by tides with modified flow pathways including the increased recirculation of oxic seawater through the aquifer (Figures 3.4d and 3.5d). Tidal fluctuations cause fresh groundwater to migrate downwards around the tide-induced flow recirculations (and upper saline plume) where it discharges near the low tide mark rather than directly at the shoreline as occurs

in the absence of tides. Discharge of the groundwater-derived species occurs in a narrow zone between the upper saline plume and the saltwater wedge. For the conservative transport simulations the low nitrate and ammonium concentrations in the intertidal region are due to the presence of the tide-induced recirculating seawater with low nitrate and ammonium concentrations and its mixing with the nitrate- and ammonium-rich fresh groundwater (Figures 3.4d and 3.5d).

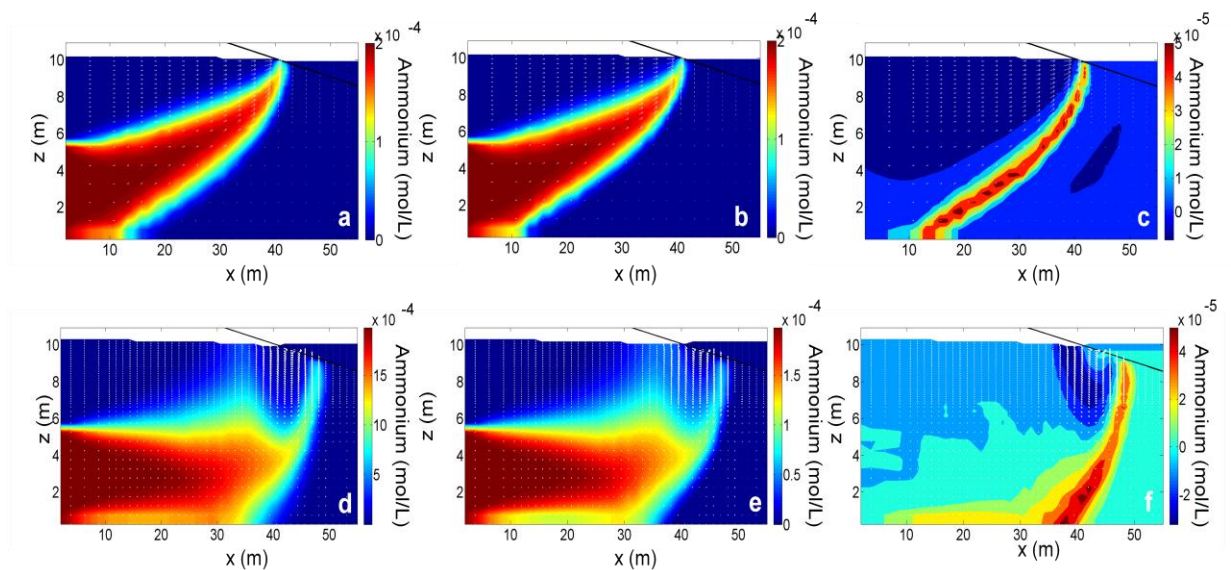


**Figure 3.5:** Concentration profiles of ammonium after 300 days for simulations with (a) conservative transport without oceanic forcing (Case 1), (b) reactive transport without oceanic forcing (Case 2), (c) change in concentration due to reaction between Cases 1 and 2 (positive change corresponds to a decrease in concentration) (d) conservative transport with tides (Case 3), and (e) reactive transport with tides (Case 4) (f) change in concentration due to reaction between Cases 3 and 4 (positive change corresponds to a decrease in concentration).

By comparing the conservative and reactive transport simulations with tides present (Figures 3.4e and 3.5e) it can be seen that there is significant production of nitrate and

ammonium in the upper mixing zone. With tide-induced recirculating seawater delivering more oxygen to the intertidal sediments, ammonium is nitrified and produces nitrate. Despite nitrification occurring, the ammonium concentration increases in the upper mixing zone as ammonium is also produced as the increased availability of oxygen also leads to the oxic degradation of land-derived DOM in this zone (Figures 3.4f and 3.5f).

The concentrations of nitrate and ammonium along the aquifer-ocean interface for the cases without oceanic forcing and with tides are shown in Figures 3.6a, and 3.6b respectively. For the simulations with conservative transport only (Cases 1, 3) the tide-induced seawater recirculation leads to a decrease in the nitrate and ammonium concentrations along the interface due to dilution effects. However with reactions considered, tides lead to an increase in the nitrate concentrations along the interface. This is due to the increased oxygen availability in the upper mixing zone inhibiting denitrification and enhancing nitrification. For the reactive transport simulation without oceanic forcing (Case 2) (Figure 3.6a), the concentration of nitrate along the interface decreases in the upper aquifer ( $x = 37 - 47$  m) and increases near the saltwater wedge interface ( $x = 47 - 50$  m). This is because, unlike the tidal case, there is no oxygen available in the upper aquifer to inhibit denitrification in this region. For tidal reactive transport (Case 4), the exit concentration of nitrate increases along the interface ( $x = 35 - 52$  m) (Figure 3.6a). The density-driven recirculation causes groundwater-derived ammonium to mix with the recirculating oxygen from seawater in the mixing zone of the saltwater wedge and so nitrification increases the nitrate concentration and decreases the ammonium concentration near the saltwater wedge interface. For both the tidal and non tidal reactive transport cases (Cases 4 and 2), the exit concentration of ammonium

decreases near the shoreline ( $x = 47 - 50$  m) due to nitrification (Figure 3.6b). However, in the upper aquifer ( $x = 37 - 47$  m), an increase in ammonium concentration for the tidal reactive case is observed due to the oxic degradation of land-derived DOM which subsequently leads to nitrate formation via nitrification (Figure 3.6b).

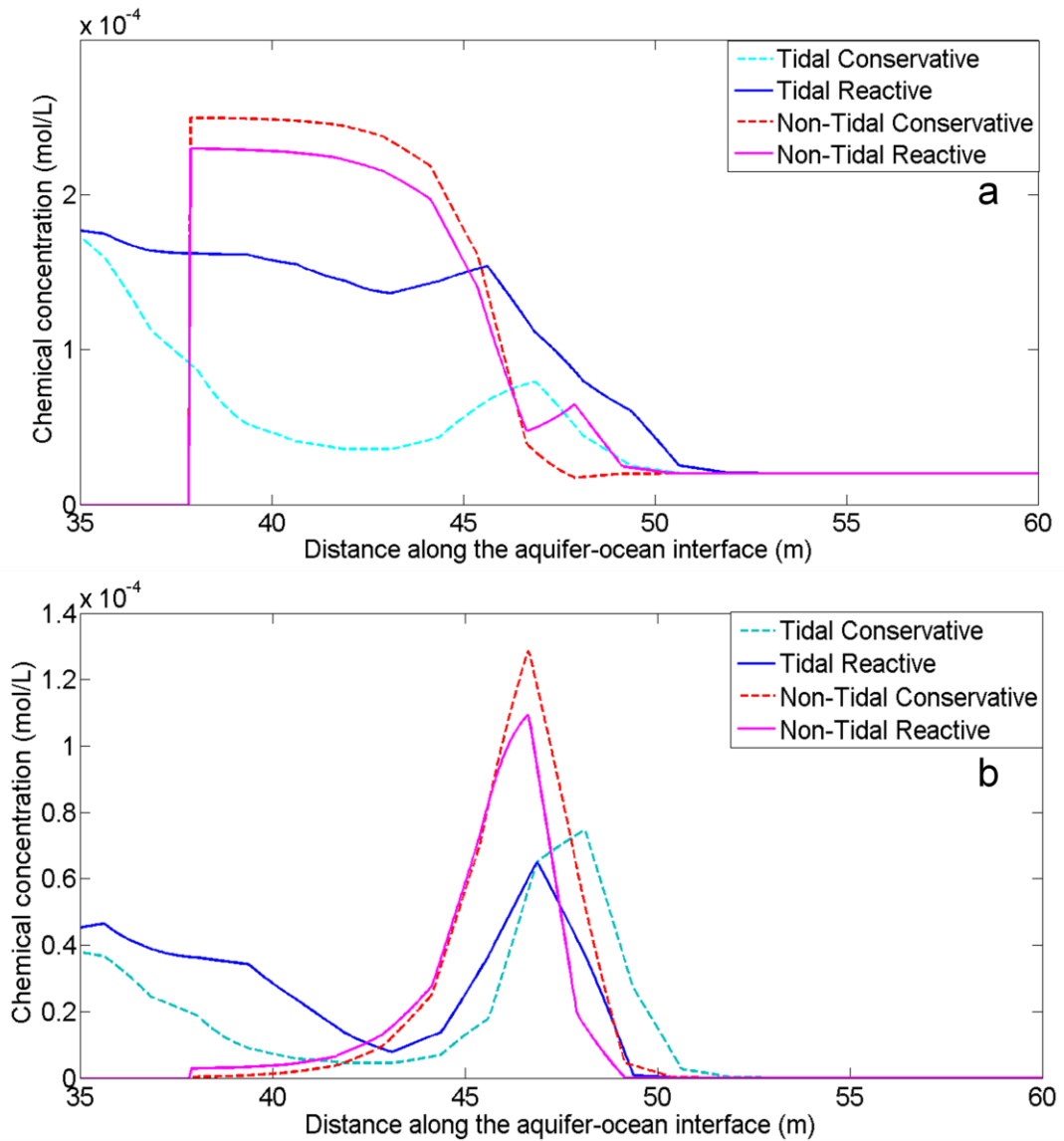


**Figure 3.6:** Exit concentration of (a) nitrate and (b) ammonium along the aquifer-ocean interface after 300 days for Cases 1-4.

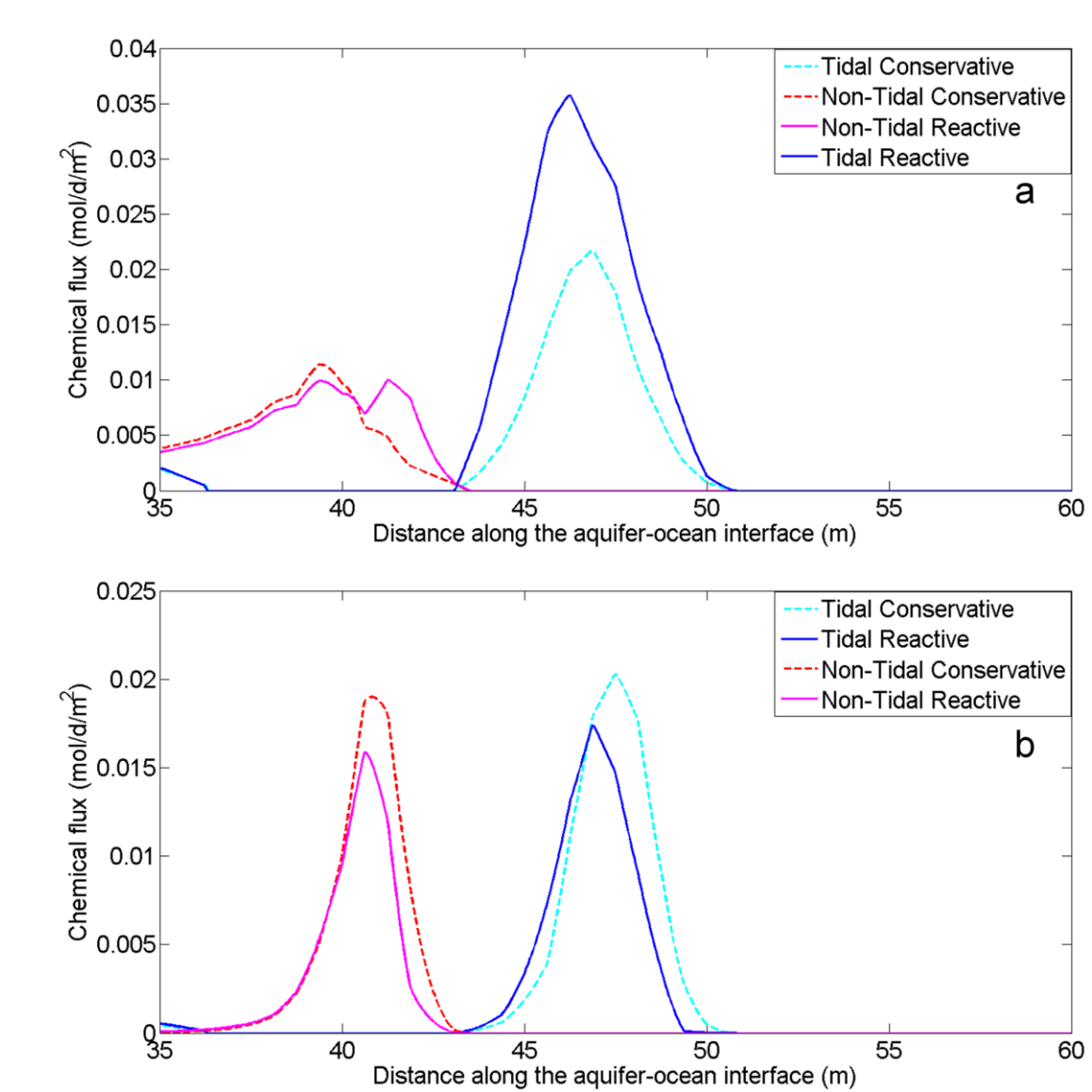
Figure 3.7 shows the fluxes of nitrate and ammonium discharging across the aquifer-ocean interface. The discharge zone for both nitrate and ammonium is moved seaward by tides as the fresh groundwater discharges near the low tide mark rather than at the mean shoreline as occurs for simulation with no oceanic forcing. The nitrate flux is highest for the case with tides and with reactions considered due to the enhanced nitrification in the aquifer. Although the nitrate concentrations along the interface are lower for the tidal case (Cases 3,4) compared with the no oceanic forcing case (Cases 1,2) (Figure 3.6a), high tide-induced recirculation across the aquifer-ocean interface results in a higher nitrate discharge flux compared to the cases with no oceanic forcing (Figure 3.7a). It can be seen that the discharge flux of ammonium decreases for both the no oceanic forcing and tidal cases as it is removed by nitrification.

Table 3.5 summarizes the percentage removal or production of nutrient species in the near-shore aquifer for the simulations conducted. This is calculated by:

$$\text{Percentage removal} = \left( \frac{\text{Inflow rate of species } \mathbf{k} - \text{Outflow rate of species } \mathbf{k}}{\text{Inflow rate of species } \mathbf{k}} \right) \times 100$$

With reactions considered, 23.6% of ammonium entering the aquifer is attenuated for the no oceanic forcing case (Case 2) compared to 39.3% with tides present (Case 4). This indicates that, for the conditions simulated the tide-induced recirculation enhances the removal of ammonium in the near-shore aquifer. There is however a significant increase in the net discharge of nitrate due to tidal fluctuations. The net discharge of nitrate increases by 108% with tides (Case 4) compared to only a 3.5% net discharge increase for the simulation with no oceanic forcing (Case 2).





**Figure 3.7:** Discharge of chemical fluxes of (a) nitrate and (b) ammonium along the aquifer-ocean interface for Cases 1-4 after 300 days.

**Table 3.5:** Production and consumption of species in the near-shore aquifer for simulated cases 1-8 (without the presence of labile DOM).

Species	$\text{NO}_3^-$	$\text{NH}_4^+$	$\text{PO}_4$	$\text{Fe}(\text{OH})_3$ (s)	$\text{PO}_4$ (ads)
Case 2 <b>No forcing</b>	3.5% increase	23.6% decrease	96.5% decrease	3.83 moles precipitation	0.96 moles adsorption
Case 4 <b><math>A = 0.5 \text{ m}</math></b>	108% increase	39.3% decrease	100% decrease	4.5 moles precipitation	1.3 moles adsorption
Case 6 <b><math>H_{rms} = 1 \text{ m}</math></b>	9.4% increase	29.3% decrease	100% decrease	3.6 moles precipitation	1.12 moles adsorption
Case 8 <b><math>H_{rms} = 2 \text{ m}</math></b>	15% increase	41.7% decrease	100% decrease	3.3 moles precipitation	1.1 moles adsorption

### 3.3.1.3 Transport and fate of phosphate and iron

The distributions of phosphate and ferrous iron in the near-shore aquifer for the no oceanic forcing and tidal cases after 300 days are presented in Figures 3.8 and Figure 3.9. As was shown previously for the transport of ammonium and nitrate, the tide significantly alters the flow pathways for dissolved phosphate and ferrous iron and reactions occurring along these pathways. For the conservative transport simulation of no oceanic forcing (Case 1) phosphate is transported along the bottom of the aquifer and discharges near the shoreline (Figure 3.8a). The transport pathway is the same for the simulation with reactive transport considered, but phosphate is attenuated near the aquifer-ocean interface prior to its discharge to coastal waters (Figure 3.8b). For the case with no oceanic forcing (Case 2, Figure 3.9b), the groundwater-derived ferrous iron is

oxidized by the oxygen-rich recirculating seawater along the interface of the saltwater wedge and  $\text{Fe}(\text{OH})_3$  precipitates. The dissolved phosphate adsorbs to  $\text{Fe}(\text{OH})_3$  and it is predicted that 96.7% is removed in the aquifer prior to its discharge to the sea.

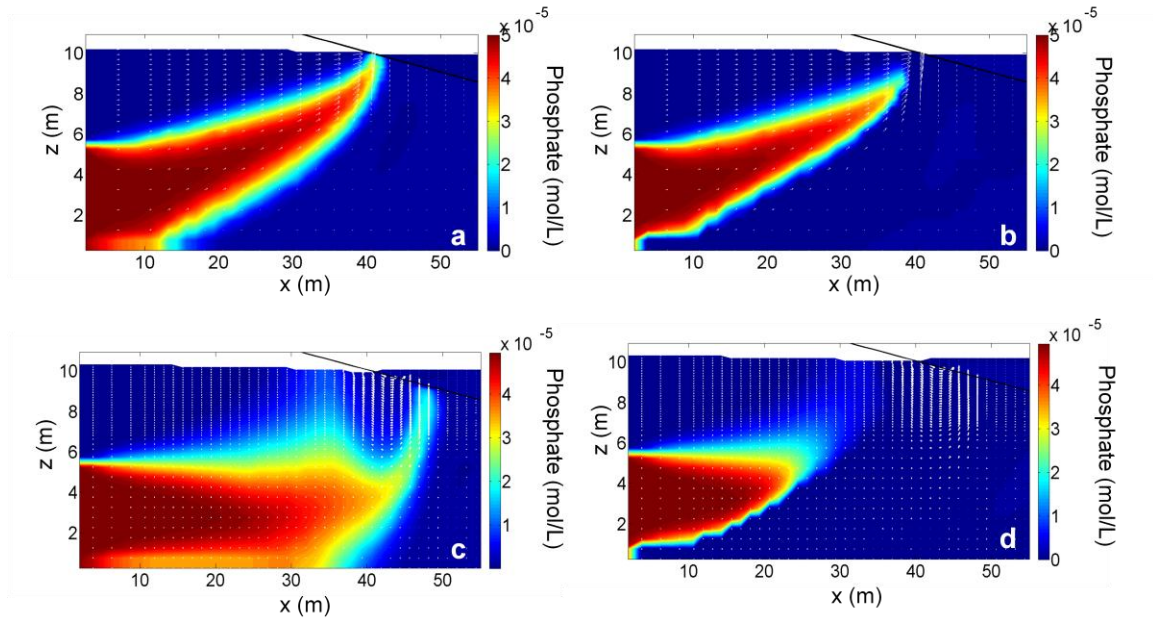


**Figure 3.8:** Concentration profiles of dissolved phosphate after 300 days for simulations with (a) conservative transport without oceanic forcing (Case 1), (b) reactive transport without oceanic forcing (Case 2), (c) conservative transport with tides (Case 3), and (d) reactive transport with tides (Case 4).

The tide-induced recirculation leads to a greater availability of oxygen in the near-shore aquifer leading to greater precipitation of  $\text{Fe}(\text{OH})_3$ . Over the 300 days simulation period 4.5 moles of  $\text{Fe}(\text{OH})_3$  precipitates in the subsurface for tidal reactive transport case (Case 4). This is greater than that for the reactive case with no oceanic forcing (Case 2) where 3.83 moles of  $\text{Fe}(\text{OH})_3$  precipitate in aquifer (Table 3.5). Subsequently all the land-derived phosphate is adsorbed in the near-shore aquifer with negligible discharge to

coastal waters with tides present (1.3 moles adsorbed for tidal case compared with 0.96 moles for the no oceanic forcing case).

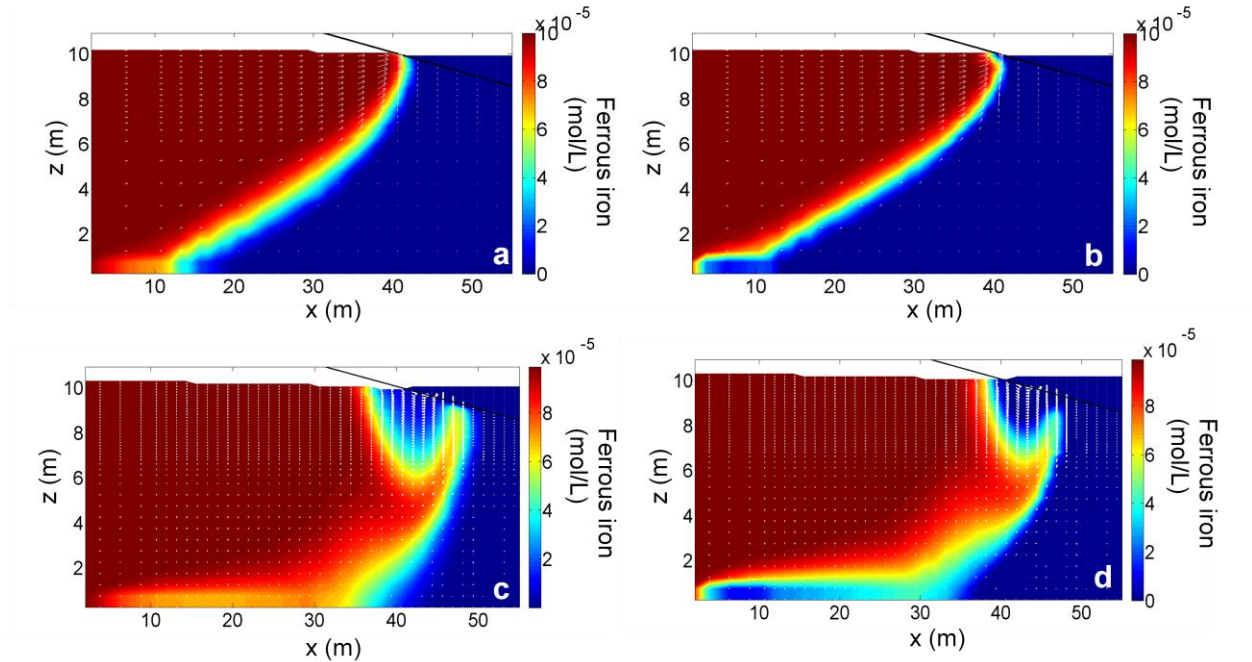


**Figure 3.9:** Concentration profiles of dissolved ferrous iron after 300 days for simulations with (a) conservative transport without oceanic forcing (Case 1), (b) reactive transport without oceanic forcing (Case 2), (c) conservative transport with tides (Case 3), and (d) reactive transport with tides (Case 4).

Figures 3.10a and 3.10b show that for the simulations with conservative transport the concentrations of phosphate and ferrous iron along the aquifer-ocean interface are decreased by tides due to the dilution of the phosphate- and iron-rich groundwater plume with the recirculating seawater. For the non-tidal case with reactions considered (Case 2), only 3.3% of the phosphate entering through the landward boundary is predicted to discharge to the sea (Figure 3.8b, 3.10a). However, with tides considered the dissolved phosphate plume is completely (100%) attenuated in the aquifer due to the higher

$\text{Fe}(\text{OH})_3$  precipitation and there is negligible phosphate discharge to the sea (Figures 3.8e and 3.10a). The adsorption rate for phosphate is high and hence in all cases (no oceanic

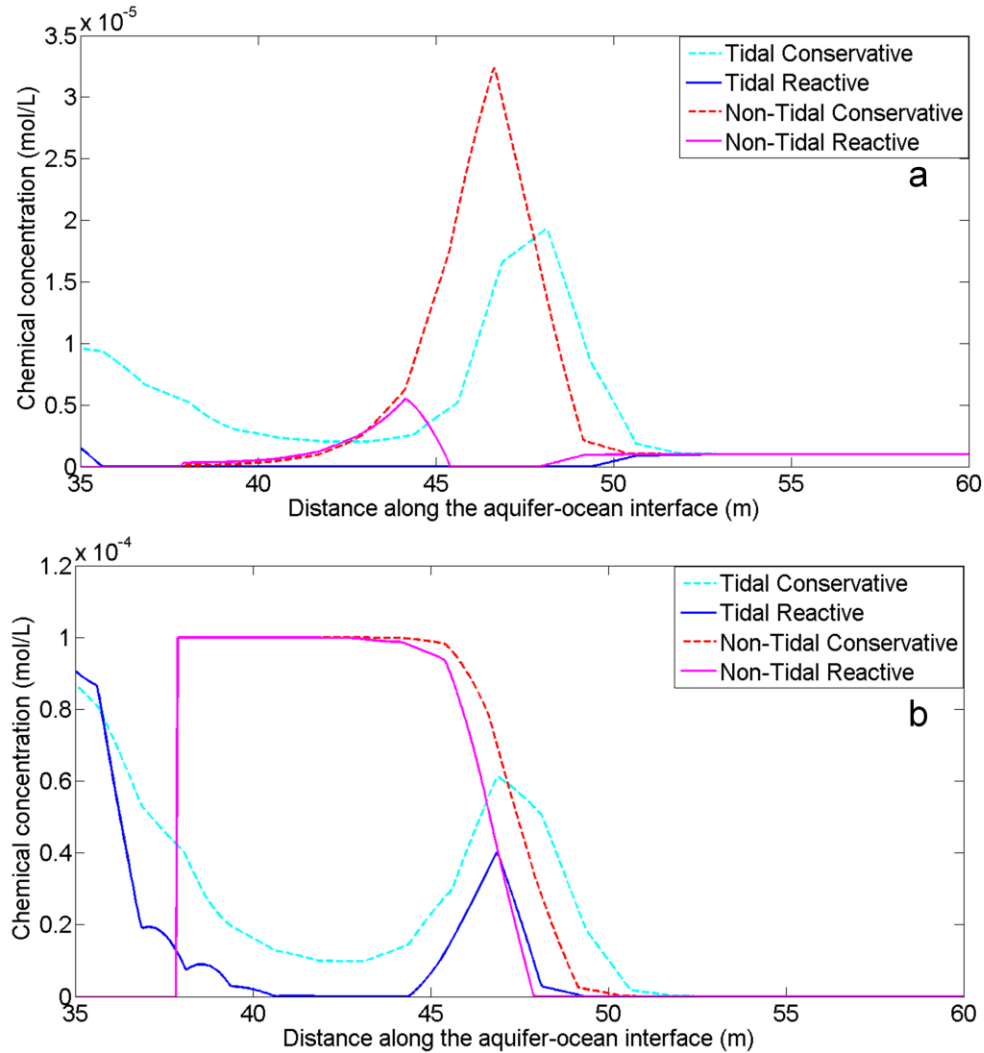


**Figure 3.10:** Concentrations of (a) dissolved phosphate and (b) ferrous iron along the aquifer-ocean interface for Cases 1-4 after 300 days.

forcing, and tidal fluctuation) more than 96% phosphate gets attenuated. This is because of the high sorption coefficient adopted which is consistent with the field data and simulations presented by Spiteri et al. (2008b). For the conservative and reactive transport simulations, the discharge occurs near the low tide mark ( $x = 37 - 43$  m) when

tides are present and near the shoreline ( $x = 43 - 50$  m) for the no oceanic forcing case. Although the exit concentrations of ferrous iron are higher for the no oceanic forcing case (Figure 3.10b), the ferrous iron flux is higher for the tidal case (Figure 3.11b). The higher chemical flux is due to the higher velocities across the aquifer-ocean interface for the tidal case.

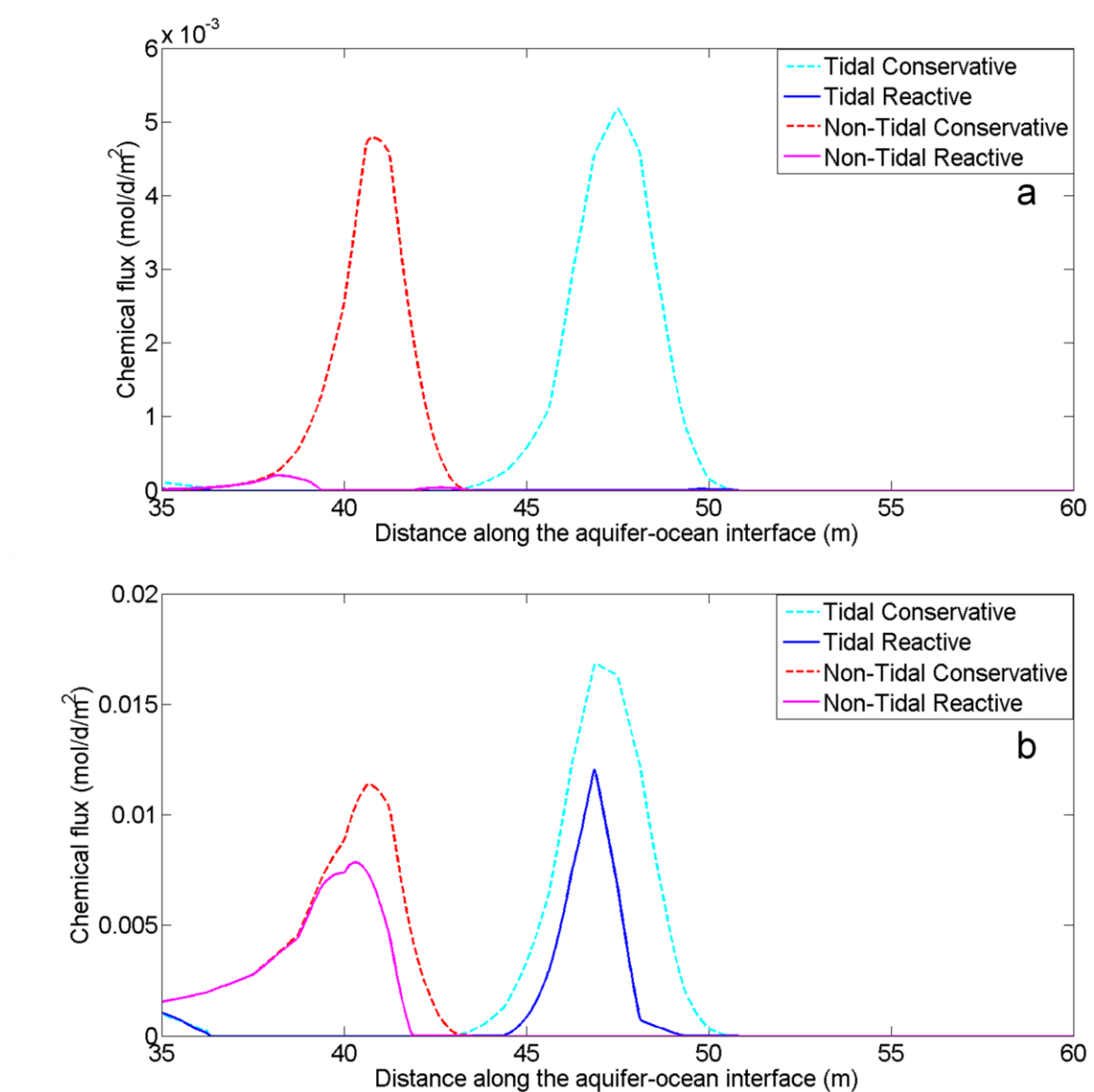


**Figure 3.11:** Discharge fluxes of (a) dissolved phosphate and (b) ferrous iron along the aquifer-ocean interface for Cases 1-4 after 300 days.

### 3.3.2 Effect of waves

#### 3.3.2.1 Salinity and oxygen distribution

Similar to tides, wave set-up generates a seawater recirculation cell in the near-shore aquifer and this leads to the formation of an upper saline plume (Figures 3.12a, 3.12b). Two wave heights (1 m, 2 m) were simulated and as expected the wave-induced seawater recirculation cell is stronger and thus the upper saline plume is larger for the simulation with higher  $H_{rms}$  (2 m). The larger upper saline plume in turn limits the landward intrusion of the saltwater wedge. For both wave cases ( $H_{rms} = 1$  m and 2 m) the saltwater wedge does not intrude as far inland as for the cases with no oceanic forcing and with tides (Figures 3.3a, b).

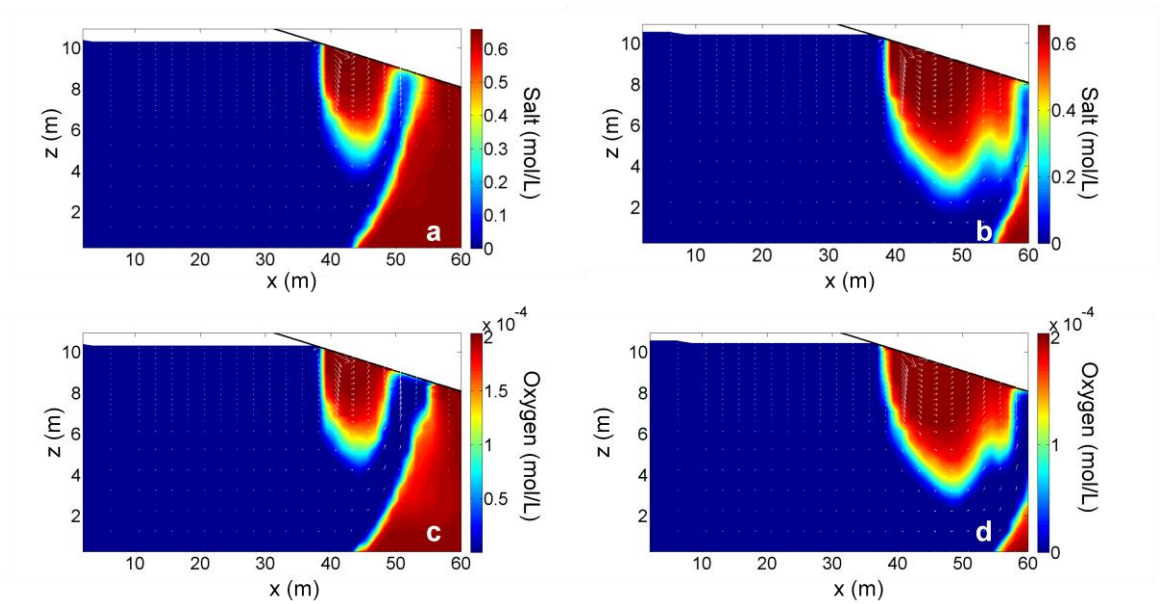


**Figure 3.12:** Salt distribution in the near-shore aquifer for (a)  $H_{rms} = 1$  m (Cases 5, 6) and (b)  $H_{rms} = 2$  m (Cases 7, 8), and oxygen distribution for reactive transport simulations with (c)  $H_{rms} = 1$  m (Case 6) and (d)  $H_{rms} = 2$  m (Case 8) after 300 days.

Without reactions considered the oxygen distribution with waves present is the same as the salt distribution differing only in magnitude. It can be seen that, less oxygen is consumed in the upper saline plume for the simulated wave cases (Figures 3.12c, and 3.12d) compared to the tidal cases (3.3d). This is because the tide causes greater mixing between the fresh groundwater and seawater along the boundary of the upper saline plume compared to the regular wave conditions simulated via wave set-up. This result is consistent with Xin et al. (2010). From this it is expected that the transformation of nutrients in the mixing zone of the upper saline plume may be less for the wave cases (Cases 6, 8) compared to the tidal case (Case 4) despite the larger upper saline plume.

### **3.3.2.2 Transport and fate of nutrients with wave set-up**

Presence of waves changes the groundwater discharge pathway of nutrients significantly compared to the cases with no oceanic forcing and tides (Figures 3.13a, d, g, l). Figure 3.13 shows the nutrient concentrations considering conservative and reactive transport with wave set-up simulations with  $H_{rms} = 1$  m (Cases 5, 6).



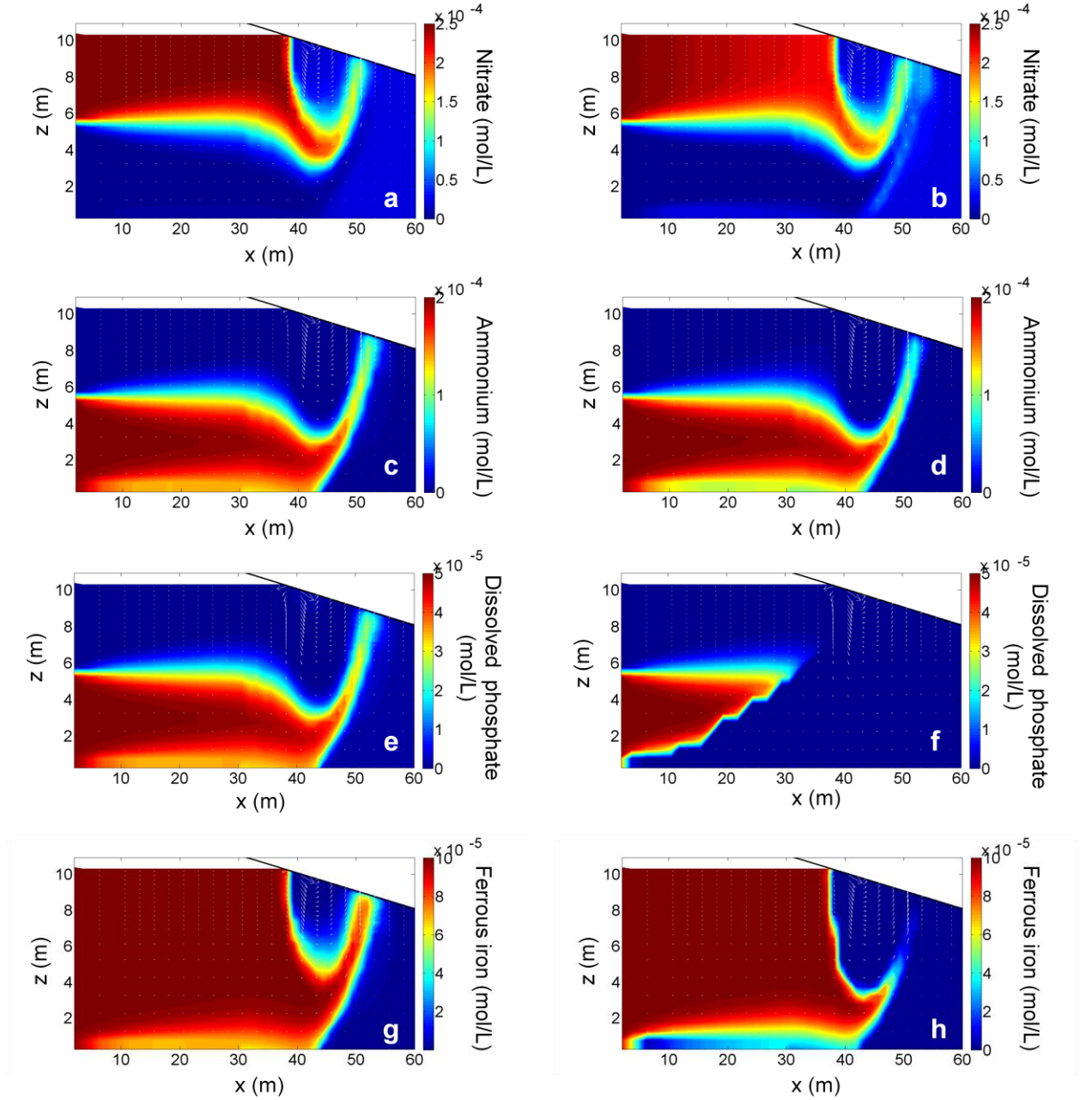


**Figure 3.13:** Concentration profiles from simulations with  $H_{rms} = 1$  m with conservative transport (Case 5) of (a) nitrate, (c) ammonium, (e) phosphate, and (g) ferrous iron; and reactive transport (Case 6) of (b) nitrate, (d) ammonium, (f) phosphate, and (h) ferrous iron after 300 days.

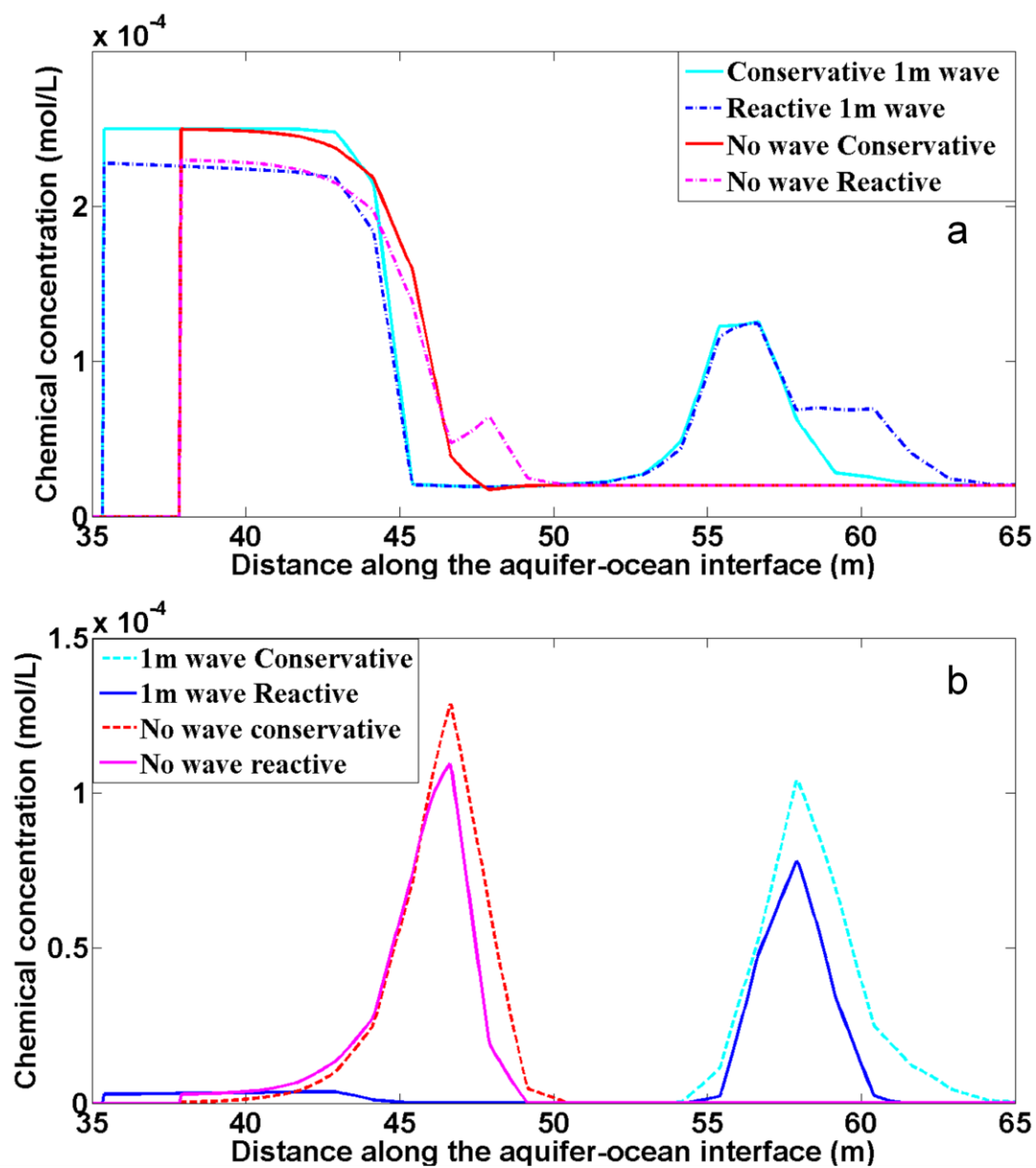
Comparing the nutrient distributions between Figures 3.4a and 3.13a, it can be seen that wave set-up up modifies the transport pathways for nitrate with nitrate discharging further offshore, near the wave set-down zone ( $x = 47 - 52$  m) with waves present. Similar to the other cases (Cases 2, 4) nitrification occurs at the saltwater wedge interface (Figure 3.13b). As there is less mixing occurring at this interface compared to the tidal case the extent of nitrification is less. Due to less salt-freshwater mixing in the upper saline plume for wave cases compared to the tidal cases, there is less production of nitrate and less consumption of ammonium in this mixing zone (Figures 3.4e, 3.5e, 3.13b, and 3.13d). However, compared to the case with no oceanic forcing (Case 2), there is increase in nitrate and decrease in ammonium in the aquifer (Case 6). There is 9.4% increase in the net discharge of nitrate and 29.3% decrease in the net discharge of ammonium for  $H_{rms} = 1$  m wave. Similar to the tidal case this is primarily due to oxic degradation combined with nitrification occurring in the upper saline plume. As the wave height increases ( $H_{rms} = 2$  m) the net production of nitrate and the consumption of ammonium in the aquifer increases. For  $H_{rms} = 2$  m, the net discharge increases by 15% for nitrate and decreases 41.7% for ammonium. This is because as expected an increase in wave height enhances mixing between fresh groundwater and recirculating seawater with more oxic degradation and nitrification occurring around the upper saline plume. The increased oxygen recirculation and availability in the near-shore aquifer also further inhibits denitrification.

Figure 3.14 shows the exit concentration of nitrate, ammonium, dissolved phosphate and ferrous iron for the cases with no oceanic forcing and  $H_{rms} = 1$  m. For wave-induced recirculation, the exit concentration for the conservative transport of all species decreases

compared to no oceanic forcing scenario due to dilution (Figure 3.14a, b). However, for wave-induced reactive transport, the nitrate exit concentration increases further seaward ( $x = 58 - 64$  m) as the formation of larger upper saline plume modifies the transport pathways and enhances nitrification as well as oxic degradation. In both cases, oxygen from the recirculating seawater cause nitrification which decreases the reactive ammonium concentrations and increases nitrate concentrations.

Similar to the tidal case (Case 4), phosphate is completely (100%) removed from the aquifer in the presence of waves (Cases 6, and 8, Figure 3.14c). This is because the ferrous iron is oxidized and precipitates as  $\text{Fe}(\text{OH})_3$  around the upper saline plume and along the saltwater wedge interface (Figure 3.13h). The dissolved phosphate is adsorbed to the  $\text{Fe}(\text{OH})_3$ . The adsorption rate for phosphate is high similar to no oceanic forcing and tidal cases. Over the 300 day simulation period 3.6 moles and 3.3 moles of  $\text{Fe}(\text{OH})_3$  precipitates in the aquifer for  $H_{rms} = 1$  m and  $H_{rms} = 2$  m respectively. The total moles that precipitate is less for the wave cases compared to both the no oceanic forcing and tidal forcing as only regular, constant wave conditions via simulation of wave set-up is considered. The formation of a larger upper saline plume by waves pushes the saltwater wedge further seaward and this reduces the length of the mixing zone along the saltwater wedge where  $\text{Fe}(\text{OH})_3$  precipitates. In addition, the presence of a large upper saline plume lengthens the discharge flow path and travel time for the land-derived ferrous iron. This increase in travel time means that the time for the ferrous iron to reach the salt-freshwater mixing zones near the aquifer-ocean interface is longer for wave cases compared to the tidal and no oceanic forcing cases. This increased travel time also results in less ferrous iron precipitation in the aquifer over the 300 d simulation period. Despite

the lower total iron precipitation observed the ferrous iron concentrations along the interface are much lower for the reactive transport simulations with waves present compared with the case with no oceanic forcing (Figure 3.14d,  $x = 50 - 65$  m). This is because once the ferrous iron does reach the mixing zones more iron oxidation and  $\text{Fe(OH)}_3$  oxidation occurs due to the higher availability of oxygen in the subsurface.



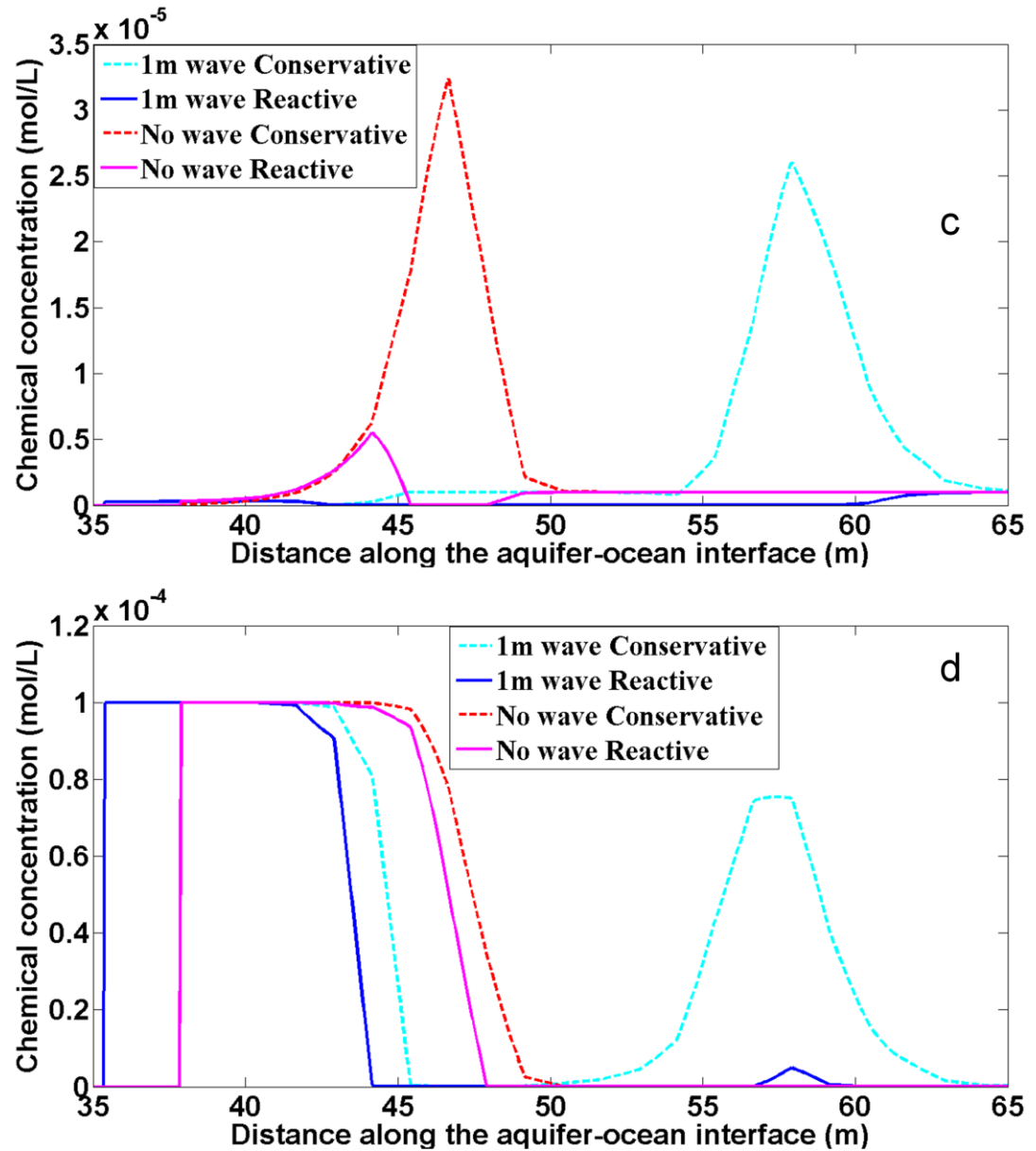


**Figure 3.14:** Exit concentrations for (a) nitrate, (b) ammonium, (c) dissolved phosphate, and (d) ferrous iron for cases with  $H_{rms} = 1$  m (Cases 5, 6) and no oceanic forcing (Cases 1, 2) after 300 days.

### 3.4 Influence of labile DOM from seawater

It was shown by Spiteri et al. (2008b) that the presence of labile (reactive) DOM in seawater can significantly alter the reactions occurring in a subterranean estuary and consequently change the fluxes of nutrients to coastal waters. Simulations were performed to quantify the influence that increased availability of labile DOM from seawater may have on the fate of nutrients in a near-shore aquifer exposed to oceanic forcing. For these simulations, the concentration of DOM in seawater is 0.2 mM and the reactivity of the seawater-derived DOM is modified by increased  $k_{fox}$  to  $3.0 \times 10^{-7} \text{ s}^{-1}$ . Simulation results show that for the case with no oceanic forcing the transport and fate of all chemical species are significantly modified by the presence of labile DOM (Case 9, Figure 3.15). The labile DOM consumes all of the oxygen in the saltwater wedge via oxic degradation (Figures 3.15a and 3.15b). This reaction also produces ammonium as can be seen by the increase of ammonium concentration in the saltwater wedge (Figure 3.15c and 3.15d). Unlike previous cases the ammonium produced is not nitrified as the abundance of labile DOM rapidly consumed all oxygen in the system. This means that nitrate is not produced in the saltwater wedge or along its mixing zone. However, similar to Case 2 denitrification still occurs and nitrate is consumed in the upper aquifer due to the availability of land-derived DOM and anoxic conditions (Figure 3.15c and 3.15d).

Table 3.6 summarizes the consumption and production of nutrients in the near-shore aquifer. The net discharge of nitrate is reduced by 32.7% whereas the net discharge of ammonium increases by 4.5% for Case 9. This is opposite to Case 2 where a net production of nitrate and net consumption of ammonium was observed. The total precipitation of  $\text{Fe}(\text{OH})_3$  in the aquifer over the 300 day simulation period is 3.52 mol.

This amount is less than for Case 2 (3.83 mol), as there is less oxygen available to ferrous iron for oxidation along the interface of saltwater wedge. Despite this the total phosphate adsorbed over the 300 d simulation period is 0.97 moles which is almost similar to that of Case 2 (0.96 moles). This is due to the high adsorption coefficient used to simulate phosphate adsorption which causes 94% sorption of phosphate for Case 9.

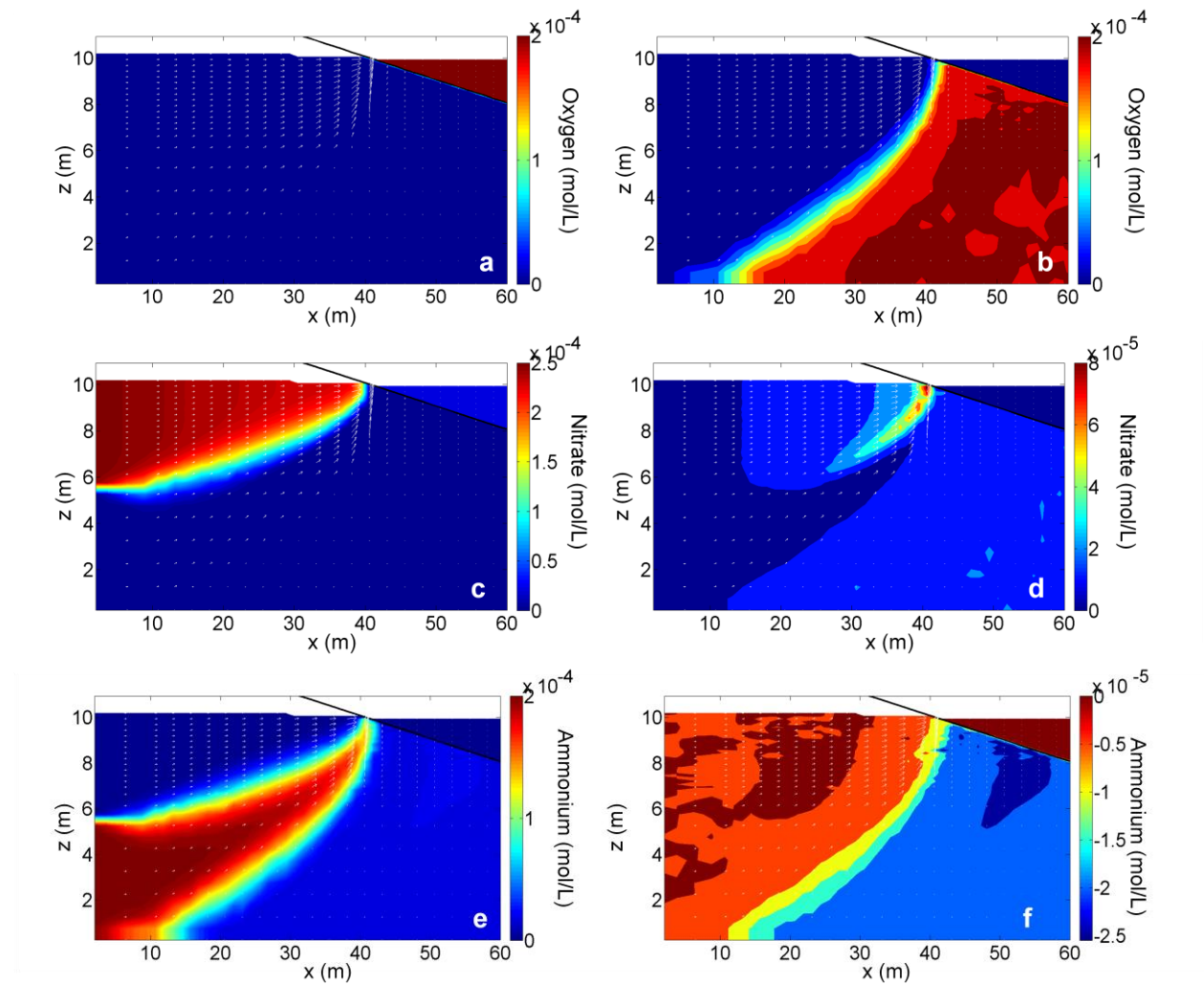


**Figure 3.15:** Simulated (a) oxygen, (c) nitrate and (e) ammonium distributions for reactive transport case with no oceanic forcing and labile DOM (Case 9) and change in concentrations due to reaction for (b) oxygen, (d) nitrate, and (f) ammonium (positive change corresponds to a decrease in concentration) after 300 days.



**Table 3.6:** Production and consumption of species in the near-shore aquifer for simulated cases 9-11 with labile DOM.

Species	$\text{NO}_3^-$	$\text{NH}_4^+$	$\text{PO}_4$	$\text{Fe}(\text{OH})_3$ (s)	$\text{PO}_4$ (ads)
Case 9 <b>No forcing</b>	32.7% decrease	4.5% increase	94% decrease	3.52 moles precipitation	0.97 moles adsorption
Case 10 <b><math>H_{rms} = 1</math> m</b>	99% decrease	61.6% increase	25.7% decrease	3.11 moles precipitation	1.7 moles adsorption
Case 11 <b><math>H_{rms} = 2</math> m</b>	100% decrease	73.6% increase	16.7% decrease	2.88 moles precipitation	1.3 moles adsorption

### 3.4.1 Wave effects on nutrients in the presence of labile DOM

The fate of nutrients in the subterranean estuary are also significantly modified by the presence of labile DOM with waves present (Case 10,  $H_{rms} = 1$  m, Figure 3.16). Oxygen in both the saltwater wedge and the upper saline plume is rapidly consumed by the labile DOM (Figure 3.16a and 3.16b). Ammonium is produced at the interface of the upper saline plume due to denitrification of the land-derived nitrate by the recirculating labile DOM (Figure 3.16c and 3.16d). Oxidic degradation of the labile DOM in the saltwater wedge and upper saline plume also increases the subsurface ammonium production (Figure 3.16e and 3.16f). It is predicted that with the labile DOM present, nitrate is mostly consumed in the aquifer prior to discharge across the aquifer-ocean interface with 99% removal for the simulation with  $H_{rms} = 1$  m and 100% removal for  $H_{rms} = 2$  m. The net discharge of ammonium is increased by 61.6% and 73.6% for  $H_{rms} = 1$  m and  $H_{rms} = 2$  m respectively. More ammonium is produced for  $H_{rms} = 2$  m as the wave-induced

seawater recirculation rate is higher and thus the rate of oxic degradation of the labile DOM and thus ammonium production is also be greater. Similar to the case with no oceanic forcing it can be seen that the presence of labile DOM significantly alters the production and consumption of nutrients in the subterranean estuary.

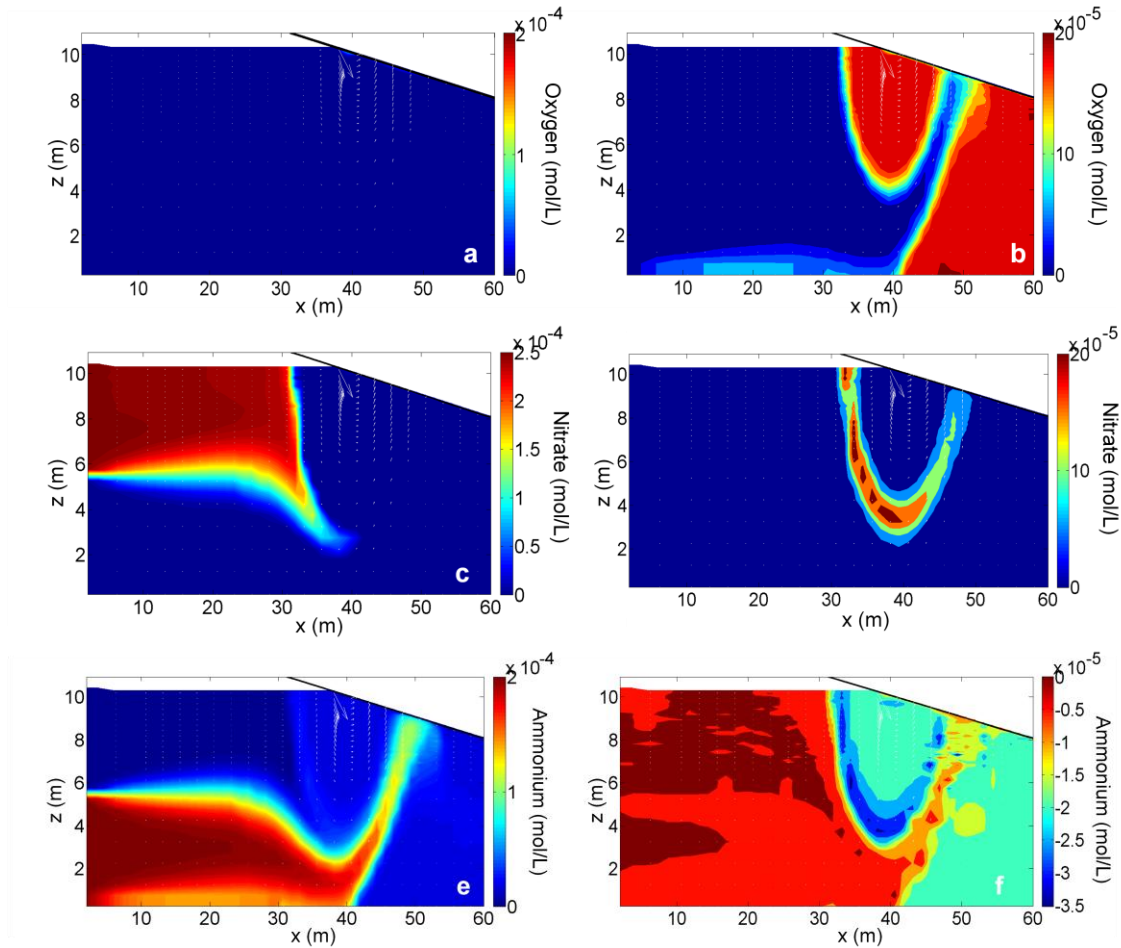


**Figure 3.16:** Simulated (a) oxygen, (c) nitrate and (e) ammonium distributions for reactive transport case with  $H_{rms} = 1$  m and labile DOM (Case 10) and change in concentrations due to reaction for (b) oxygen, (d) nitrate, and (f) ammonium (positive change corresponds to a decrease in concentration) after 300 days.

Over the 300 d simulation period 3.11 mol and 2.88 mol of  $\text{Fe}(\text{OH})_3$  precipitates in the aquifer for  $H_{rms} = 1$  m and  $H_{rms} = 2$  m respectively. The total  $\text{Fe}(\text{OH})_3$  formed is less in for these cases compared to both the no oceanic forcing (Cases 2 and 9) as well as no labile DOM cases with waves (Cases 6 and 8). This is because the increased input of labile DOM as the wave conditions increase rapidly consumes the oxygen in the subsurface so less oxygen is available to oxidize ferrous iron. In addition, for  $H_{rms} = 2$  m, the larger upper saline plume formed increases the travel time for land-derived ferrous iron to reach the mixing zones near the aquifer-ocean interface compared to  $H_{rms} = 1$  m. This results in less precipitation of  $\text{Fe}(\text{OH})_3$  over the 300 d simulation period for  $H_{rms} = 2$  m. For the wave cases with labile DOM present phosphate is not completely removed from the aquifer prior to discharge. The phosphate discharge reduces 25.7% (Case 10) and 16.7% (Case 11). This is because of increased phosphate production in the aquifer by the enhanced oxic degradation of the labile seawater-derived DOM as well as denitrification by the sea-derived labile DOM. Although the phosphate adsorption coefficient is high not all the phosphate produced is adsorbed to the  $\text{Fe}(\text{OH})_3$  prior to discharge across the aquifer-ocean interface. The total phosphate adsorbed over the 300 d simulation period for the wave cases with labile DOM are 1.7 moles (Case 14), and 1.3 moles (Case 16) compared to 1.12 moles (Case 6) and 1.1 moles (Case 8) for the wave cases without labile DOM. This increased phosphate adsorption is consistent with the higher phosphate production and concentrations in the aquifer. Although significant phosphate is generated in the upper saline plume by oxic degradation it only has a small subsurface residence time and flow path available for adsorption to  $\text{Fe}(\text{OH})_3$  prior to its discharge to coastal waters. Hence, net discharge of phosphate via SGD is high.

### 3.5 Conclusions

In this study the influence of tides and waves on nutrient dynamics in a near-shore aquifer has been examined. SEAWAT-2005 combined with PHT3D v2.10 provides a powerful modeling platform for simulation and quantification of the multi-component reactive transport processes occurring in a near-shore aquifer influenced by oceanic forcing. It was shown that the transport and fate of nutrients in a near-shore aquifer are strongly influenced by oceanic forcing as these forces alter the subsurface nutrient transport pathways and intensify the mixing of fresh groundwater and recirculating seawater. The enhanced mixing and modified pathways caused by tides and waves greatly influence the reaction processes occurring in the near-shore aquifer. For the conditions simulated, oceanic forcing was shown to increase the discharge flux of nitrate and decrease the discharge flux of ammonium in the absence of reactive DOM in the recirculating seawater. For the cases with oceanic forcing without labile (reactive) DOM it was shown that tide- and wave-induced oxic seawater recirculation through the aquifer caused a high rate of nitrification and inhibited denitrification. Tides increased the precipitation of  $\text{Fe}(\text{OH})_3$  in the aquifer due to the increased subsurface oxygen availability but surprisingly wave effects reduced the total  $\text{Fe}(\text{OH})_3$  that precipitated over the 300 d simulation period. This is likely because the simulations only considered regular, constant wave conditions via simulation of wave set-up. Although the spatial extent of the upper saline plume was greater with the inclusion of waves, the intensity of salt-freshwater mixing around the upper saline plume was not significantly enhanced. Irregular wave conditions (i.e., varying wave heights, wave storm events) will likely greatly increase the salt-freshwater mixing around the upper saline plume and this is

likely to lead to greater precipitation of  $\text{Fe}(\text{OH})_3$ . For all the simulation cases without the seawater-derived labile DOM, the sorption of phosphate to  $\text{Fe}(\text{OH})_3$  in the aquifer was high with minimal or negligible amounts discharging across the aquifer-ocean interface.

Availability of reactive DOM from recirculating seawater alters the geochemical reactions and nutrient production/consumption in the subterranean estuary. The seawater-derived reactive DOM causes a net consumption of nitrate and production of ammonium in the aquifer. The oxygen is rapidly consumed in the saltwater wedge and upper saline plume as the DOM degrades and this enhances the production of phosphate and ammonium in the aquifer.

This numerical study illustrated that oceanic forcing and the chemical composition of the terrestrial groundwater and recirculating seawater strongly controls the fate of nutrients in a subterranean estuary prior to their discharge to near-shore waters. The model applied was verified using simulation results from Spiteri et al (2008a). However model validation with field data from a tide or wave-influenced near-shore aquifer system would enhance the applicability of the model to the real aquifer systems. While the model considers a complex suite of chemical reactions that typically control subsurface nutrient dynamics, further model validation may indicate that additional reactions should be considered including annamox, pyrite denitrification and co-precipitation of species. Finally, in future work it is recommended that the model be applied to conduct detailed sensitivity analysis of the reactions and reaction rates considered, species concentrations, landward freshwater flux, tidal amplitude and wave conditions which will also provide a broader understanding of the factors controlling nutrient dynamics in a near-shore coastal aquifer.

## References

- Andersen, M. S., L. Baron, et al. (2007). "Discharge of nitrate-containing groundwater into a coastal marine environment." Journal of Hydrology 336 (1-2 ): 98-114.
- Beck, A. J., Y. Tsukamoto, et al. (2007). "Importance of geochemical transformations in determining submarine groundwater discharge-derived trace metal and nutrient fluxes." Applied Geochemistry 22(2): 477-490.
- Berner, E. K. and R. K. Berner (1996). Global Environment: Water, Air and Geochemical cycles. New Jersey, Prentice Hall.
- Boufadel, M. C. (2000). "A mechanistic study of nonlinear solute transport in a groundwater-surface water system under steady state and transient hydraulic conditions." Water Resources Research 36(9): 2549-2565.
- Capone, D. G. and M. F. Bautista (1985). "A Groundwater source of nitrate in nearshore marine-sediments." Nature 313: 214-216.
- Charette, M. A. and M. C. Allen (2006). "Precision ground water sampling in coastal aquifers using a direct-push, shielded-screen well-point system." Ground Water Monitoring and Remediation 26(2): 87-93.
- Charette, M. A. and E. R. Sholkovitz (2006). "Trace element cycling in a subterranean estuary: Part 2. Geochemistry of the pore water." Geochem et Cosmochim Acta 70: 811-826.
- Charette, M. A., E. R. Sholkovitz, et al. (2005). "Trace element cycling in a subterranean estuary: Part 1. Geochemistry of the permeable sediments." Geochem et Cosmochim Acta 69(8): 2095-2109.
- Cooper, H. H. (1959). "A hypothesis concerning the dynamic balance of fresh water and salt water in a coastal aquifer." Journal of Geophysical Research 64(4): 461-467.
- Destouni, G. and C. Prieto (2003). "On the possibility for generic modelling of submarine groundwater discharge." Biogeochemistry 66: 171-186.
- Garrison, G. H., C. R. Glenn, et al. (2003). "Measurement of submarine groundwater discharge in Kahana Bay, O'ahu, Hawai'i." Limnology and Oceanography 48(2): 920-928.
- Guo, W. and C. D. Langevin (2002). User's Guide to SEAWAT: A computer program for simulation of three-dimensional variable-density ground-water flow. Tallahassee, Florida, US Geological Survey: pp. 77.

- Horn, D. (2006). "Measurements and modelling of beach groundwater flow in the swash-zone: a review." Continental Shelf Research 26: 622-652.
- Howarth, R. W., G. Billen, et al. (1996). "Regional nitrogen budgets and riverine N&P fluxes for the drainages to the North Atlantic Ocean: Natural and human influences." Biogeochemistry 35(1): 75-139.
- Hunter, K. S., Y. F. Wang, et al. (1998). "Kinetic modeling of microbially-driven redox chemistry of subsurface environments: coupling transport, microbial metabolism and geochemistry." Journal of Hydrology 209(1-4): 53-80.
- Iversen, T. M., R. Grant, et al. (1998). "Nitrogen enrichment of European inland and marine waters with special attention to Danish policy measures." Environmental Pollution 102: 771-780.
- Johannes, R. E. (1980). "The ecological significance of the submarine discharge of groundwater." Marine Ecology - Progress Series 3: 365-373.
- Kroeger, K. D. and M. A. Charette (2008). "Nitrogen biogeochemistry of submarine groundwater discharge." Limnology and Oceanography 53(3): 1025-1039.
- Krom, M. D. and R. A. Berner (1980). "Adsorption of phosphate in anoxic marine-sediments." Limnology and Oceanography 25(5): 797-806.
- Langevin, C., W. B. Shoemaker, et al. (2003). Modflow-2000, The U.S. Geological Survey modular ground-water model - Documentation of the Seawat-2000 version with the variable density flow process (VDF) and the integrated MT3DMS transport process (IMT). Tallahassee, Florida: pp. 57.
- Lapointe, B. E. and J. D. O'Connell (1989). "Nutrient-enhanced growth of *Cladophora prolifera* in Harrington Sound, Bermuda: Eutrophication of a confined, phosphorus-limited marine ecosystem." Estuarine, Coastal and Shelf Science 28: 347-360.
- Li, L. and D. A. Barry (2000). "Wave-induced beach groundwater flow." Advances in Water Resources 23: 325-337.
- Li, L., D. A. Barry, et al. (2000). "Beach water table fluctuations due to spring-neap tides: moving boundary effects." Advances in Water Resources 23: 817-824.
- Li, L., D. A. Barry, et al. (1999). "Submarine groundwater discharge and associated chemical input to a coastal sea." Water Resources Research 35(11): 3252-3259.
- Mao, X., P. Enot, et al. (2006). "Tidal influence on behaviour of a coastal aquifer adjacent to a low-relief estuary." Journal of Hydrology 327(1-2): 110-127.

- Moore, W. S. (1999). "The subterranean estuary: A reaction zone of ground water and sea water." Marine Chemistry 65: 111-125.
- Nyvang, V. (2003). Redox processes at the salt-/freshwater interface in an anaerobic aquifer, Technical University of Denmark. Ph. D.
- Parkhurst, D. L. and C. A. J. Appelo (1999). User's guide to PHREEQC (version 2) - A computer program for speciation, batch-reaction, one dimensional transport, and inverse geochemical calculations. Denver, US Department of the Interior, Water-Resources Investigations Report 99-4259.
- Postma, D., C. Boesen, et al. (1991). "Nitrate reduction in an unconfined sandy aquifer-water chemistry, reduction processes, and geochemical modeling." Water Resources Research 27(8): 2027-2045.
- Prieto, C. and G. Destouni (2005). "Quantifying hydrological and tidal influences on groundwater discharges to coastal waters." Water Resources Research 41: W12427.
- Prommer, H. and V. Post (2010). A reactive multicomponent transport model for saturated porous media
- Robinson, C., A. Brovelli, et al. (2009). "Tidal influence on BTEX biodegradation in sandy coastal aquifers." Advances in Water Resources 32 16–28.
- Robinson, C., B. Gibbes, et al. (2007a). "Salt-freshwater dynamics in a subterranean estuary over a spring-neap tidal cycle." Journal of Geophysical Research 112: C09007.
- Robinson, C., B. Gibbes, et al. (2006). "Driving mechanisms for flow and salt transport in a subterranean estuary." Geophysical Research Letters 33: L03402.
- Robinson, C., L. Li, et al. (2007b). "Effect of tidal forcing on a subterranean estuary." Advances in Water Resources 30: 851-865.
- Robinson, C., L. Li, et al. (2007c). "Tide-induced recirculation across the aquifer-ocean interface." Water Resources Research 43: W07428.
- Robinson, M. A., D. Gallagher, et al. (1998). "Field observations of tidal and seasonal variations in groundwater discharge to tidal estuarine surface water." Ground Water Monitoring and Remediation 18(1): 83-92.
- Santos, I. R., W. C. Burnett, et al. (2009). "Tidal pumping drives nutrient and dissolved organic matter dynamics in a Gulf of Mexico subterranean estuary." Geochimica et Cosmochimica Acta 73(5): 1325-1339.



- Santos, I. R., M. I. Machado, et al. (2008). "Major ion chemistry in a freshwater coastal lagoon from southern Brazil (Mangueira Lagoon): Influence of groundwater inputs." Aquatic Geochemistry 14(2): 133-146.
- Slomp, C. P. and P. van Cappellen (2004). "Nutrient inputs to the coastal ocean through submarine groundwater discharge: controls and potential impact." Journal of Hydrology 295: 64-86.
- Smith, A. J. (2004). "Mixed convection and density-dependent seawater circulation in coastal aquifers." Water Resources Research 40(8): 16.
- Spalding, R. F. and M. E. Exner (1993). "Occurrence of nitrate in groundwater-a review." Journal of Environmental Quality 22(3): 392-402.
- Spiteri, C., P. Regnier, et al. (2005). "pH-dependent iron oxide precipitation in a subterranean estuary." Journal of Geochemical Exploration 88: 399-403.
- Spiteri, C., C. P. Slomp, et al. (2008b). "Flow and nutrient dynamics in a subterranean estuary (Waquoit Bay, MA, USA): Field data and reactive transport modeling." Geochimica et Cosmochimica Acta 72(14): 3398-3412.
- Spiteri, C., C. P. Slomp, et al. (2008a). "Modeling biogeochemical processes in subterranean estuaries: Effect of flow dynamics and redox conditions on submarine groundwater discharge of nutrients." Water Resources Research 44(4): W04701.
- Tromp, T. K., P. V. Cappellen, et al. (1995). "A global model for the early diagenesis of organic carbon and organic phosphorous in marine sediments." Geochimica et Cosmochim Acta 59(7): 1259-1284.
- Turner, I. L. and R. I. Acworth (2004). "Field measurements of beachface salinity structure using cross-borehole resistivity imaging." Journal of Coastal Research 20(3): 753-760.
- Valiela, I., J. Costa, et al. (1990). "Transport of groundwater-borne nutrients from watersheds and their effects on coastal waters." Biogeochemistry 10: 177-197.
- Valiela, I., K. Foreman, et al. (1992). "Coupling of watersheds and coastal waters: Sources and consequences of nutrient enrichment in Waquoit Bay, Massachusetts." Estuaries 15(4): 443-457.
- Valiela, I., J. M. Teal, et al. (1978). "Nutrient and particulate fluxes in a salt-marsh ecosystem: Tidal exchanges and inputs by precipitation and groundwater." Limnology and Oceanography 23(4): 798-812.

- Van Cappellen, P. and Y. Wang (1995). "Metal cycling in surface sediments: modeling the interplay of transport and reaction." IN: Allen, H.E. (Ed.), Metal contaminated Sediments. Ann Arbor Press, Chelsea, MI: 21-64.
- Vandenbohede, A. and L. Lebbe (2005). "Occurrence of salt water above fresh water in dynamic equilibrium in a coastal groundwater flow system near De Panne, Belgium." Hydrogeology Journal 14(4): 462 - 472.
- Werner, A. D. and D. A. Lockington (2006). "Tidal impacts on riparian salinities near estuaries." Journal of Hydrology 328(3-4): 511-522.
- Xin, P., C. Robinson, et al. (2010). "Effects of wave forcing on a subterranean estuary." Advances in Water Resources 46: W12505.
- Zheng, C. and M. C. Wang (1999). MT3DMS-A modular three-dimensional multispecies transport model for simulation of advection, dispersion and chemical reactions of contaminant in ground-water systems; documentation and user's guide. Washington, DC, U.S Army Corps of Engineers.

## Chapter 4

---

### Summary and Recommendations

#### 4.1 Summary

The groundwater flow, salt-freshwater mixing and geochemical reaction processes occurring in a near-shore coastal aquifer are complex and understanding and predicting the fate of nutrients in a near-shore coastal aquifer is challenging. In this study a numerical model has been developed to evaluate the influence of oceanic forcing and factors affecting the transport and transformation of nutrients in a near-shore coastal aquifer. The model was developed by combining the variable-density groundwater flow model SEAWAT-2005 (Guo and Langevin 2002) with the reactive multi-component transport model PHT3D v2.10 (Prommer and Post 2010). The numerical model, including the geochemical code was first verified against previously reported numerical simulation results (Spiteri et al. 2008a). Once verified, the numerical model was used to evaluate effects of oceanic forcing on nutrients in a near-shore aquifer exposed to (i) no oceanic forcing, (ii) tides, and (ii) waves. The simulation results were post-processed using MATLAB to quantify the nutrient exit concentrations, chemical fluxes across the aquifer-ocean interface and also the consumption/production of nutrients in the near-shore aquifer. The model was also applied to examine the influence of recirculating labile DOM from seawater on the geochemical reactions and nutrient transformations in the near-shore aquifer.

When estimating groundwater-derived nutrient loading rates to coastal waters, coastal managers typically only consider the landward concentration of nutrients in the aquifer.

The present study shows that tides and waves lead to dynamic subsurface flows and salt-freshwater mixing in the near-shore region and this significantly modifies the transport pathways as well as the nutrient distributions. Therefore considering only the landward concentration of nutrients will not provide an accurate prediction of nutrient discharge from coastal aquifers as it neglects important nutrient transformations that can occur close to the aquifer-ocean interface. In some cases this approach may underestimate the nutrient fluxes (e.g., in the absence of labile DOM in recirculating seawater oceanic forcing may significantly enhance the nitrate discharge flux) and in some cases it may overestimate nutrient fluxes (e.g., oceanic forcing may reduce the nitrate discharge flux when labile DOM is available from recirculating seawater). While previous studies have indicated that only a small amount of nitrate removal in the near-shore aquifer prior to its discharge to coastal waters (Spiteri et al. 2008b), the present study shows that tide- and wave-induced recirculation may lead to significant nitrate production or removal depending on the availability of chemical species in the recirculating seawater. Also as the water exchanging across the aquifer-ocean interface is higher when tides and waves are present the chemical discharge fluxes are increased even though the exit concentrations are lower due to dilution of the land-derived groundwater with the recirculating seawater.

Prior studies have indicated that the reactive processes occurring in a subterranean estuary, particularly phosphate adsorption and only marginal nitrate removal, may lead to the discharge of N-limited groundwater (low N:P ratio) to coastal waters. In contrast the results from this study suggest that presence of tides and waves along with the availability of labile DOM in recirculating seawater may increase the N:P ratio by

enhancing the removal of nitrate and production of phosphate in the near-shore aquifer. Oxidic degradation and denitrification by the reactive DOM delivered by the tide- and wave-induced recirculating seawater are the major reactions leading to the increased N:P ratio. However, if the labile DOM concentration is not significant in the seawater, the tide- and wave-induced recirculation will not increase phosphate production in the subterranean estuary and there may be close to complete adsorption of phosphate in the aquifer to iron (hydr)oxides. Also nitrification combined with high water exchange fluxes may enhance nitrate loading to coastal waters.

Consistent with the findings of previous study (Xin et al. 2010), the numerical simulations show that tides cause greater salt-freshwater mixing in the near-shore aquifer compared to regular wave forcing. This leads to a higher transformation of the nutrients in a subterranean estuary subject to tides compared to waves which in turn influences the nutrient fluxes across the aquifer-ocean interface.

The numerical model developed is able to enhance the conceptual understanding of the dynamic salt-freshwater mixing and complex reaction processes occurring in a near-shore aquifer and is a valuable tool for examining the influence of oceanic fluctuations on nutrient fluxes to coastal waters. As required to better predict the nutrient loadings rates to coastal waters via SGD, this model provides valuable information on the natural attenuation/production of nutrients in a coastal aquifer due to the presence of oceanic fluctuations.

## 4.2 Recommendations

While the model is able to significantly enhance conceptual understanding of the processes controlling the fate of nutrients in a near-shore aquifer, model validation with field data and sensitivity analysis to quantify the influence of additional variables would further enhance understanding of nutrient dynamics in this complex system. The following recommendations are provided to form the basis of future work:

- Only regular, constant wave forcing was considered in the present study via simulation of wave set-up. The influence of random wave conditions (e.g., storm surges) should be examined in future studies. It is expected that random wave conditions will enhance the mixing of recirculating seawater with fresh groundwater in a near-shore aquifer. This will significantly influence the geochemical reactions and alter the nutrient fluxes to coastal waters.
- Simulations should be performed with varying tidal amplitudes to analyze the sensitivity and response of the system to the strength of tidal forcing.
- The influence of the fresh groundwater discharge rate, including seasonal variations, and also aquifer properties (hydraulic conductivity, porosity, depth of the aquifer) were not considered in the present study. These variables may significantly impact the transport and fate of nutrients in a near-shore aquifer.
- The sensitivity of nutrient fate to the reactions considered, reaction rate constants adopted and species concentrations should be examined in future studies. The model developed was verified using an existing numerical model that has been used to simulate nutrient transport in a coastal aquifer not subject to oceanic forcing. Validation of the model with field data collected in tide- or wave-

influenced coastal aquifer is recommended. Extending the geochemical reaction network; for example, including reactions such as anammox, pyrite denitrification, and co-precipitation of species may be required to better predict nutrient fate in a coastal aquifer.

- The combined effects of both tides and waves acting on a coastal aquifer should be examined as many shoreline areas are exposed to both these forcing mechanisms.

## References

- Guo, W. and C. D. Langevin (2002). User's Guide to SEAWAT: A computer program for simulation of three-dimensional variable-density ground-water flow. Tallahassee, Florida, US Geological Survey: pp. 77.
- Prommer, H. and V. Post (2010). A reactive multicomponent transport model for saturated porous media
- Spiteri, C., C. P. Slomp, et al. (2008b). "Flow and nutrient dynamics in a subterranean estuary (Waquoit Bay, MA, USA): Field data and reactive transport modeling." Geochimica et Cosmochimica Acta 72(14): 3398-3412.
- Spiteri, C., C. P. Slomp, et al. (2008a). "Modeling biogeochemical processes in subterranean estuaries: Effect of flow dynamics and redox conditions on submarine groundwater discharge of nutrients." Water Resources Research 44(4): W04701.
- Xin, P., C. Robinson, et al. (2010). "Effects of wave forcing on a subterranean estuary." Advances in Water Resources 46: W12505.

## Appendix A

---

### Numerical Model Verification

#### A.1 Introduction

The reactive variable-density groundwater flow and transport model including the reaction kinetics was verified by simulating the numerical results of Spiteri et al. (2008a) who developed a numerical model to examine the flow dynamics and transport of nutrients in a near-shore aquifer not exposed to oceanic forcing.

#### A.2 Groundwater flow and multi-species transport geochemical model setup

A brief summary of numerical model presented by Spiteri et al (2008a)) is provided here with a schematic of the model domain shown in Figure A1. The model represents a cross-shore transect through a sandy coastal aquifer. The model domain is divided into two zones: a surface water zone (zone A) and an aquifer zone (zone B). A very high hydraulic conductivity of  $10^5 \text{ md}^{-1}$ ,  $n_e = 1$  and a constant salt concentration of  $27 \text{ gL}^{-1}$  is applied in zone A to represent surface water. To simulate a sandy aquifer, the permeability is  $7 \times 10^{-12} \text{ m}^2$ , porosity is 0.3, longitudinal dispersivity is 0.5m ( $\alpha_L$ ), and transverse dispersivity is 0.05m ( $\alpha_T$ ) in zone B. The model domain is 95 m long. Spiteri et al. (2008a) considered a 60 m long model with a rectangular domain (vertical aquifer-ocean interface at seawater right-hand boundary). This two zone approach is required in our study to simulate the tidal oscillations. Due to difficulties in simulations of tides with a rectangular model, for model verification we used a 95 m two zone model with 60 m extent in the landward side representing the same domain of Spiteri et al. (2008a). A



shallow coastal aquifer system is simulated with an aquifer depth ( $H$ ) of 20 m. The model domain is discretized into 72 layers and 89 columns with greater refinement around the sloping beach interface. Grid discretization test were performed to ensure the numerical solution was independent of the grid sizing.

No flow boundary condition was applied on the bottom boundary and also at the vertical seaward boundary. A constant head of 0.4 was applied at the landward interface ending up with  $0.0067 \text{ mm}^{-1}$  gradient. The upper boundary is a phreatic surface and recharge to the aquifer is not considered.

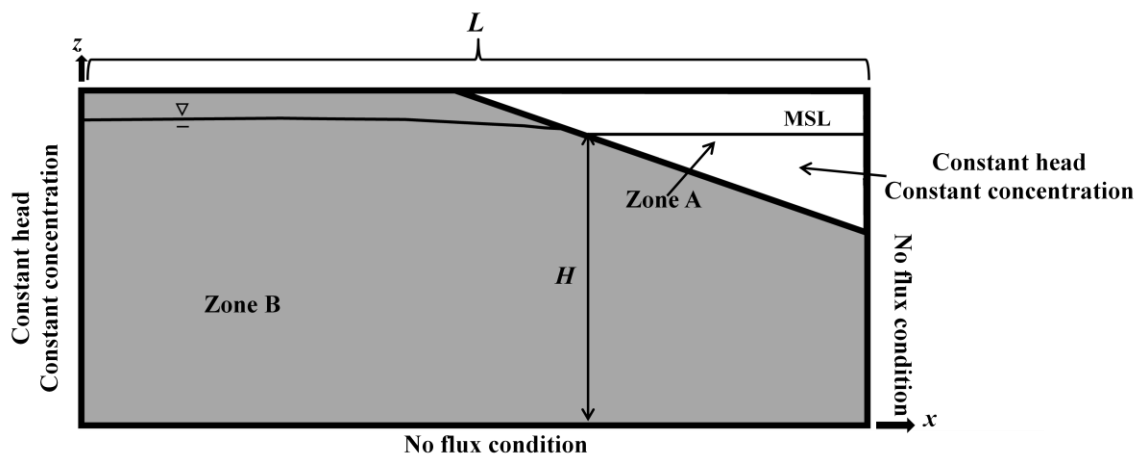


**Figure A.1:** Model domain and flow boundary conditions.

The solute species considered in the reactive transport model are salt, ammonium ( $\text{NH}_4^+$ ), nitrate ( $\text{NO}_3^-$ ), phosphate ( $\text{PO}_4$ ), oxygen ( $\text{O}_2$ ), ferrous iron ( $\text{Fe}^{2+}$ ), dissolved organic matter (DOM), adsorbed phosphate ( $\text{PO}_{4(\text{ads})}$ ) and iron hydroxide ( $\text{Fe}(\text{OH})_3$ ). The reactions and rate expression included in the model are the same as Spiteri et al. (2008a) who examined the nutrient dynamics in a sandy near-shore aquifer not exposed to oceanic forcing. The reactions simulated and the kinetic rate expressions and rate constants adopted are shown in Tables 3.1 and 3.2 respectively. Constant concentrations

of species were set along the landward boundary and also for cells in zone A. The concentration values for each species are provided in Table 3.3. These concentrations represent the anoxic groundwater and oxic seawater concentrations (Case 3 from Spiteri et al. 2008a) used by Spiteri et al. (2008a). The land-derived nitrate plume occurs at a depth of 8-12m from the top of the aquifer and an ammonium/phosphate plume occurs at a depth of 12-16m from the top of the aquifer. The model was first run to reach steady state with regards to the salt distribution and groundwater flows. The reactive transport simulation was then run for 1000 days as this simulation time was required for the chemical species from the landward boundary to reach the seaward boundary.

### A.3 Salt distribution

The concentration distribution of salt is shown in Figure A.2. It can be seen that the model developed for this study predicts that the saltwater wedge intrudes into the coastal aquifer to a distance of approximately 15 m from the landward boundary (Figure A.2a). This matches with salt distribution of Spiteri et al. (2008a) (Figure A.2b) as well as Glover's solution. The fresh groundwater discharges into the sea near the shore line.

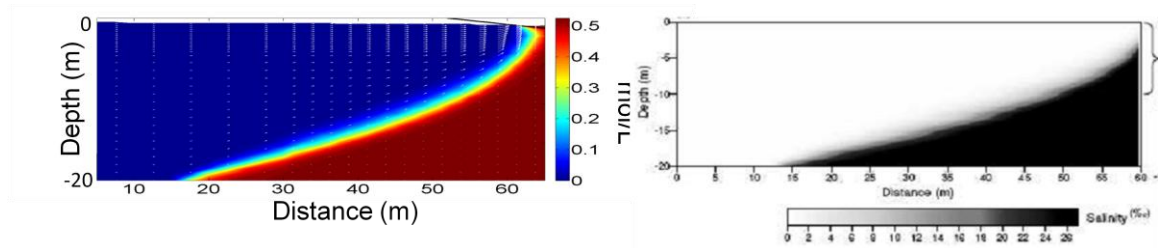


**Figure A.2:** Simulated steady state salt distribution in the coastal aquifer from (a) model developed, and (b) Spiteri et al. (2008a).

Figure A.3 represents the vertical steady state salt distribution profiles at different  $x$  locations from the present study. Consistent with Figure A.2 the salt intrusion depth decreases towards landward boundary (Figure A.3a).

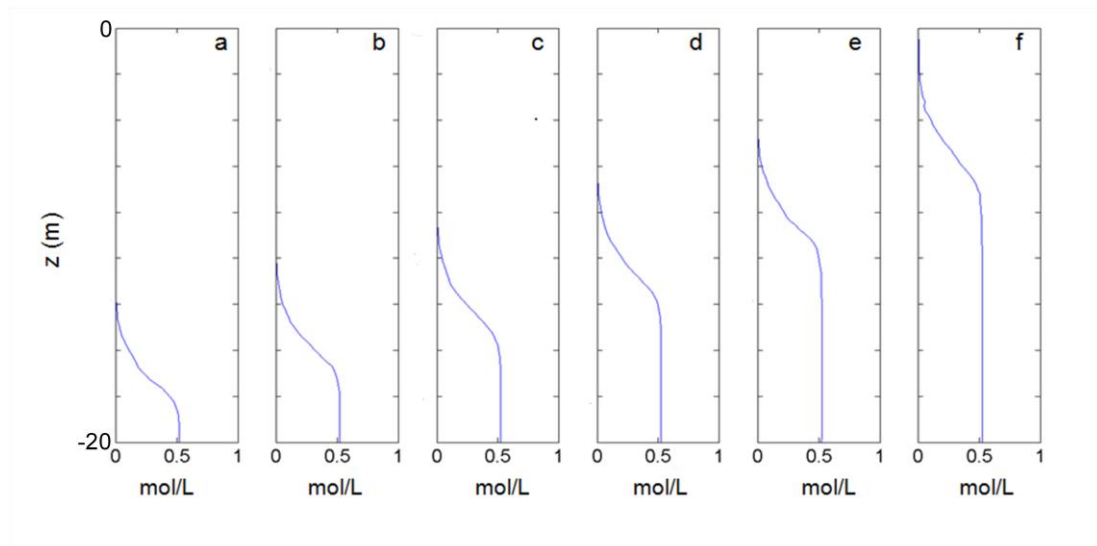


**Figure A.3:** Vertical salt distribution profiles at (a) 35 m, (b) 40 m, (c) 45 m, (d) 50 m, (e) 55 m, and (f) 60 m from landward boundary in the model at steady state.

#### A.4 Nutrient distribution

The steady state reactive concentration distribution profiles for nitrate, ammonium and phosphate from our numerical model simulations and from Spiteri et al. (2008a) are shown in Figure A.4. Figure A.5 illustrates the steady state conservative and reactive concentration profiles along a vertical profile at 60m for the present study and at seaward boundary for Spiteri et al. (2008a). Due to different seaward boundary configuration in the present study (sloped rather than vertical boundary), the concentration profiles are slightly different however the distribution profiles are very similar to that of Spiteri et al. (2008a).

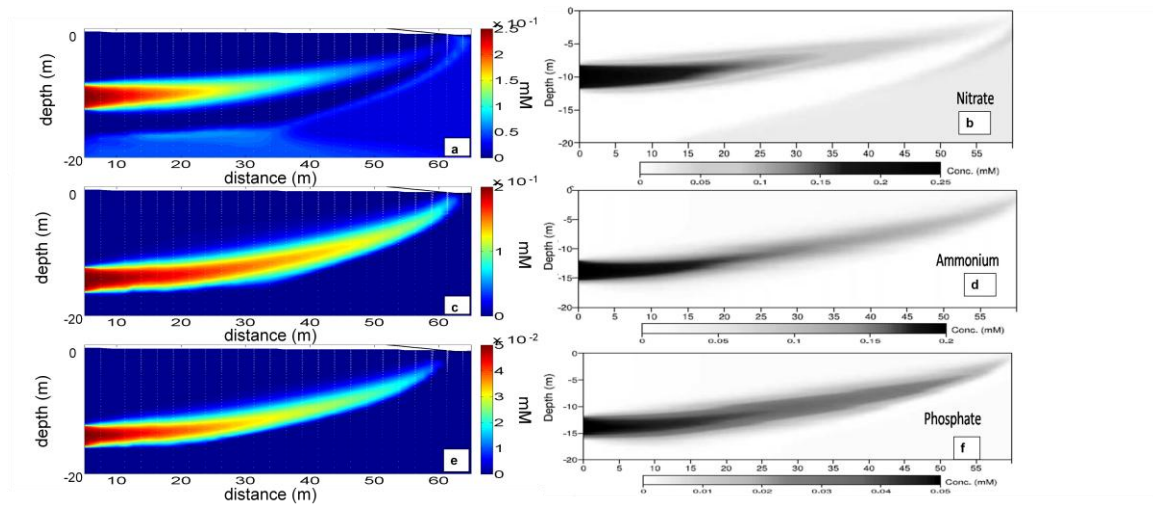


**Figure A.4:** Simulated concentration profiles for (a, b) nitrate, (c, d) ammonium; and (e, f) phosphate from present study and Spiteri et al. (2008a) respectively. The subplots on the right hand side (b), (d) and (f) are modified from Spiteri et al. (2008a).

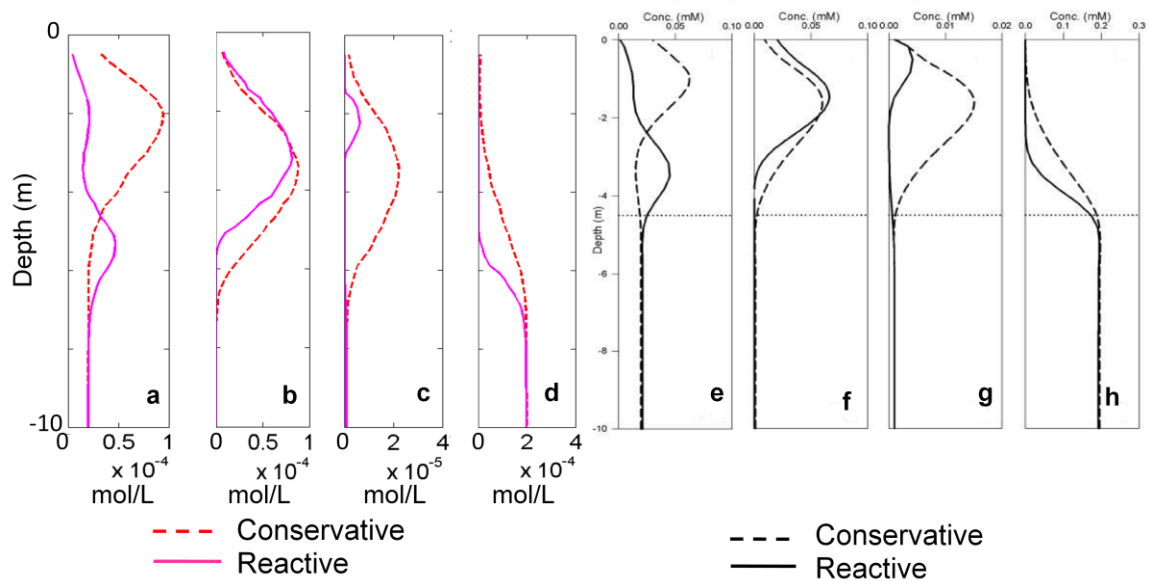


**Figure A.5:** Steady state vertical concentration profiles of (a,e) nitrate, (b,f) ammonium, (c,g) phosphate and (d,h) at interface and seaward boundary from present study and Spiteri et al. (2008a) study respectively after 1000 days. Dashed lines represent

simulation results conservative transport simulations and solid lines represent simulation results from reactive transport simulations.

Comparing Figure A.5a and A.5b it is evident that both denitrification and nitrification occurs along the nitrate discharge flow path and this results in nitrate attenuation at lower depth and nitrate production at higher depth in the aquifer. Similar reaction processes are observed in the model by Spiteri et al. (2008a) (Figure A.5e and A.5f). For both simulations, the phosphate concentration is significantly decreased due to sorption (Figure A.5c and A.5g) and this results in significant attenuation of phosphate in the coastal aquifer prior to discharge via SGD. Due to the reaction processes occurring in the near-shore aquifer, the landward depth of the nutrient plume (i.e., nitrate and ammonium rich plumes) becomes reversed prior to discharging to coastal waters. This is consistent with the numerical results of Spiteri et al. (2008a). At the landwater boundary the nitrate plumes overlies the ammonium and phosphate plume however mixing and reactions in the subterranean estuary cause an ammonium and phosphate plume to discharge above a nitrate plume at the aquifer-ocean interface.

## **A.5 Conclusion**

This model verification provides a basis for using the reactive transport model developed in SEAWAT-2005 and PHT3D v2.10 to evaluate the mixing and nutrient reaction processes in a near-shore coastal aquifer subject to oceanic forcing.

## **References**

Spiteri, C., C. P. Slomp, et al. (2008a). "Modeling biogeochemical processes in subterranean estuaries: Effect of flow dynamics and redox conditions on

submarine groundwater discharge of nutrients." Water Resources Research 44(4): W04701.

## Appendix B

---

### MATLAB code for post processing data

#### B.1 Parameters Calculated

A MATLAB code was written for post-processing the numerical model results. This script includes the procedure for extracting and plotting the concentration distribution profiles and calculating the exit concentrations and chemical flux of nutrients (nitrate, ammonium, and phosphate) after 300 days. The total moles of precipitates (iron hydroxides), and total adsorbed moles of phosphate after 300 days are also calculated. For the tidal cases, a tide-averaged velocity approach is adopted for calculating the chemical fluxes and exit concentrations.

#### B.2 Extracting data for ammonium

```
clear all

%Model parameters

column=56
layer=49

%SEAWAT model information

str=('Reading SEAWAT model information.....')

%Bottom of layers

B=textread('grid/bottom.txt','%f','delimiter','whitespace');
for i=0:layer-1;
    k=3+i*column;
    l=2+(i+1)*column;
    B1(i+1,:)=B(k:l,1)';
end;
```

```

%Top of layers

T=textread('grid/top.txt','%f','delimiter','whitespace');
for i=0:layer-1;
    k=3+i*column;
    l=2+(i+1)*column;
    T1(i+1,:)=T(k:l,1)';
end;

Z=(T1+B1)/2;           %elevations in middle of cell
dz=T1-B1 ;             %z discretisation

%Column data

x=xlsread('grid/column.xls');
x1=x(:,1);
x1=x1';
for i=1:layer;
    x2(i,1:column)=x1;
end

dx=x(:,2);
dx=dx';
for i=1:layer;
    dx1(i,1:column)=dx;
end

%Porosity data

nee=textread('grid\porosity.txt','%f','delimiter','whitespace');

for i=0:layer-1;
    k=3+i*column;
    l=2+(i+1)*column;
    ne(i+1,:)=nee(k:l,1)';
end;

%Read concentration results

p_amm_ss_raw=textread('p_amm_ss');
p_amm_ss=p_amm_ss_raw(2:end,:);

m_amm_ss_raw=textread('m_amm_ss');
m_amm_ss=m_amm_ss_raw(2:end,:);

%Set dry/inactive cells (Where concentration is  $1 \times 10^{30}$ ) to be NaN (Not a number)

```



```

for i=1:column;
    for j=1:layer;
        if p_amm_ss(j,i)>=1000;
            p_amm_ss(j,i)=NaN;
        end
        if m_amm_ss(j,i)>=1000;
            m_amm_ss(j,i)=NaN;
        end
    end
end

%Change in ammonia

diff_amm_ss=m_amm_ss-p_amm_ss;

% %Reading and extracting flow data
%Extract flow data for stress period 200

k1=199;
sp=1;

str=('Reading budget.dat.....')

%Opens binary file for reading

fid=fopen('budget.dat');

extra=9;

%Repositioning in indicator in file ie. location in files to start reading in data

k=((k1)*(6*column*layer+6*extra))*4;
fseek(fid, k,'bof');

%Reading in data

m=(6*column*layer+6*extra)*sp;
L=fread(fid,m,'single');

%Extracting budget data

str=('Extracting flow data.....')

%Replace dry cells with NaN

```

```

for i=1:length(L);
    if L(i,:) <= -1000;
        L(i,:)=NaN;
    end;
end;

%Replace inactive cells with NaN

for i=1:length(L);
    if L(i,:) >= 100;
        L(i,:)=NaN;
    end;
end;

%Converts column results into a matrix of layer * column
M=L';
%Flow through right face (m3/day)

for n=1:sp
    for i=0:(layer-1);
        p=i*column+(6*(n-1)+2)*column*layer+(6*(n-1)+3)*extra+1;
        j=p+column-1;
        C_ss(i+1,1:column,n)=M(1,p:j);
    end

    vC_ss(:,:,n)=C_ss(:,:,n)./dz; %Darcy velocity through right face
    lvC_ss(:,:,n)=vC_ss(:,:,n)./ne; %Linear velocity through right face

    %Flow through lower face (m3/day)

    for i=0:(layer-1);
        p=i*column+(6*(n-1)+3)*column*layer+(6*(n-1)+4)*extra+1;
        j=p+column-1;
        D_ss(i+1,1:column,n)=M(1,p:j); %Flow per stress period
    end

    vD_ss(:,:,n)=D_ss(:,:,n)./dx1; %Darcy velocity through bottom
    face
    lvD_ss(:,:,n)=vD_ss(:,:,n)./ne; %Linear velocity through bottom
    face
end

%Set velocities in surface water region and near interface = 0

I=find(ne>0.9);

```

```

vC_ss(I)=0;           %set velocity at zero for surface water cells
vD_ss(I)=0;

%Locations where to calculate fluxes from

aa=30:0.05:70;

%Step back from interface at increments

dist=[0.15 0.25 0.5 0.75 1];

NL=5                  %number of locations back from interface where recirculation will be
                    %calculated as specified in variable 'dist'

for i=1:NL;
    aa1(i,:)=aa;
end;

%Angle of interface ie. beach slope

beta=atan(1/10);

distx=dist/sin(beta); %distance to step in x-direction
distz=distx/tan(beta); %distance to step in z-direction

for i=1:NL
    aa20(i,:)=aa-distx(1,i);
end

for i=1:NL
    bb20(i,:)=(aa20(i,:)-aa20(i,1))*0.1+11;
end

xx=x2+dx1/2;         %matrix with right hand faces

%Unit vector normal to interface

uvz=10/(10^2+1^2)^0.5;
uvx=1/(10^2+1^2)^0.5;

%Calculate concentrations perpendicular to the interface

for i=1:NL;
    EC(i,:)=interp2(x2,Z,p_amm_ss(:,:),aa20(i,:),bb20(i,:));
end

```

```

%If the concentration == NaN, set it to zero

EC_nan=isnan(EC);
for i=1:NL;
    for j=1:length(aa20);
        if EC_nan(i,j)==1;
            EC(i,j)=0;
        end;
    end;
end;

%Calculate exchange based on the flow fields (m3/d)

for i=1:NL;
    U20av(i,:)=interp2(xx,B1,lvc_ss,aa20(i,:),bb20(i,:));
    V20av(i,:)=interp2(xx,B1,-lvd_ss,aa20(i,:),bb20(i,:));
    EX(i,:)=0.25*(0.05/cos(beta))*(uvx.*U20av(i,:)+uvz.*V20av(i,:));
end

% Where the EX = NAN, let the EX = zero

for j=1:length(aa);
    for i=1:NL
        TF = isnan(EX(i,j));
        if TF==1;
            EX(i,j)=0;
        end;
    end;
end;

%To calculate exfiltration rates set all infiltration cells to zero

EXex=EX;
for j=1:length(aa);
    for i =1:NL
        if EXex(i,j)<=0;
            EXex(i,j)=0;
        end;
    end;
end;

%To calculate infiltration rates set all exfiltration cells to zero

EXin=EX;
for j=1:length(aa);
    for i =1:NL

```

```

        if EXin(i,j)>=0;
            EXin(i,j)=0;
        end;
    end;
end;

%Calculate chemical fluxes for exfiltration as C (mol/L) x EX_tidal (m3/d at each point)
* 1000 (L/m3)

CF_av=EC.*EXex.*1000;

%Calculate chemical fluxes for infiltration as C (mol/L) x EX_tidal (m3/d at each point)
* 1000 (L/m3)

CF_in=EC.*EXin.*1000;

%Total mass flux exfiltrating

CF=sum(CF_av')

%Total mass flux infiltrating

Cin=sum(CF_in')

%Total water flux exfiltrating

EXex_total=sum(EXex')

%Total water flux infiltrating

EXin_total=sum(EXin')

%Inland flow

for i=1:sp;
    Inland(:,i)=C_ss(:,1,i);           %Creates a matrix with first column from each
    stress period                       stress period
end
Inlandt=sum(Inland(:,1:sp));           %Sums the columns to calculate the total freshwater
discharge per stress period             discharge per stress period
Itt=sum(Inlandt)/(sp)                   %total freshwater flow through interface per day

%Calculate total moles in aquifer
%Zeroth moment - Total moles in aquifer
%If the concentration == NaN, set it to zero

```

```

C_tot=p_amm_ss;
C_nan=isnan(C_tot);

for i=1:column;
    for j=1:layer;
        if C_nan(j,i)==1;
            C_tot(j,i)=0;
        end;
    end;
end;
M=ne.*C_tot*1000.*dx1.*dz;
M0=sum(sum(M))

%Plot results

%Total Chemical flux versus x

figure(101)
plot(aa20(4,:),CF_av(4,:)/0.0502,'k');
hold on

title('Total chemical flux along the aquifer-ocean interface')
xlabel('Distance along the aquifer-ocean interface (m)')
ylabel('Chemical flux (mol/d/m^2)')
xlim([35 65])

%Exit concentration versus x

figure(102)
plot(aa20(1,:),EC(4,:), 'g');
hold on

title('Exit concentrations along the aquifer-ocean interface')
xlabel('Distance along the aquifer-ocean interface (m)')
ylabel('Ammonia concentration (mol/L)')
xlim([35 65])

%Contour plots for ammonium

figure(103);

vfilled_amm_m_ss=( [0:max(max(m_amm_ss))/100:max(max(m_amm_ss))] );
contourf(x2,Z,m_amm_ss,vfilled_amm_m_ss);
caxis([0 max(max(m_amm_ss))]);
shading flat
colorbar

```

hold on

%Plot aquifer-ocean boundary

```
for j=1:column;
A{1,j} = find(ne(:,j)>0.5);           %Finds the interface cells
G(1,j)=length(A{1,j})+1;
if G(1,j)==layer+1;
    G(1,j)=layer;
end;
end;
```

```
plot(x1,T1(G,1),'k','LineWidth',3);
hold on
```

%Plot velocity vectors

```
quiver(x2(1:2:layer,1:2:column),Z(1:2:layer,1:2:column),vC_ss(1:2:layer,1:2:column),-
vD_ss(1:2:layer,1:2:column),'w');
hold on
```

```
xlim([2 60]);
xlabel('x (m)');
ylabel('z (m)');
title('Ammonium Concentrations - No reaction ');
```

figure(104);

```
vfilled_amm_p_ss=(0:max(max(p_amm_ss))/100:max(max(p_amm_ss)));
contourf(x2,Z,p_amm_ss,vfilled_amm_p_ss);
caxis([0 max(max(p_amm_ss))]);
shading flat
colorbar
hold on
```

%Plot aquifer-ocean boundary

```
for j=1:column;
A{1,j} = find(ne(:,j)>0.5);           %Finds the interface cells
G(1,j)=length(A{1,j})+1;
if G(1,j)==layer+1;
    G(1,j)=layer;
end;
end;
```

```
plot(x1,T1(G,1),'k','LineWidth',3);
hold on
```

```

%Plot velocity vectors

quiver(x2(1:2:layer,1:2:column),Z(1:2:layer,1:2:column),vC_ss(1:2:layer,1:2:column),-
vD_ss(1:2:layer,1:2:column),'w');
hold on

xlim([2 60]);
xlabel('x (m)');
ylabel('z (m)');
title('Ammonium Concentrations - Reaction');

figure(105);

vfilled_amm_diff_ss=(0:max(max(diff_amm_ss))/100:max(max(diff_amm_ss))];
contourf(x2,Z,diff_amm_ss);
shading flat
colorbar
hold on

%Plot aquifer-ocean boundary
for j=1:column;
A{1,j} = find(ne(:,j)>0.5);           %Finds the interface cells
G(1,j)=length(A{1,j})+1;
if G(1,j)==layer+1;
    G(1,j)=layer;
end;
end;

plot(x1,T1(G,1),'k','LineWidth',3);
hold on

%Plot velocity vectors

quiver(x2(1:2:layer,1:2:column),Z(1:2:layer,1:2:column),vC_ss(1:2:layer,1:2:column),-
vD_ss(1:2:layer,1:2:column),'w');
hold on

xlim([2 60]);
xlabel('x (m)');
ylabel('z (m)');
title('Ammonium Concentrations - Change from reaction ');

```



## Vita

---

<b>Name:</b>	Nawrin Anwar
<b>Birthplace:</b>	Dhaka, Bangladesh.
<b>Date of Birth:</b>	September 21, 1987.
<b>Post-secondary Education and Degrees:</b>	Bangladesh University of Engineering and Technology, Dhaka, Bangladesh. B. Sc. in Civil Engineering, 2004 - 2009.
<b>Honours and Awards:</b>	Dean Scholarship Bangladesh University of Engineering and Technology, Dhaka, Bangladesh. 2005 - 2009.  University Merit Scholarship Bangladesh University of Engineering and Technology, Dhaka, Bangladesh. 2005 - 2009.
<b>Related Work Experience:</b>	Graduate Research and Teaching Assistant, The University of Western Ontario, 2010 - 2012.  Lecturer, Civil Engineering Department, University of Asia Pacific, Dhaka, Bangladesh. October 2009 – April 2010.
<b>Conference Proceedings:</b>	1) Anwar, N; Lee J; Weber, S; and Robinson, C. (2011). “Nutrient and heavy metal concentration in the groundwater At beaches of the Great Lakes”, Proceedings of the 11 <sup>th</sup> Great Lake Beach Association Conference, Michigan City, Indiana, September 26-28, 2011.  2) Anwar, N; and Robinson, C. (2011). “Nutrient transport and transformation in a tidally influenced subterranean estuary”, Proceedings of the 21 <sup>st</sup> Conference of the Coastal Estuarine Research Federation, Daytona Beach, Florida, November 6-10, 2011.

- 3) Anwar, N; and Robinson, C. (2011).  
“Influence of tides on the transport and fate of groundwater-derived nutrients to coastal waters”, Proceedings of the AGU Fall Meeting 2011, San Francisco, California, December 5-9, 2011.
- 4) Anwar, N; and Robinson, C. (2012).  
“Fate of groundwater-derived nutrients in tidally influenced coastal aquifers: numerical simulations”, Proceedings of the 22<sup>nd</sup> V.M. Goldschmidt 2012 Conference, Montreal, Quebec, June 24-29, 2012.